DEVELOPMENT OF LOOP-MEDIATED ISOTHERMAL AMPLIFICATION TECHNOLOGY FOR RAPID DIAGNOSTICS

Johnny Xiangyi Zhou

Linacre College

Department of Engineering Science

University of Oxford

A thesis submitted for the degree of

Doctor of Philosophy

Michaelmas 2024

Acknowledgements

My time at Oxford has been marked by deep personal growth. Arriving during COVID lockdowns, I initially faced an isolating loneliness, confined to college with little opportunity for connection. Yet, in time, I formed friendships and mentorships that I will cherish for life, from those who directly helped me to those who supported me simply by being great friends.

To my selfless parents, who have never stopped believing in me. My ambitions are fundamentally built on honouring the countless sacrifices you've made. And to my sister Jess, who has always been by my side and on my team. You all taught me the true meaning of family, and words cannot fully capture my gratitude.

To my beloved fiancée, Evie, whose constant love and support sustained me through my DPhil journey. You have been my motivation and my peace, and I look forward with excitement to stepping into our next adventure together.

To my teachers, Professor Zhanfeng Cui and Professor Wei Huang, I consider you life mentors. Who I was before meeting you feels like an empty vessel compared to who I am now, thanks largely to your wisdom and guidance. Your nurturing will never be forgotten.

To Professor Wen Wang, who has mentored and guided me throughout my higher education, your support has been instrumental in getting me to where I am today.

Special thanks to Dr. Richard Yu, for your unrelenting aid in the laboratory and genuine friendship. And to all my wonderful friends in our lab: Phoebe Yuan, Yutong Yin, Siqi Dai, Shuai Ren, Jane Tsu, and Boon Lim. May our friendship last forever and extend beyond Oxford!

To Tongshan Liu, Marek Rychetský Zelimhan Raduev, Barnum Swannell, Jeff Liu, Mingshan Tsai, and Kumeren Govender, life at Oxford would have been far less bright without you all in it.

Finally, to my close friends outside of Oxford, even across the world in Beijing, some bonds are timeless. Endless love and gratitude to you all.

Abstract

The urgent need for rapid, reliable diagnostic technologies has been underscored by global health challenges like the COVID-19 pandemic. Conventional diagnostic methods, such as Polymerase Chain Reaction (PCR), are effective but rely on complex infrastructure, making them less accessible for decentralized or resource-limited settings. Loop-Mediated Isothermal Amplification (LAMP) technology offers a faster and simpler alternative, but traditional LAMP assays face limitations, including the inability to quantify pathogen load, cold-chain dependency, limited multiplexing, and interference from sample pH.

This thesis addresses these gaps through multiple innovations, resulting in the development of OxLAMP, a third-generation LAMP assay designed for versatile point-of-care diagnostics. Key advancements include the advancement of quantitative LAMP (qLAMP

) for pathogen quantification, akin to PCR's CT values. qLAMP was verified by 64 clinical samples (25 positives and 39 negatives) and LAMP threshold time (TT) values showed linear relationships to pathogen load. Novel lyophilisation and Matrix-Assisted Room Temperature (MART) drying techniques for reagent stabilization were developed, demonstrating capabilities of preserving reagents for six months at 45°C, eliminating the need for cold-chain storage. Additionally, the OxLAMP platform was further developed by incorporating pH-independent colorimetric diagnostic capabilities, improving robustness and ensuring consistent diagnostic accuracy across pH ranges of 2.0 to 9.0. Custom primer sets were designed and validated for pathogens, including six variants of SARS-CoV-2, seven different bacterial bloodstream pathogens, and Herpes Simplex Virus (HSV), enabling multiplex detection of pathogens within a single platform. False positives, a common challenge in LAMP, were eliminated through stringent primer design and experimental validation, with a specificity of 100% in clinical testing.

These innovations culminated in the integration of the OxLAMP assay into a multiplex diagnostic device, the Sinopharm Colorimetric Photometer, which facilitates high-throughput and quantitative pathogen detection from clinical samples. Validation using 20 clinical specimens (14 positives and 6 negatives) demonstrated the platform's reliability and diagnostic accuracy across diverse healthcare settings.

By addressing key limitations in traditional diagnostic tools, OxLAMP bridges the gap between laboratory innovation and real-world application. This work not only enhances the scalability and accessibility of rapid diagnostic technologies but also provides a robust framework for managing current and emerging infectious diseases in both clinical and resource-limited environments.

Contents

List of Figures

List of Tables

List of Publications and Manuscripts

1. A quantitative RT-qLAMP for the detection of SARS-CoV-2 and human gene in clinical application. Yu, Y., Zhou, J.X.Y., Li, B., Ji, M., Wang, Y., Carnaby, E., Andersson, M.I., Huang, W.E., Cui, Z., 2022. A quantitative RT-qLAMP for the

detection of SARS-CoV-2 and human gene in clinical application. *Microb Biotechnol* 15, 2619–2630. https://doi.org/10.1111/1751-7915.14112

2. Thermostabilising Functional Proteins with Matrix Assisted Room Temperature Drying. Authors: Yejiong Yu, Siqi Dai, Johnny Xiangyi Zhou, Wei E Huang, Zhanfeng Cui. *Engineering*. Date submitted: April 2024
3. Lyophilised pH-Independent Colorimetric LAMP Assays for Detection of Herpes Simplex Virus (HSV) in Clinical Applications. Authors: Johnny Xiangyi Zhou, Yejiong Yu, Yasaman Ahmaid, Monique Andersson, Wei E Huang, Zhanfeng Cui.

Chapter 1 Introduction

1.1 Background: Need for rapid testing

1.1.1 Devastation from a pandemic

The SARS-CoV-2 (Covid-19) pandemic represents one of the most devastating global health crises in modern history. Since the Spanish Flu of 1918, there has been no pandemic, excluding HIV/AIDS, that has brought about such widespread consequences on a global scale[1]. What began as a seemingly isolated outbreak of a novel coronavirus in Wuhan, China, quickly spiralled into a global emergency within the span of four months[2]. The initial reports from Wuhan described patients with flu-like symptoms, but these early indicators did not prompt an immediate or urgent response from international authorities. As a result, the virus was able to spread rapidly across the world [3]. By the time national governments and health organizations realized the gravity of the situation, it was too late to contain its spread effectively.

The global death toll caused by COVID-19 is estimated to have reached approximately 4.4 million, while confirmed cases exceeded 210 million when this research project began. [4]. Hospitals worldwide, even those in well-developed nations with advanced healthcare systems, struggled to cope with the sudden influx of patients, leading to waves of overwhelming demand on medical services [5].The pandemic placed unprecedented strain on healthcare infrastructures, resulting in shortages of essential medical supplies such as face masks, gowns, gloves, and oxygen tanks [6]. Beyond this, national economies were brought to a near standstill, and international supply chains were disrupted due to quarantine measures and movement restrictions [7]. These economic consequences were felt at both the local and global levels, with businesses closing, millions of people losing their jobs, and household isolation cutting off the support that small businesses rely on to stay afloat [8,9]. The pandemic led to a feedback

loop of financial strain: businesses struggled or went bankrupt, leaving workers unemployed, which in turn reduced consumer spending, further contributing to economic decline [10].

The social isolation brought on by lockdowns and social distancing policies proved to be one of the most detrimental aspects of the pandemic for mental health. While social distancing was vital in controlling the spread of the virus [11], its psychological effects were severe. People around the world faced prolonged periods of isolation from loved ones, leading to increased rates of anxiety, depression, insomnia, and obsessive-compulsive disorders [12,13]. Many stress-relieving activities, such as outdoor recreation, were restricted, adding to the mental health burden faced by millions during the pandemic [14]. Suicide rates and incidents of self-harm saw a concerning rise, as individuals struggled to cope with the stress and isolation brought on by the pandemic [15]. Humans are social animals by nature, and the prolonged periods of enforced isolation only exacerbated the emotional toll of the pandemic.

Beyond its immediate health impacts, COVID-19 had profound implications on global geopolitics. The pandemic heightened tensions between nations, as borders were closed and countries prioritized national interests over international cooperation. Nations pointed fingers at one another over issues of containment failures and debated the virus's origins [16,17]. The World Health Organization's (WHO) decision to name variants using the Greek alphabet, rather than geographical labels such as "Indian variant" or "South African variant," was partially motivated by the desire to reduce stigmatization and the potential for xenophobia [18]. Unfortunately, the pandemic did spark waves of racism, particularly against people of Asian descent, with Chinese individuals being the primary targets [19]. As a person of Chinese ethnicity, I have personally witnessed examples of this discrimination among friends and family members. The pandemic laid bare the deep-seated social biases that can be exacerbated by global crises.

While COVID-19's effects have been devastating, it also serves as a stark reminder that global pandemics can and will continue to emerge. The world must prepare for the possibility of future pandemics by learning from the lessons of this crisis. Among these lessons, the importance of quality diagnostic testing has been highlighted as a critical tool in pandemic management. Emerging infectious diseases have become increasingly common in recent decades, with new human infectious diseases arising approximately every eight months [20]. Globalization, urbanization, climate change, and human migration all contribute to the spread of infectious diseases, creating a perfect storm for future pandemics [21]. Even in the absence of pandemics, diseases of varying scales can be controlled and mitigated with rapid, accurate diagnostic technologies.

1.1.2 The role of testing in pandemic management

The importance of mass testing during a pandemic cannot be overstated. As COVID-19 spread, it became evident that robust diagnostic capabilities were essential for identifying infected individuals, controlling the spread of the virus, and implementing public health measures to prevent widespread transmission. Many of the societal and economic impacts of the pandemic could have been mitigated if rapid, accurate, and accessible testing had been available on a larger scale from the outset [22]. Although the development and deployment of vaccines offered hope for controlling the virus [23,24], testing remained crucial. Vaccinated individuals could still act as carriers of the virus, posing a risk to vulnerable populations. Thus, testing prior to interacting with at-risk individuals, particularly in care homes or hospitals, continued to be a necessary preventative measure [25].

Early diagnosis allows for reduced time to targeted isolation, help control outbreaks, and lower the burden on healthcare systems by enabling earlier intervention [26]. The speed of test results therefore became a critical factor in the efficacy of pandemic control efforts. Early in the pandemic, Loop-Mediated Isothermal Amplification (LAMP) technology, a form of nucleic acid amplification testing (NAAT), was rapidly adapted for COVID-19 diagnostics. Researchers, including Professor Huang et al., developed SARS-CoV-2-specific primers for the LAMP assay, providing a faster and more accessible alternative to the widely used polymerase chain reaction (PCR) tests [27].

LAMP-based testing, particularly Reverse Transcriptase-LAMP (RT-LAMP), was shown to have a significantly shorter turnaround time, with results being delivered in approximately 30 minutes, as compared to the 2-hour processing time typically required for PCR testing [28]. While PCR remains the "gold standard" for diagnostic testing due to its high sensitivity and specificity, it has several limitations in the context of pandemic management. PCR tests require specialized equipment, trained personnel, and batch processing in centralized laboratories, leading to delays in result reporting [29]. The logistical challenges of PCR testing were particularly evident when rapid, point-of-care testing was needed in locations such as airports, care homes, and hospitals.

The urgent need for faster, more accessible testing was underscored as governments around the world sought to implement mass testing strategies as part of their efforts to reopen economies and return to a semblance of normalcy. Lateral flow tests (LFTs), another form of rapid testing, were introduced as a cheaper and quicker alternative to PCR. However, early evaluations of antigen-based LFTs revealed significant drawbacks, including lower specificity and sensitivity, especially when administered by untrained individuals [30,31]. This made LFTs unsuitable for critical settings where accuracy was paramount, such as care homes or airplanes, where the risk

of spreading the virus to vulnerable individuals was high. In such contexts, the need for a rapid, accurate, and scalable testing platform remained unmet. LAMP may also be susceptible to human error, and therefore, consideration should be in place to manage them through built-in procedural controls. These could include objective readout methods (fluorescent or photometric), the use of negative controls, and the inclusion of human gene targets as internal positive controls in multiplex testing.

In the airline industry, where tourism accounts for a significant portion of global economic activity, the limitations of existing testing technologies became evident. With tourism contributing approximately 10% to the UK's GDP [32], the inability to quickly and accurately test passengers resulted in delays and financial losses for both the airline and tourism sectors. On-site PCR testing, with its 2-hour turnaround time, was simply too slow to be practical for airport use. During the winter lockdown of 2020, I volunteered as a supervisor for Prenetics™ lab technicians at Heathrow Airport, overseeing the use of RT-LAMP tests for passenger testing. Despite the one hour and a half faster turnaround time of LAMP compared to PCR, delays were still common, and there was an evident demand for even faster diagnostic solutions, even if by just a few minutes.

1.2 Aims and objectives

This project aims to advance the next generation of LAMP technology by enhancing its advantages over PCR and addressing current limitations. It also addresses key challenges in point-of-care diagnostics, with the ultimate goal of developing a comprehensive solution, branded as OxLAMP.

1 Development of quantitative LAMP (qLAMP) for fluorescence-based diagnostics, an alternate reading methodology for faster detection times, and verification of pathogen load for clinical samples.

2 Design of LAMP primers for Sars-Cov-2 and all its major variants during the mid to latter stages of the global pandemic. Develop LAMP primer sets for six of the most common bloodstream pathogens present in sepsis, as well as Herpes-Simplex-Virus (HSV) 1 and 2. Prove interchangeability of primer sets within OxLAMP reaction mix and potential for multiplex testing. Criteria for success with multiplex testing would be the simultaneous running of three or more different nucleic acid target samples in one LAMP reaction cycle.

3 Incorporation of lyophilisation and Matrix-Assisted Room Temperature (MART) drying techniques and creation of formulations to improve the stability of LAMP reaction mix. Allowing LAMP tests to be stored at room temperature or above temperatures for five days or more and easing the burden of cold-chain transportation.

4 Development of pH-independent colorimetric LAMP testing. Allowing for diagnostics to occur with naked eye colour change observation at POC settings, without relying on colour changing pH indicators.

5 Incorporation of lyophilised pH-independent LAMP into a multiplex testing device, which can allow for diagnosis via colour change observation or photometer reading.

The next section provides an overview of the thesis chapters, indicating which chapters address each specific objective.

1.3 Structure of thesis and achievements

Chapter 2 reviews the current landscape of diagnostic testing, beginning with the details of the current gold standard for pathogen detection, qPCR, and moving to isothermal amplification

techniques better suited for point-of-care (POC) diagnostics. LAMP is emphasized as the chosen nucleic acid amplification method for this project, and thus, a substantial portion of the literature review will focus on recent advancements in LAMP technology. Together with the introduction, this chapter clarifies the research direction of the project and how the objectives aim to address existing gaps and challenges in the field.

Chapter 3 broadens the potential of LAMP diagnostics by designing primers for additional pathogens, including bacterial pathogens involved in sepsis and Herpes Simplex Virus (HSV) 1 and 2. This chapter also demonstrates the viability of custom assays with various primer options, paving the way for multiplex capabilities.

Main achievements:

- Designed and optimized primers for seven key bacterial pathogens responsible for bloodstream infections (e.g., Pseudomonas aeruginosa, Escherichia coli, and Staphylococcus aureus) as well as SARS-CoV-2 and HSV.
- Validated qLAMP for direct detection of bacterial DNA from colony samples, bypassing complex nucleic acid extraction steps.
- Verified compatibility of primer sets with the OxLAMP reaction mix, paving the way for future multiplex diagnostic applications.

Chapter 4 marks a key progression in this DPhil project: the implementation of a fluorescence-based quantitative LAMP (qLAMP) approach. This work integrates real-time fluorescence detection to improve diagnostic speed and facilitate estimation of pathogen load

through time-to-threshold analysis. Its application here demonstrates feasibility under our LAMP assay conditions, providing an alternative to qPCR for quantitative diagnostics.Main achievements:

- Improvement of fluorescence techniques to LAMP assays to provide quantitative results analogous to PCR's CT values, enabling pathogen load assessment.
- Demonstrated the use of both fluorescent and colorimetric detection for qLAMP, offering flexibility in diagnostic settings.
- Established a strong linear relationship between template copy number and time-to-threshold (TT) values, enhancing qLAMP's clinical utility.
- Verified qLAMP’s applicability across various sample types, including 65 clinical specimens and cell lines, emphasizing its utility in real-world diagnostics.

Chapter 5 addresses the cold-chain challenge by exploring drying techniques for LAMP assays, such as lyophilisation and Matrix-Assisted Room Temperature (MART) drying. Stabilizing the assays at higher temperatures greatly enhances their transportability to POC locations and extends their shelf life.

Main achievements:

- Created tailored lyophilisation recipes incorporating protective agents to maintain enzyme activity and reaction stability over extended periods.
- Introduced and validated MART drying as a novel, cost-effective alternative for LAMP assays, ensuring reagent stability without requiring specialized equipment.

- Demonstrated extended shelf life and robustness of dried LAMP reagents under simulated transport conditions, confirming their suitability for point-of-care (POC) diagnostics.

Chapter 6 introduces the development of a pH-independent colorimetric LAMP assay, which enables diagnostics through a colour change without relying on pH indicators. This assay maintains qLAMP functionality, offering increased flexibility. The new colour-change system allows LAMP tests to work with a wider range of potential samples, as sample pH is no longer a significant obstacle. This chapter also combines all the advancements of our LAMP assays into an existing multiplex testing platform, the Sinopharm Colorimetric Photometer. Multiple freeze-dried, pH-independent LAMP assays were successfully run simultaneously on this device. The functionality of our assays within this system has been validated using clinical samples, and the sensitivity of the tests has been thoroughly established.

Main achievements:

- Developed a pH-independent assay that eliminates reliance on traditional pH indicators, ensuring diagnostic accuracy regardless of sample pH variability.
- Demonstrated enhanced reliability of the pH-independent assay using both fluorescent and colorimetric detection methods across diverse sample types.
- Confirmed the assay's diagnostic performance using 17 clinical samples, showcasing its sensitivity and specificity for pathogen detection in real-world scenarios.
- Demonstrated the feasibility of using the Sinopharm reader for multiplex diagnostics, tracking reaction progress in real time and eliminating subjectivity in result interpretation.

Finally, Chapter 7 concludes the thesis by reflecting on the accomplishments of this research and its contributions to the field of point-of-care diagnostics.

Chapter 2 Literature Review

2.1 Loop Mediated Isothermal Amplification (LAMP)

Quantitative PCR (qPCR) is the gold standard for nucleic acid amplification due to its high sensitivity of up to 3 copies of DNA per reaction [33], specificity often exceeding 95% [34], and quantitative ability [35]. However, it requires thermal cycling, trained personnel, and laboratory infrastructure, making it less suitable for rapid, decentralised, or resource-limited settings [36,37]. In contrast, isothermal amplification methods operate at a constant temperature, offering faster turnaround and simplified equipment requirements, which are key advantages for point-of-care (POC) diagnostics. LAMP was chosen as the core diagnostic method in this project due to its established use in our laboratory during the early stages of the COVID-19 pandemic. The lab had already developed SARS-CoV-2-specific LAMP primers, and prior publications by Professors Huang and Cui had demonstrated the feasibility of LAMP for rapid diagnostics under field conditions [27]. Building on this foundation allowed for immediate progression into assay development, optimization, and application, without the need to establish an entirely new platform. This practical alignment with ongoing work also enabled faster iteration and clinical relevance during a time of urgent diagnostic need. The following section outlines the core principles and recent developments in LAMP technology. LAMP was initially introduced in the year 2000 with four primers (inner primers: FIP&BIP, outer primers:

F3&B3) with the reaction time exceeding one hour [38]. It was further enhanced in 2002 by the addition of loop primers (LF&LB), which accelerated the reaction [39]. As shown in Figure 2.1, the LAMP inner primer, FIP, binds to the targeted sequences (I) and is elongated by a strand-displacing polymerase, usually polymerase Bst 2.0. Strand (II) is separated from the target DNA duplex after the elongation of the LAMP outer primer, F3 (III). Upon elongation by another inner primer, BIP, and outer primer, B3, a dumbbell-shaped DNA structure (IV) is formed. This structure acts as a seed for exponential amplification. Subsequently, structures of various sizes are generated. The addition of loop primers (LF and LB) can accelerate this process, typically finishing within 30 minutes [40]. For RNA templates, the targeted sequence must undergo reverse transcription into complementary DNA before amplification with reverse transcriptase [41,42].

After amplification, except for using the conventional gel electrophoresis for visualizing amplicons [44,45], various detection methods are employed to interpret the results by targeting the different products of the LAMP reaction, including amplicons, pyrophosphate, and hydrogen ions. These methods can include techniques such as fluorescent reading for real-time or endpoint monitoring of amplicon generation, lateral flow testing, colorimetric assays for visualizing results through colour changes, turbidity measurement to detect pyrophosphate precipitation, and electrochemical detection. Each detection method offers unique advantages, enabling the versatile application of LAMP in diverse diagnostic settings.

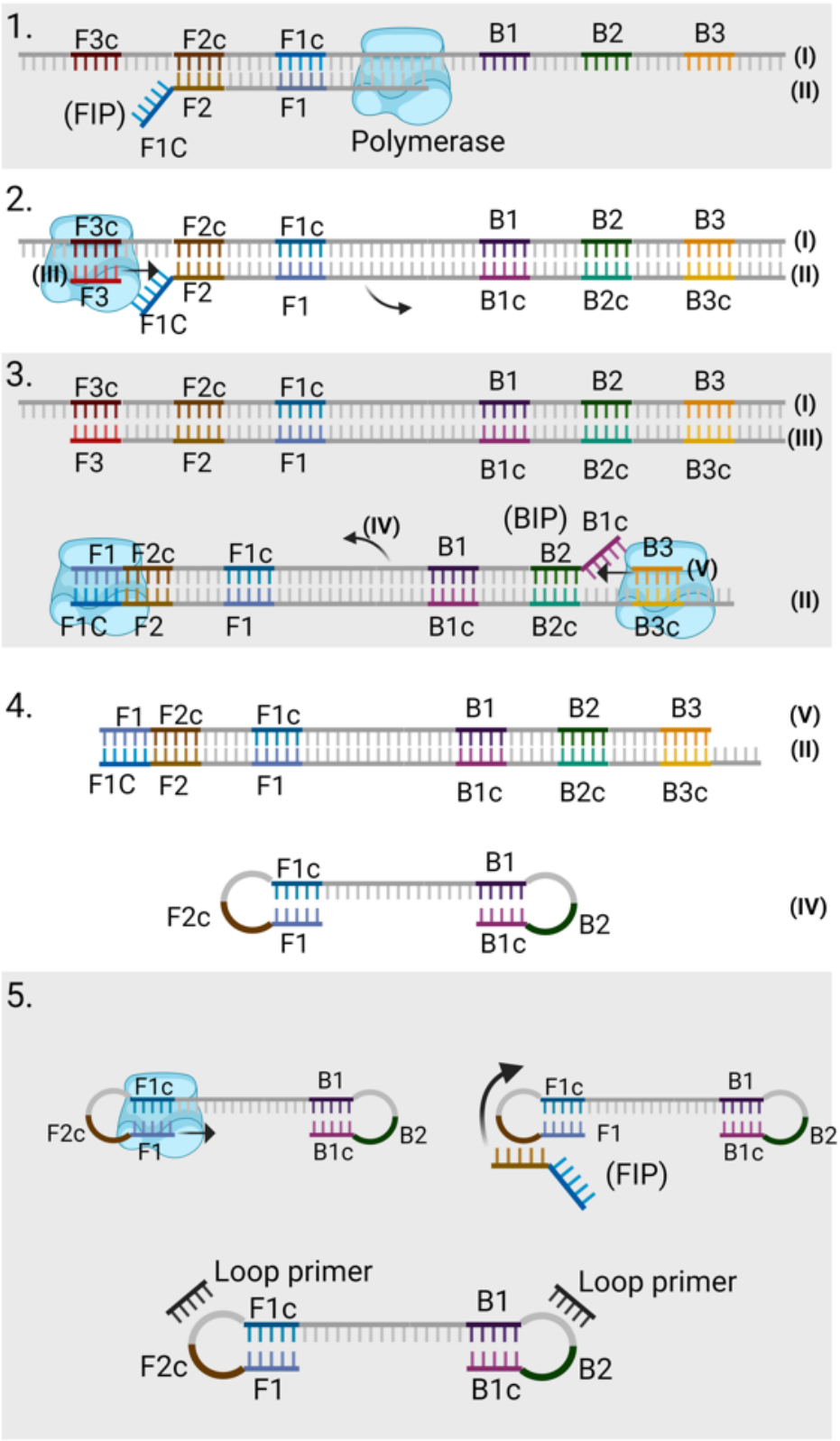

Figure 2.1 *Schematic representation illustrating the LAMP assay amplification process. Begins with FIP and BIP primers leading to the formation of dumbbell structures. Exponential amplification then occurs from these dumbbell structures resulting in the formation of DNA products of various sizes and shapes. Adapted from Ahmadi et al., 2025* [43].

LAMP was chosen for this project primarily because it had already proven its effectiveness during the COVID-19 pandemic, where LAMP assays were successfully deployed for the rapid detection of SARS-CoV-2. As my project commenced during the height of the pandemic, LAMP's track record for delivering quick and reliable results was a significant factor in its selection. Among other isothermal amplification techniques, LAMP stood out for its speed, typically completing reactions within 30 minutes, which provided a clear advantage in POCT scenarios where rapid turnaround times are essential. Furthermore, LAMP's robustness, simplicity, and ability to operate without complex thermal cycling equipment made it highly suitable for resource-limited settings and decentralized testing environments. These qualities aligned perfectly with the goals of my project, particularly in developing a diagnostic platform capable of responding efficiently to both current and future pathogen detection needs.

2.2 Cold-Chain challenges during the COVID-19 pandemic and future pandemics

One of the most significant challenges during pandemics is the requirement for an efficient cold-chain system to store and transport sensitive biological materials. The cold-chain refers to the temperature-controlled supply chain necessary to preserve the stability and efficacy of temperature-sensitive products, such as vaccines, diagnostic assays, and therapeutic reagents. During the pandemic, the cold-chain became a critical bottleneck in the timely delivery and administration of life-saving treatments and tests, particularly in regions with limited infrastructure [46,47].

The cold-chain was also crucial for the transportation of diagnostic test assays, particularly those based on molecular technologies like PCR and LAMP. The enzymes and reagents used in these tests are highly sensitive to temperature and must be kept refrigerated or frozen to

maintain their stability. In many parts of the world, the lack of cold storage infrastructure meant that testing capabilities were severely constrained [48,49].

This challenge was especially pronounced in point-of-care testing scenarios, where rapid, on-site diagnostics were essential to prevent virus transmission. Healthcare workers in remote and resource-limited areas often faced difficulties obtaining and using diagnostic tests because the reagents had degraded during transport, rendering the tests inaccurate or unusable [50,51]. Without a reliable cold-chain, even the most advanced diagnostic technologies would be rendered ineffective in the very settings where they were most needed [52].

The long-term solution lies in reducing dependency on cold-chain logistics by developing products that are stable at ambient temperatures. By focusing on innovative drying solutions, creating diagnostic tools, and vaccines that are more adaptable to a wider range of environments. This will not only improve pandemic preparedness but also enhance the ability to combat a wide range of infectious diseases in both routine and emergency settings [53].

2.3 LAMP within the field of diagnostics and its developments

This section shifts the focus to LAMP, the chosen diagnostic method for this project. This section delves into the recent advancements in LAMP technology, highlighting the various methodologies used to interpret LAMP results, including colorimetric, fluorescence, and turbidity-based readings. Each methodology brings unique advantages, such as colorimetric assays that allow for easy visual interpretation and fluorescence-based detection that offers greater sensitivity. Additionally, this part of the review examines the challenges LAMP faces in clinical applications, such as issues with sample preparation, sensitivity, and real-world implementation in diverse settings.

2.3.1 Fluorescent LAMP

LAMP amplicon detection often utilizes fluorescent dyes, such as SYBR green, which chelate with double-stranded DNA (dsDNA), emitting fluorescence signals during or after amplification [54,55]. While SYBR green, a common fluorescent dye used in real-time PCR, has been found to exhibit a high binding affinity to dsDNA, shifting the melting temperature and stabilising dsDNA. At relatively low reaction temperatures compared to the PCR melting step, it resulted in the inhibition of LAMP reactions, generating false negative results [56–58]

Therefore, SYBR Green is recommended to be added after amplification. To avoid opening the cap after reaction, causing contamination, one method is to place SYBR Green on the inner side of the tube or cap, avoiding contact with the reagents, and then spin or invert the tubes to allow the SYBR Green to dissolve into the reagents [59,60]. Another method involves encapsulating the SYBR Green in agarose gel, which is added after the samples [61]. After amplification, the dissolved SYBR Green can be used to measure endpoint fluorescent intensity or exhibit a colour change, as shown in Figure 1.[62,63].

In addition to using fluorescent dyes directly, some studies employ CRISPR-Cas systems after amplification to enhance specificity and reduce false positive rates. A typical protocol involves first using LAMP with a modified FIP primer that contains a CRISPR-Cas enzyme recognition site to amplify the target DNA. Subsequently, the CRISPR-Cas system is added. The Cas enzyme, directed by the guide RNA, specifically binds to the target site of the amplicons. The binding of Cas enzyme to the target activates its collateral cleavage activity, resulting in the cleavage of nearby non-target single-stranded DNA molecules labelled with fluorescence tags and quenchers. Quenchers on these fluorescence probe molecules keep fluorescence levels low

until CRISPR-Cas enzyme cleavage occurs, allowing for a clear and specific signal indicating the presence of the target DNA [42,64,65].

Due to the observed inhibition of the LAMP assay upon addition of the CRISPR-Cas system [66], it is recommended that this system be added after amplification. While this approach enhances specificity and significantly reduces false positive rates, it also introduces additional steps, increasing cost, time, and the risk of cross-contamination [42].

2.3.2 LAMP with Lateral Flow Test

LAMP amplification with labelled primers can visualize results on a lateral flow strip. Fluorescein (FAM) and biotin groups are linked to the FIP and BIP primers, respectively. After amplification, the amplicons are dual labelled with both FAM and biotin. When applying the amplicons to the lateral flow strip along with phosphate buffer, the FAM-labelled portion of the amplicons binds to anti-FITC antibodies conjugated with gold nanoparticles (Au-NP) that are previously adsorbed on the strip. Capillary action drives the Au-NP-labelled amplicons across the lateral flow strip until they are captured by streptavidin at the test line via biotin-streptavidin interaction. The results can be visually interpreted without the need for specialized equipment [67–69]. The limitations were also evident. Opening the reaction tubes to mix the liquid with buffer and then dripping it onto the lateral flow strip could potentially lead to cross-contamination. The integrated device of LAMP assay and lateral flow test could potentially eliminate the cross-contamination [70].

2.3.3 Colorimetric LAMP assay

Except for aiming at the amplicons, some detection methods target the byproduct, hydrogen ions or pyrophosphate. The release of hydrogen ions could reduce the pH, which could be visualised by colour change of the pH indicator, typically phenol red and hydroxynaphthol blue [27,71,72]. The formulation of the LAMP assay needs to be tuned to minimize the concentration of pH buffer, and the initial pH of the reagents needs to be carefully adjusted [73]. However, a significant drawback of this readout method is that the initial pH of the samples may cause an immediate colour change upon addition, potentially interfering with the final results [74].

Pyrophosphate, another byproduct of LAMP, precipitates with certain metal ions such as Magnesium, Zinc, and Manganese. This property allows for a colorimetric metal ion detection method to be incorporated with the LAMP assay to visualize the results. For instance, 5-Br-PAPS, a sensitive metal ion indicator dye, originally appears yellow and changes to pink when chelated with metals like zinc or manganese [75]. The addition of this colorimetric system to LAMP assay, where zinc ions initially bind to 5-Br-PAPS, presents a pink colour. During LAMP amplification, pyrophosphate is released, causing the metal ions to dissociate from the complex and precipitate with the pyrophosphate. This results in a colour change of the reaction solution from pink to yellow, indicating a positive amplification. Although this colorimetric assay effectively eliminates interference from sample pH, the addition of zinc or manganese can inhibit enzyme activities, particularly reverse transcriptase, thereby extending the reaction time [76,77]. In Szobi's work [77], the reaction volume is doubled to increase the concentration of enzymes, mitigating the effects of zinc addition. However, reaction time was still extended to 1 hour.

2.3.4 Turbidity LAMP

This reading methodology focuses on the generation of pyrophosphate during the amplification, resulting in the precipitation with magnesium [78–81]. This precipitation can be detected using a turbidimeter [60,82,83]. Alternatively, in the absence of a turbidimeter, a brief centrifugation of the LAMP products can be used as an alternative method to observe the white precipitation, which is visible to the naked eye [60,84].

2.3.5 Electrochemical detection LAMP

The release of hydrogen ions will generate current and can be detected by electrochemical measurements [85]. However, often the current generated from hydrogen ions alone is not enough to produce a strong signal for detection, therefore, various techniques help to amplify the signal for electrochemical detection. One method utilises the released hydrogen ions to induce dimer-I motifs, which aid in signal transduction for specific biosensors [86]. Another technique uses hydrogen ions to induce a conformational switch in DNA nanostructures. Electroactive ferrocene probes attached to these DNA molecules would then be released and bind to a detection electrode, amplifying the signal [87].

2.3.6 LAMP assay in diagnosis and key challenges in clinical applications

LAMP is distinguished by its simplicity, minimal equipment requirements, and rapid results within 30 minutes. Consequently, LAMP assays have been extensively developed for the detection of various pathogens, including viruses [88–91], bacteria [92–94], fungi [95–97], and protozoa [98–101].

Apart from the LAMP kits authorized by the FDA for emergency use in detecting COVID-19, there are only a few LAMP kits available on the market. One notable example is the Meridian Bioscience illumigene platform (now known as Alethia), which has been granted FDA approval for detecting a range of pathogens, including *Clostridioides difficile toxin, Cytomegalovirus, Streptococcus pyrogenes, Streptococcus agalatiae, Mycoplasma pneumoniae, Bordetella pertussis, Chlamydia trachomatis, Neisseria gonorrhoeae, and Herpes Simplex 1 & 2* [102]. The LAMP kits developed by Eiken Ltd. for the detection of tuberculosis and malaria have been widely used in Southeast Asia and Africa [103,103,104]. There are three main challenges hindering the application of LAMP assay in the point-of-care setting and low resourced setting, which are complex methodology, reliability, stability.

2.3.6.1 Complex Methodology

The logistics of the LAMP assay are relatively straightforward, involving the collection of samples, sample pretreatment, addition of samples to reagents, and the interpretation of results. Sample pretreatment is often the most complex and critical step, as it significantly influences the sensitivity of the assay [105].

In PCR assays, all samples undergo nucleic acid extraction prior to amplification. This pretreatment step ensures that, regardless of the sample type or transport medium, the resulting extract is purified, containing only nucleic acids in the elution buffer. The elution buffer is normally water or TE buffer, which will not affect the amplification [106].

Integrating DNA extraction into LAMP assays has been shown to enhance sensitivity [105]. However, standard DNA extraction typically requires automated machines or skilled technicians, making it impractical for point-of-care or resource-limited settings. Simpler and instrument-free sample pretreatment techniques with minimal human intervention could enhance the feasibility and speed of LAMP in field detection.

The variability in sample types and the lack of standardized sample pretreatment protocols pose significant challenges for the widespread adoption of LAMP assays. Even within the same sample type, multiple pretreatment methods may exist, further complicating the standardization process. Additionally, even with the same samples, for instance, the whole blood can be treated with a small Flinders Technology Associates (FTA) disc in the micropipette tip to lyse and trap DNA from blood and applied to detect E. coli [107]. No purification was required for the detected HIV-1 from the whole blood [108]. Since different pathogens were targeted, the effectiveness of using the FTA card for treating blood is still unknown. This lack of comparability underscores the need for standardized protocols and rigorous validation studies to ensure the reliability and accuracy of LAMP-based diagnostics across different sample types and target pathogens.

Uses of membranes for nucleic acid extraction from samples and subsequent elution into LAMP reagents have been commonly employed. Various types of membranes have been investigated for this purpose, including filter papers [109,110], FTA card [111,112], and polyethersulfone membrane [113,114]. Notably, a commercial rapid nucleic acid extraction method based on Whatman filter paper has been developed, known as dipstick DNA extraction (Bento, UK). This method involves dipping a dipstick made of Whatman filter paper into heat-inactivated samples, washing it with Tris-HCl buffer, and then dipping it into reagents to elute DNA. The process could be finished in 30 seconds. This methodology holds potential for use with different sample types [115]. If a simple device based on this technique could be developed, it could streamline sample preparation and significantly reduce human error.

These membranes offer advantages such as simplicity, rapid processing times, and compatibility with point-of-care settings. Additionally, they can help standardize the sample pretreatment process, thereby improving the reliability and reproducibility of LAMP-based diagnostics.

Moreover, LAMP tests that have been used in clinical applications for different pathogens do not have a standardized protocol to abide by. Different reagent compositions and personnel will result in dissimilar levels of test sensitivity and reproducibility. Separate research entities are fine-tuning reagent lists to achieve an optimum reaction mix for which there is yet to be an 'industry standard'[116].

2.3.6.2 Reliability:

LAMP, as a nucleic acid amplification technique relying on six different primers, inherently exhibits high specificity for the targeted sequence. However, this characteristic also heightens the potential for primer-primer hybridizations, which can result in template-free amplification and consequently lead to false-positive results, reducing the reliability of the assay [117,118].

First, primer design is essential to mitigate these challenges and increase the sensitivity and specificity of LAMP assays. In addition to primer design, molecular switches have been proven to be effective in increasing the specificity, inhibiting false-positive results [119]. A molecular switch is a short sequence complementary to one of the primers, with its 3′-end modified by a dark quencher molecule, such as Iowa Black RQ (IBRQ). The molecular switch serves as a temperature-dependent mechanism that binds to an essential primer, such as the forward inner primer (FIP). When the reaction temperature is lower than the optimal working temperature of LAMP, the FIP primer is bound to the switch oligonucleotide and cannot participate in the amplification. This prevents non-specific amplification, thereby enhancing the overall specificity of the LAMP assay. A similar approach has been applied to the polymerase enzyme, WarmStart Polymerase Bst 2.0. An aptamer is utilized to block the active site of the polymerase when the temperature is below 45°C. However, when the temperature rises above 45°C, the structure of the aptamer changes, exposing the active site of the polymerase and allowing the

amplification process to proceed [120]. These temperature-dependent regulations help to ensure the specificity of the amplification reaction.

Adjusting the reaction temperature can also reduce non-specific binding and improve assay sensitivity. While most LAMP reactions occur at 65 °C, the optimal working temperature for the polymerase, primer binding efficiency may be compromised at this temperature. Balancing enzyme activity and primer binding efficiency by tuning the reaction temperatures can improve sensitivity [116]. Additionally, touchdown-LAMP, which progressively transitions to lower temperatures over the time course, can enhance sensitivity, as reported in Wang's work [116]. LAMP assay with heating at 63 °C for 5 minutes, 61 °C for 5 minutes, 59 °C for 5 minutes, and finally at 57 °C for 60 minutes, detected 10 fg per reaction of Listeria monocytogenes DNA template, whereas the sensitivity of the conventional LAMP assay (57 °C for 60 min) was 1000 fg. However, this technique requires precise temperature control, which increases the complexity of designing and programming the heating process, making it less applicable for field tests.

Another challenge with LAMP assays is the risk of cross-contamination, as aerosols released from positive tubes can easily contaminate the testing area, making it difficult to remove amplicons [121]. To mitigate this risk, in-tube detection methods such as real-time fluorescence acquisition, colorimetric assays, or turbidity measurements can be employed, avoiding the need to open the caps and reducing the risk of aerosol contamination. Additionally, implementing a hot lid can substantially reduce the generation of aerosols and prevent condensation of reagents on the cap. This is crucial as condensation can alter the concentration of reagents and potentially lead to false-positive results [122]. Alternatively, applying low-melting-temperature wax or mineral oil can achieve similar effectiveness [123–126]. The addition of deoxyuridine triphosphate (dUTP) and uracil-DNA-glycosylase (UDG) can help mitigate the effects of cross-contamination. When amplicons from previous positive tubes are inadvertently introduced into

new reaction tubes, UDG can cleave these amplicons to reduce the risk of cross-contamination. However, it may not eliminate the cross-contamination, and the reaction time will be extended due to the replacement [127]. These strategies collectively contribute to improving the reliability and accuracy of LAMP assays, particularly in environments where contamination risks are high.

2.3.6.3 Stability:

Another challenge is that the reagents are commonly temperature-sensitive and susceptible to freeze-thaw cycles, requiring storage at -20°C during transportation and storage [128,129]. Additionally, storage space is often limited in point-of-care or resource-limited settings [130]. Consequently, reagents typically need to be thermostabilized to extend their shelf life. Freeze-drying, or lyophilization, is a common method used to achieve thermostabilization [119,131–133].

If the testing occurs in PCR tubes, the freeze-drying process is relatively straightforward. LAMP reagents are formulated with protective agents and lyophilized in the freeze dryer with a certain program [119]. Approved test kits provided by Eiken Ltd. and Meridian Bioscience Ltd. are also supplied in this format.

In the context of in vitro diagnostic (IVD) devices, direct lyophilization of reagents onto the IVD chip can result in inefficient use of space in the freeze dryer and may damage the chip due to the low temperature and vacuum conditions. Moreover, most IVD chips are made of plastic to reduce costs, but the low thermal conductivity of plastic prolongs freeze-drying cycles and may decrease production efficiency. Consequently, reagents are typically freeze-dried in the form of beads (lyobeads/lyospheres) to facilitate easier handling and optimize the lyophilization process [134].

Compared to freeze-drying in PCR tubes, the process of manufacturing lyobeads is much more complex. The typical method involves dripping the formulated reagents, mixed with protective agents, into liquid nitrogen at the desired volume. The droplets float on the surface of the liquid nitrogen before immersing. Afterward, the lyobeads need to be collected and stored in liquid nitrogen during transportation. Before transferring into the freeze dryer, the freeze dryer must be precooled to prevent the collapse of the lyobeads. In this case, the IVD chip did not need to be in the freeze drying, which significantly increases the production effectiveness. Additionally, the formulation must not only maintain enzyme activity after storage but also ensure sufficient mechanical strength for handling and transportation [135].

Moreover, the formulations and freeze-drying recipes are typically patented, requiring each company to develop its own formulations. This results in high capital expenses, significant operational and maintenance costs, and a prolonged development phase, which collectively impose a substantial economic burden on companies [136].

2.4 Key challenges in LAMP

Consolidating all of the above, we can see that even though there have been numerous developments in nucleic acid amplification technologies, current methods still face several key limitations, particularly in the context of point-of-care diagnostics. The COVID-19 pandemic underscored the need for rapid, reliable, and scalable testing solutions that can be easily deployed in diverse clinical and resource-limited settings. While LAMP has demonstrated potential as a faster, simpler alternative to PCR, several challenges remain unaddressed, limiting its widespread clinical adoption. These challenges, which include the need for better quantitative capabilities, cold-chain dependency, multiplexing potential, and adaptability to a broad range of pathogens, form the basis of the research gap that this thesis seeks to address.

Firstly, although LAMP is known for its speed and simplicity, there is a limited set of reliable methods for quantifying pathogen load, a feature that is critical in clinical diagnostics for assessing the severity of infections. While qPCR provides quantitative data through CT-values, LAMP has traditionally been limited to qualitative or semi-quantitative results. Current LAMP assays also suffer from cold-chain dependency, which limits their use in remote and resource-limited settings where refrigeration is not readily available. The stability of enzymes and reagents in LAMP assays is a major barrier to scalability, particularly in low-resource environments. Existing freeze-drying formulations have issues or are patented, making their ubiquity for different diseases limited. Advancements or alternatives are needed for making LAMP assays more accessible and deployable in POC diagnostics, particularly in regions where cold-chain logistics are impractical.

There is a need for diagnostic platforms that can detect multiple pathogens simultaneously, especially in cases where symptoms overlap or multiple infections may occur concurrently. While multiplexing is well established in PCR, LAMP has yet to fully realize its multiplex potential. Having a test with the above traits needs an assay that has proven to be compatible with a variety of different pathogen primers as well as a compatible testing device.

Lastly, while colorimetric assays have made LAMP more user-friendly for POC diagnostics, they often rely on pH indicators, which can be affected by the sample's acidity or alkalinity, reducing the assay’s robustness. Addressing this limitation with a pH-independent colorimetric LAMP assay would allow diagnostics to be performed based on a colour change that is independent of sample pH, improving the assay’s compatibility with a broader range of clinical samples and enhances its potential for use in diverse diagnostic environments.

By addressing these critical gaps, this thesis aims to advance LAMP technology into a more robust, flexible, and scalable diagnostic tool that can meet the demands of both current and future infectious disease challenges.

Chapter 3 Expansion of OxLAMP for pathogen diagnostics: Primer design, optimisation and verification

3.1 Introduction

In this chapter, I describe the process of designing and optimizing primers for eight of the top ten bacterial pathogens most commonly seen in bloodstream infections (BSIs). The targeted pathogens—*Pseudomonas aeruginosa*, *Escherichia coli*, *Staphylococcus epidermidis*, *Staphylococcus aureus*, *Staphylococcus haemolyticus*, *Enterococcus faecium*, and *Enterococcus faecalis*—are among the most prevalent bacteria implicated in BSIs [137,138]. Bloodstream infections represent a significant clinical challenge, contributing to high rates of morbidity and mortality, particularly in critically ill or immunocompromised patients. Timely and accurate detection of these pathogens is crucial for guiding effective antimicrobial therapy, as delays in diagnosis can lead to the progression of sepsis, multi-organ failure, and increased mortality [139]. This highlights the urgent need for reliable, rapid diagnostic tools in clinical practice. The species targets were provided by a clinical collaborator of Professor Huang, based at a hospital in China, where these organisms represented some of the most commonly encountered pathogens in routine diagnostics. While the selection was not exhaustive or systematic, it allowed for an initial proof-of-concept of our diagnostic approach.

The primers designed for these pathogens were carefully developed to ensure both high sensitivity and specificity. Special attention was given to their genetic diversity and virulence factors, aiming to detect a broad spectrum of strains within each bacterial species. While some of the primers were optimized exclusively for qLAMP assays, others were made compatible with both qLAMP and colorimetric LAMP, thereby expanding their use across different

diagnostic platforms. The inclusion of colorimetric LAMP offers a significant advantage for point-of-care testing, particularly in resource-limited or decentralized settings where access to advanced instrumentation may not be available. This capacity for visual readout simplifies the testing process, making it feasible to implement rapid diagnostics in a variety of healthcare environments.

In addition to these bacterial primers, this work also builds upon the SARS-CoV-2 primers described in Chapter 3 and the HSV primers detailed in Chapter 6, further expanding the diagnostic capabilities of the LAMP platform. The integration of these viral primers alongside the bacterial primers establishes a versatile multiplex testing platform capable of identifying a wide range of infectious agents. This combined approach enhances the platform's utility for diagnosing bloodstream infections, respiratory illnesses, and viral infections, providing a comprehensive diagnostic tool for clinical use. This expansion not only increases diagnostic versatility but also enables more rapid and targeted treatment interventions, improving patient outcomes in various healthcare settings.

3.2 Materials and Methods

3.2.1 Primer design

All forward (F3), backward (B3), forward-inner (FIP), and backward-inner (BIP) primers were designed using the Primer Explorer software (https://primerexplorer.jp/e/) with a detailed set of selection criteria to ensure optimal performance in the LAMP assays. The length of each primer was carefully controlled, with a minimum threshold of 16 base pairs to ensure adequate binding to the target sequence. F3 and B3 primers were restricted to a maximum length of 30 base pairs, as longer primers can lead to inefficient binding and amplification during the LAMP

process, potentially reducing assay sensitivity. Striking this balance in primer length is critical to achieving both specificity and amplification efficiency.

A key factor in primer design is the Guanine (G) and Cytosine (C) content, which was set between 40-60% for all primers. This range was chosen to produce a sufficiently high melting temperature (Tm) to allow stable hybridization with the target DNA, without creating overly complex secondary structures or making synthesis more difficult. The GC content also impacts primer stability during the amplification process, particularly in high-sensitivity techniques like LAMP, where precise binding to the target is crucial.

To further enhance primer stability, I selected primers with a Gibbs free energy (ΔG) of less than -4 kcal/mol for both the 5' and 3' ends. This selection helps ensure that the primers will form strong, stable bonds with the template DNA at the critical initiation and termination points of the reaction. However, in cases where achieving this ΔG threshold for the 5’ and 3’ ends was not feasible due to the sequence constraints of certain pathogens, I focused instead on ensuring that the F2/B2 and F1C/B1C regions, which are essential for LAMP amplification, had a ΔG of less than -4 kcal/mol. These regions play a particularly important role in the strand displacement mechanism of LAMP, and their stability is vital for maintaining the integrity of the amplification process.

Once primers were generated based on these criteria, I performed additional specificity checks using Primer BLAST (https://www.ncbi.nlm.nih.gov/tools/primer-blast/) to ensure that the selected primers did not have significant homology with non-target sequences. This was done by running the F3/B3 and F2/B2 sequences against both the NR and RefSeq Representative genome databases, focusing on human, bacterial, and viral organisms. This step was essential to reduce the likelihood of off-target amplification, which could lead to false positives,particularly if the primers matched human genes or common environmental

microorganisms. Ensuring the specificity of each primer set was critical for the overall reliability and accuracy of the diagnostic platform.

Following the specificity validation, I returned to Primer Explorer to generate loop primers (LF/LB) for each primer set. Loop primers enhance the speed and efficiency of the LAMP reaction by accelerating the amplification process. However, in several cases, the software was unable to generate loop primers automatically, requiring me to design these primers manually. These manually designed primers were done by targeting a sequence between the F2/B2 and F1C/B1C regions, ensuring it is between 18-24 base pairs in length and has appropriate GC content. These manually designed loop primers are noted accordingly in the following section. For all generated loop primers, I applied the ΔG threshold of less than -4 kcal/mol to the 5' and 3' regions, ensuring their stability during amplification.

Once the complete primer sets, including loop primers, were finalized, they were ordered from Integrated DNA Technologies (IDT) for synthesis.

Table 3.1 ***Primer sequences for pathogen targets.***

This table presents the designed LAMP primers for the detection of common sepsis-causing bacteria, HSV and Sars-Cov-2 viruses. Primers are categorized by target pathogen, with forward (F3), backward (B3), forward-inner (FIP), backward-inner (BIP), and loop primers (LF/LB) listed for each pathogen. Some primer sets were designed to function specifically for qLAMP, while others are compatible with both qLAMP and colorimetric LAMP assays. Loop primers that were manually designed due to limitations in Primer Explorer's automatic generation are noted accordingly.

Table 3.1A

Pseudomonas aeruginosa	**5' -3'**
Target Sequence	NC_002516.2:5313676-5315340, 1665bp
FIP	CTCAGCCGTGCTTCCTCGGC-
BIP	ATCAATGCCTCCGAGCGCC-
F3	GGCTGTTCCTCGACTTCTC
B3	GTGGACTTCCGGCATCAC
LF	TCACCAGCAGGTCGATGG
LB	GGTACTGCATACCGCGCTGC

Table 3.1B

Escherichia coli	**5' -3'**
Target Sequence	NC_000913.3:1923719-1924591, 872bp
FIP	AGCGGCGTGCTTAATGCATTGT-
BIP	CAGTACGCCGATCACCGCAA-
F3	ATCACCAGGATGGCTTTGAG
B3	GCTCTGGTGTATGCAACTCA
LF	GGATTTCCCCCCACGCTTA
LB	AATGCCCGCACCAGGAAAA

Table 3.1C

Staphylococcus epidermidis	**5' -3'**
Target Sequence	NZ_CP035288.1:562934-564190; 1257bp
FIP	AAGCAGGTATTTGGTGGCCC-
BIP	ATACAGGTGAAGTCTTTGTTGGTG-
F3	AAAATACATTCAATCGCTGGA
B3	GCCAAAGTGCACTTGAGAA
LF (Manually designed)	CACCATAGTTGACGCG
LB	CACCTGAAGACATCGAGAATTGGAT

Table 3.1D

Staphylococcus aureus	**5' -3'**
Target Sequence	NC_007795.1:738977-740101, 1125bp
FIP	TCGTTCAACAATTGGTTTTTTACCT-
BIP	ACATGCATTAGATAACGACGCA-
F3	GCAGATATGAATGAAGTTGAAGG
B3	AATGCTTGTAACATACCTGC
LF	TCCCCTCGATAACGGTCATC
LB (Manually designed)	CATGTTGTAATTTCA

Table 3.1E

Staphylococcus haemolyticus	**NZ_CP013911.1:705132-706499, 1368bp**
FIP	TCCCACTCACGAAAGATCAATTG- GCGTCTTCATTTTTCGGC

BIP	TTGGTACACCCGGATATAGAAAAGC-TGGCTAGAAAATTGAAATCCTC
F3	AGATCGCTTCTATTTTCGCT
B3	ACGCCATTCATCATCAGAT
LF	TTTTTGAATCTTTGAACAGCATGAT
LB (Manually designed)	CATTTGAAAGTCATAG

Table 3.1F

Enterococcus faecium	**5' -3'**
Target Sequence	NZ_CP038996.1:1523346-1524320, 975bp
FIP	CTTCCAGTTTTTTGGCGAGCAA-
BIP	GGTATAGCCATTCTTTTCCGTTTTT-
F3	TACAATCCGGCTCCTAACC
B3	GCGACTGTACATTAGGTGTC
LF (Manually designed)	CTCTGTCATTATCGGTC
LB	CAGTCCGCCTCTTGTATAAGAAAAA

Table 3.1G

Enterococcus faecalis	**5' -3'**
Target Sequence	NZ_KB944666.1:12797-15067, 1951bp
FIP	CTTCGTTGGAAGACTTTACGGAAG-
BIP	TGGTAATTCCTAAACCGTAATTCGT-
F3	CCGATATTCTGTTCCAGGTAA
B3	TTTATTGAGGCACAAGAAGC

LF	GTTACGGATTGCTTTTAAAGAGGAC
LB	TGATTTTGGTTTCACGACAAACGC

Table 3.1H

Herpes Simplex Virus	**5’ -3’**
FIP	CTTCGTTGGAAGACTTTACGGAAG-
BIP	TGGTAATTCCTAAACCGTAATTCGT-
F3	CCGATATTCTGTTCCAGGTAA
B3	TTTATTGAGGCACAAGAAGC
LF	GTTACGGATTGCTTTTAAAGAGGAC
LB	TGATTTTGGTTTCACGACAAACGC

Table 3.1I

Sars-Cov-2 (O117 gene)	**5’-3’**
FIP	GGTTTTCAAGCCAGATTCATTATGGA
BIP	TCTTCGTAAGGGTGGTCGCAGCACA
F3	CCCCAAAATGCTGTTGTT
B3	TAGCACGTGGAACCCAAT
LF	TCGGCAAGACTATGCTCAGG
LB	TTGCCTTTGGAGGCTGTGT

Table 3.1J

Sars-Cov-2 (N1 gene)	**5’-3’**

FIP	CCACTGCGTTCTCCATTCTGGTAAAT
BIP	CGCGATCAAAACAACGTCGGCCCTT
F3	TGGACCCCAAAATCAGCG
B3	GCCTTGTCCTCGAGGGAAT
LF	TGAATCTGAGGGTCCACCAAA
LB	GGTTTACCCAATAATACTGCGTCTT

3.2.2 LAMP assay prep and reaction run conditions

All equipment, including the laminar-flow cabinet, pipettes, and working bench, was wiped with PCR clean (15-2001, Cambio) and 70% ethanol (Thermo-Fisher). For each qLAMP reaction, 12.5 μL of LAMP 2X WarmStart master mix (M1800, New England BioLabs), containing Bst 2.0 polymerase and reverse transcriptase, was mixed with 2.5 μL of 10X primer mix in each well of 96-well PCR plates (Bio-Rad). Primer sets of each respective pathogen were used for their reactions. 5 μL of SYTO 9 fluorescent dye (S34854, ThermoFisher) in the concentration of 2.5 μM was added for fluorescent reading while 5 μl RNase/DNase-free water was added for colorimetric reading. 5 μL RNA or DNA template in different concentrations was added as a positive control, while RNase/DNase-free water was used as a negative control. Each test was repeated in triplicate.

For the LAMP reaction, qPCR machines (Lepgen-96, Lepu & CFX-96, Bio-Rad) were applied for fluorescence acquisition, while using the thermostatic photometer (Sinopharm) for colorimetric reading, details of which can be seen in Chapter 6.

After placing the PCR plate into the qPCR machine, the PCR cycle conditions were set to 20 seconds at 65 °C for 90 cycles with fluorescence acquisition. The LAMP TT values were given by qPCR machines based on Cq Values. Temperature optimisation experiments utilised the

temperature gradient function of qPCR machines, whereby different rows heated reaction wells with different temperatures, ranging from 60 °C to 70 °C.

3.2.3 Direct detection of bacterial pathogens using colony samples

In this study, bacterial colonies were isolated and prepared for direct testing using qLAMP. The number of bacteria in each colony sample was estimated through cell counting under microscopy. After the colonies had grown, bacterial cells were transferred into tubes containing water for storage and further analysis. To validate the specificity and performance of the designed qLAMP primers, the original bacterial samples were first diluted with water by a factor of ten, ensuring that the primers could detect the pathogens effectively. Therefore, the initial experiments included a high concentration of around 4 million cells per reaction for qLAMP tests.

Following the confirmation of these initial results, a more comprehensive limit of detection (LOD) test was performed. The bacterial cell concentrations used in this test ranged from 2 million cells per reaction to 200 cells per reaction, allowing for the determination of the assay's sensitivity across a broad spectrum of bacterial loads. This thorough evaluation was essential for verifying the robustness of the designed primers for the detection of bacterial pathogens directly from colony samples.

3.2.4 Detection of E.coli and S.haemolyticus using synthetic gBlock DNA

Due to limited access to bacterial colonies for Escherichia coli and Staphylococcus haemolyticus, synthetic gBlock DNA was sourced from IDT for testing. These synthetic DNA fragments offer a purified form of nucleic acid, which differs significantly from actual bacterial colonies due to the absence of extraneous cellular components. While this may lead to slightly improved performance in amplification assays, the gBlock DNA still serves as an effective means to validate the efficacy of the designed LAMP primers.

Synthetic DNA is less representative of clinical samples, but it provides a useful benchmark for evaluating primer performance. Serial dilutions of the gBlock DNA were prepared, with concentrations ranging from 5 pg to 500 pg per reaction. Each concentration was tested in triplicate to ensure the reliability of the results.

3.2.5 Colorimetric LAMP experiments

All colorimetric LAMP reactions conducted to validate the primers utilized the pH-independent LAMP assay reagents and concentrations outlined in Chapter 6. For these experiments, the optimized reaction conditions for *E. faecalis* and *S. epidermidis* primers were used, as these bacterial targets showed the best performance in the qLAMP assays. The goal of these tests was to evaluate whether colorimetric LAMP could be used effectively for these bacterial targets, starting with high concentrations and progressively moving to lower concentrations to determine the analytical sensitivity.

Initial high-concentration tests were run with 200,000 cells per reaction and 1 million cells per reaction for both *E. faecalis* and *S. epidermidis*, with the reactions running for 30 minutes. The results indicated clear colour changes, confirming that the colorimetric LAMP system could successfully detect these pathogens at high concentrations. Following this, a spectrum of lower concentrations (ranging from 40,000 cells per reaction to 400,000 cells per reaction) was tested

for *S. epidermidis* and *E. faecalis* with a reaction time of 30 minutes. This was followed by a separate test for *S. epidermidis*, where the reaction time was extended to 60 minutes to compare the effects of a longer reaction on sensitivity.

In parallel, synthetic gBlock DNA for *E. coli* and *S. haemolyticus* was tested using colorimetric LAMP. These tests used a series of lower concentrations than those used in the qLAMP experiments to evaluate whether colorimetric LAMP could effectively detect the DNA in this format. Serial dilutions were prepared, and each reaction was run in triplicate.

3.3 Results

3.3.1 qLAMP results for direct detection of bacterial pathogens using colony samples

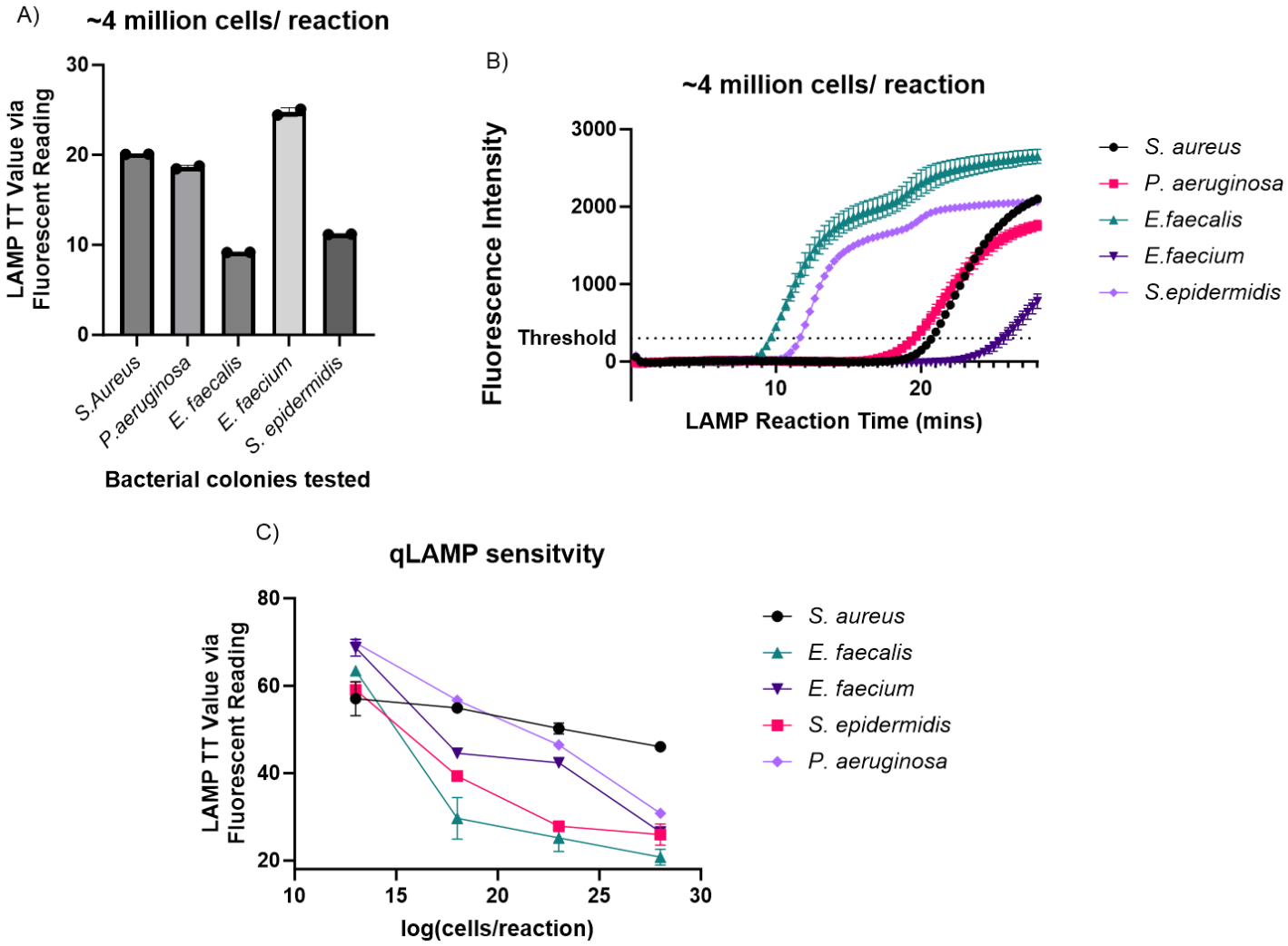

Figure 3.1 qLAMP results and sensitivity comparison between bacteria samples obtained from the cell colony. A) A bar chart shows the qLAMP results of all five bacterial pathogens at a set concentration of around 4 million cells. B) LAMP amplification curves were based on the fluorescent intensity in 30 minutes with different bacterial samples at a 4 million cells/reaction concentration. C) The line graph shows the qLAMP results of the five bacteria samples with varying concentrations ranging from around 2000 cells per reaction (~log13) to

2 million cells (~log18). Negative controls reveal no false positives in testing. TT-Value thresholds were set to be consistent with those detailed in the qLAMP experiments of Chapter 4, which were defined using Bio-Rad CFX software. All results for B and C are presented as MEAN ± SD.

The results from Figure 3.1 show that the qLAMP primers designed for all five bacterial targets were able to amplify the respective DNA successfully. Image A displays the amplification efficiency for each bacterial pathogen at a concentration of 4 million cells per reaction. Notably, *S. epidermidis* and *E. faecalis* outperformed the other bacteria, achieving fluorescence threshold times (TT values) in approximately 10 minutes, less than half the time taken by the other bacterial strains. This highlights the enhanced performance of these two bacterial targets in qLAMP assays.

Following the confirmation of primer functionality, the next step was to determine the LOD for qLAMP in detecting these bacterial pathogens. Figure 3.1b illustrates that the assay could detect concentrations as low as 2000 cells per reaction, indicating a high degree of sensitivity. However, at this low concentration, the time to reach the fluorescence threshold (TT value) increased to approximately one hour. Negative controls for all five bacterial targets showed no amplification, confirming the high specificity of the qLAMP assay.

Furthermore, as observed in Figure 3.1b, both *E. faecalis* and *S. epidermidis* demonstrated a significant improvement in performance as bacterial concentrations increased. For *E. faecalis*, the TT value was reduced by half when the concentration increased to ~log13 (20,000 cells per reaction), with a similar trend observed for *S. epidermidis*. These two bacterial targets consistently showed superior performance compared to the other pathogens across all concentration ranges tested, indicating their potential for use in rapid diagnostic applications.

3.3.2 qLAMP results for E.coli and S.haemolyticus using synthetic gBlock DNA

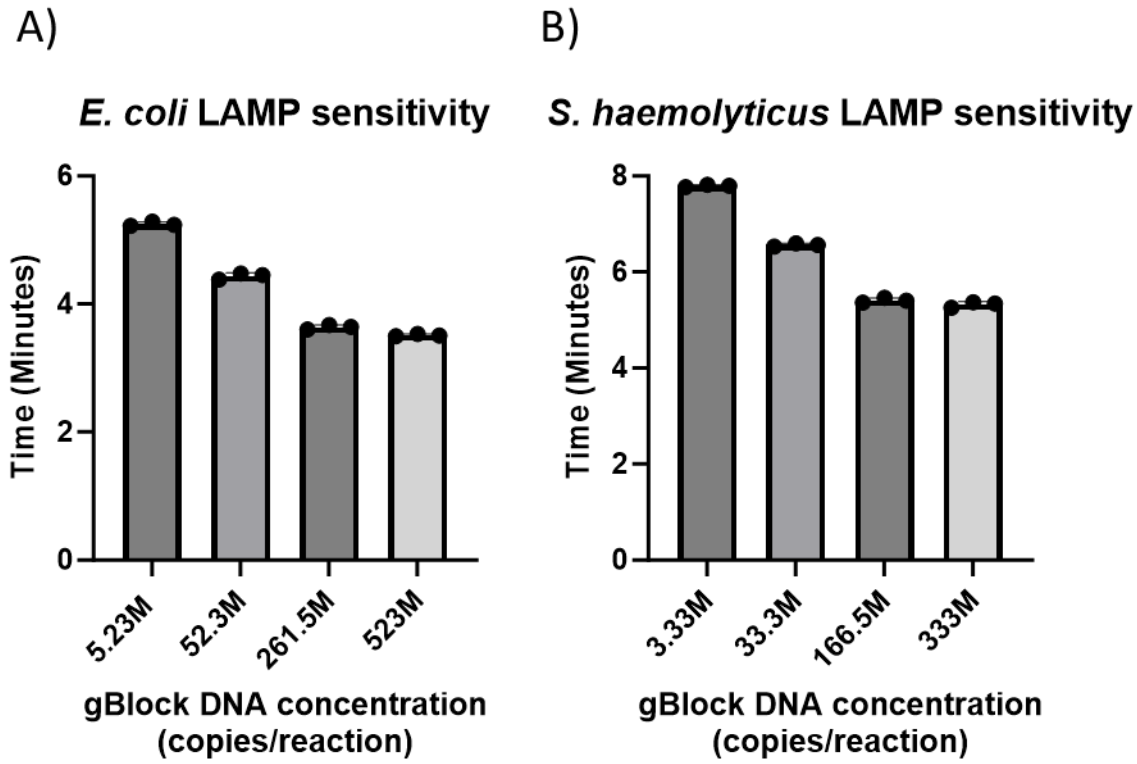

Figure 3.1 ***qLAMP results of E.coli and S.haemolyticus gDNA****. A) qLAMP sensitivity test of E.coli gDNA with concentrations ranging from 5.23 million to 523 million copies per reaction. Concentrations were tested in triplicate. B) qLAMP sensitivity test of S.haemolyticus gDNA with concentrations ranging from 3.33 million to 333 million copies per reaction. Each concentration was tested in triplicate. Results presented as MEAN + SD.*

The two bacterial targets were initially tested across the same mass-based concentration range, from 5 pg to 500 pg in 10-fold increments. To standardise reporting across experiments, these mass values were subsequently converted into DNA copy numbers using the formula: Copies = (mass (ng) ×6.022×10^23)/(length (bp)×660×10^9). Experiment results from Figure 3.2 prove that our qLAMP tests could detect E.coli and S.haemolyticus and at concentrations of 5

pg and lower, since 5 pg for both pathogens was able to be amplified at an astoundingly fast rate of less than 6 minutes.. A limit of detection (LOD) test for lower concentrations of both is done via colorimetric LAMP, which is detailed further below in Figure 3.4.

3.3.3 LAMP temperature optimisation for bacteria primers

Given the superior performance of *E. faecalis* and *S. epidermidis* in the earlier qLAMP experiments, these two bacterial targets were selected for temperature optimization. The goal was to determine the optimal temperature for running qLAMP reactions, as temperature plays a critical role in maintaining primer efficiency and ensuring rapid, accurate amplification.

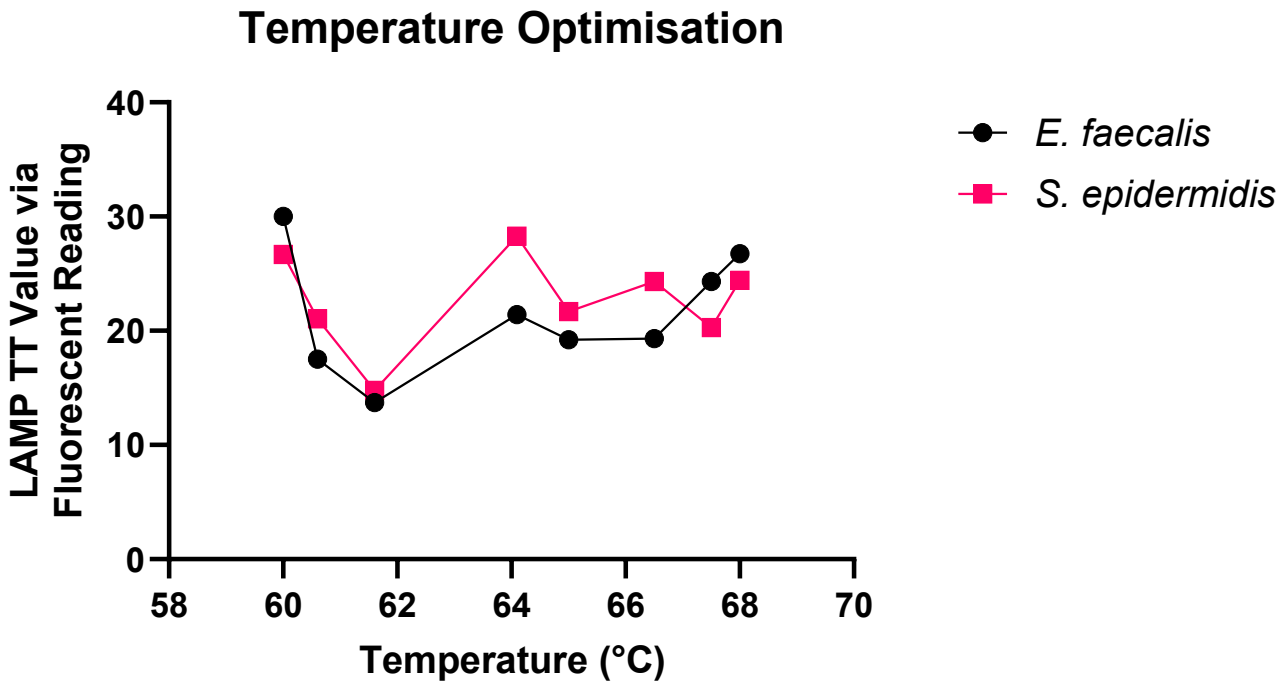

Figure 3.2 ***Temperature optimisation experiment for E.faecalis and S.epidermids qLAMP****. A temperature spectrum of eight different temperatures, 68, 67.5, 66.5, 65, 64.1, 61.6, 60.6, and 60 °C was set on a Bio-Rad qPCR machine, and eight qLAMP assays were prepared with 8k*

cells/ µL in each well for both E.faecalis and S. epidermidis. The LAMP reaction was run for 40 minutes.

The results showed that the optimal temperature for both *E. faecalis* and *S. epidermidis* was 61.6°C, where the lowest TT values, around 15 minutes, were achieved. At this temperature, the primers functioned most efficiently, producing the fastest amplification. Temperatures above 61.6°C resulted in reduced primer efficiency, leading to longer TT values and slower amplification. Similarly, at temperatures below 61.6°C, the overall efficiency of the reaction decreased, again leading to higher TT values. This experiment was conducted with only a single repeat per condition, so the results should be viewed as a rough indication of optimal temperature rather than a definitive conclusion. The same temperature range was tested for both bacteria to explore whether a single temperature could be broadly suitable across different pathogens. This approach was intended to inform future multiplex testing, where a shared reaction condition would be beneficial. It is worth noting that 61.6 °C happened to be the optimal temperature for both *E. faecalis* and *S. epidermidis*, suggesting potential for a unified protocol across the bacterial panel, though further validation is needed.

3.3.4 Colorimetric LAMP results

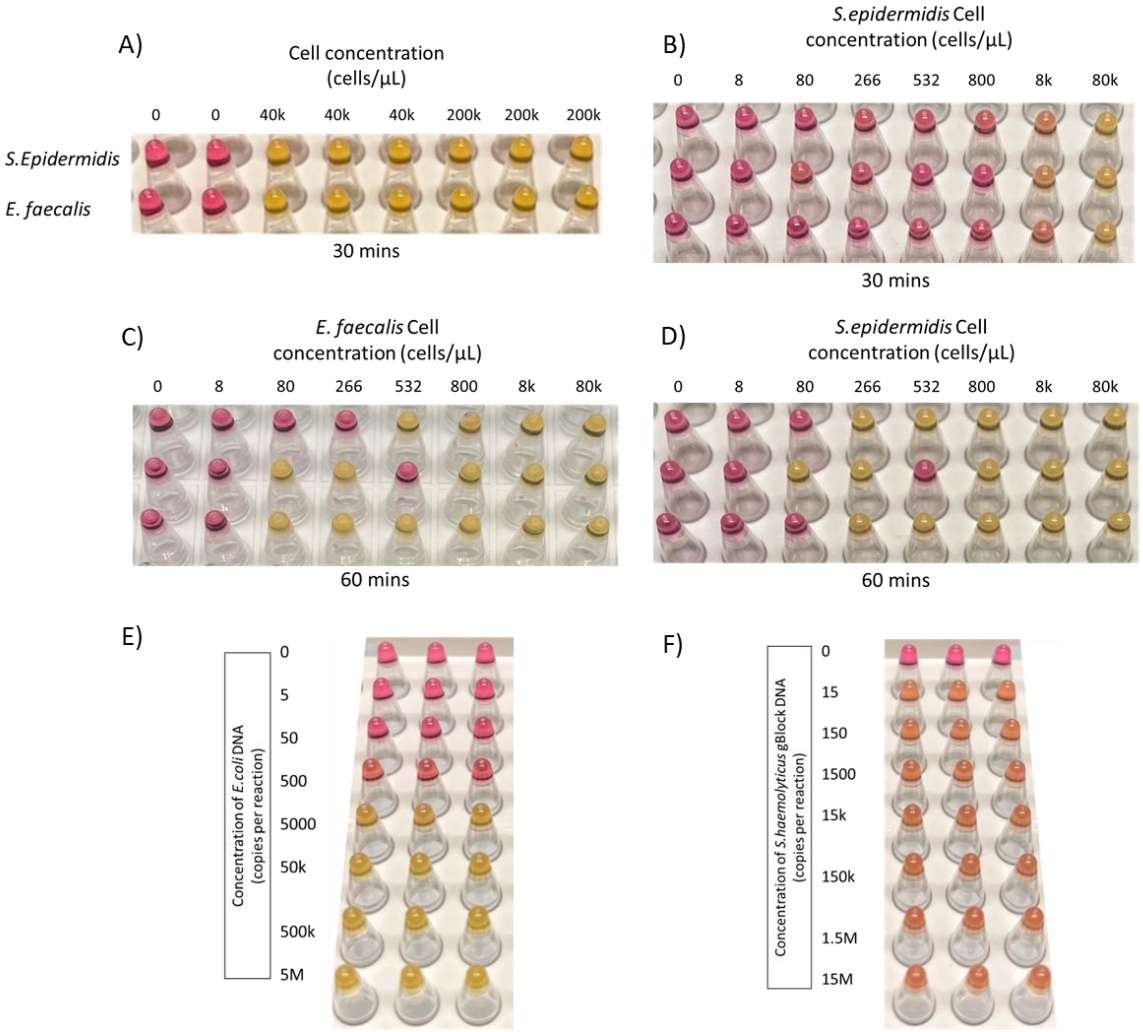

Figure 3.3 ***Colorimetric LAMP Results for Bacterial Primers****. All reactions were performed in triplicate, with negative controls included for each test. A) High-concentration colorimetric LAMP reactions for S. epidermidis and E. faecalis, with duplicate negative controls and triplicates for both 200,000 cells per reaction and 1 million cells per reaction. Reaction time: 30 minutes. B) Analytical sensitivity test for S. epidermidis, using cell concentrations ranging from 40,000 to 400,000 cells per reaction. Reaction time: 30 minutes. C) Analytical sensitivity test for E. faecalis, using cell concentrations ranging from 40,000 to 400,000 cells per reaction. Reaction time: 30 minutes. D) Repeat of the analytical sensitivity test for S. epidermidis, but with a reaction time of 60 minutes. E) Analytical sensitivity test for E. coli. Concentrations tested ranged from 5 to 5 million copies per reaction. F) Analytical sensitivity test for S.haemolyticus. Concentrations tested ranged from 15 to 15 million copies/reaction*

The results from Figure 3.4 indicate that colorimetric LAMP is a viable method for detecting *E. faecalis*, *S. epidermidis*, *E. coli*, and *S. haemolyticus*, though performance varied across the bacterial targets and conditions. Figure 3.4a shows the results of high-concentration colorimetric LAMP tests for *S. epidermidis* and *E. faecalis*, with clear positive results indicated by a colour change to bright yellow. This demonstrates that the system works effectively at high cell concentrations with a 30-minute reaction time. In Figure 3.4b, the analytical sensitivity test for *S. epidermidis* at lower concentrations shows that while a 30-minute reaction time can detect the bacteria, the colour change is not as strong, and a minimum concentration of 40,000 cells per reaction is required for a clear result. When the reaction time was extended to 60 minutes (as shown in Figure 3.4d), the test sensitivity improved significantly, with detection at concentrations as low as 1250 cells per reaction. For *E. faecalis*, the results in Figure 3.4c demonstrate that at 400 cells per reaction, two out of three reactions showed detectable colour changes after 60 minutes of reaction time. This highlights the importance of reaction time in improving the sensitivity of colorimetric LAMP.

The analytical sensitivity test for *E. coli* and *S. haemolyticus* (shown in Figure 3.4e) revealed promising results, with detection occurring at 5000 copies and 15 copies per reaction DNA concentrations, respectively. The two bacterial targets were initially tested across the same mass-based concentration range, from 5 ag to 5 pg in 10-fold increments, to enable a uniform sensitivity comparison. To standardise reporting across experiments, these mass values were subsequently converted into DNA copy numbers using the formula: Copies = (mass (ng) ×6.022×10^23)/(length (bp)×660×10^9). The colour change for *E. coli* was strong and consistent, producing a bright yellow result, while *S. haemolyticus* produced a slightly less clear colour change, shifting to orange rather than bright yellow. This variation in colour change could be attributed to differences in the DNA structure or primer efficiency, as both assays were run under the same conditions.

3.4 Discussion

In summary, the primers designed for all seven bacterial targets were successfully validated through qLAMP, though with varying degrees of performance. Among the targets, *E. faecalis* and *S. epidermidis* significantly outperformed the others, particularly in terms of amplification speed, making them prime candidates for further optimization and application in OxLAMP, a pH-independent colorimetric LAMP system with qLAMP capabilities. The robustness of the LAMP tests was further demonstrated by the fact that qLAMP successfully amplified bacterial DNA directly from colonies, without requiring any DNA extraction or purification steps, which simplifies the diagnostic process in clinical settings.

Although *E. coli* and *S. haemolyticus* were not tested using bacterial colonies, the strong performance of their gBlock DNA in qLAMP suggests that they could also be suitable candidates for future diagnostic applications. Additionally, both targets were successfully

detected via colorimetric LAMP, though the results for *S. haemolyticus* were less clear due to the orange colour change. This variation highlights one of the key challenges in using colorimetric LAMP: the subjectivity involved in interpreting colour results, which could affect diagnostic accuracy in real-world applications.

Moving forward, further optimization experiments, such as LAMP reaction temperature optimization, should be conducted on the remaining bacterial targets to improve their performance in colorimetric LAMP. Following these optimizations, a more detailed limit of detection (LOD) test for each bacterial target would provide valuable data on the assay's sensitivity across a range of concentrations. Importantly, it is encouraging that many of the pathogen-specific primers have been shown to be compatible with our LAMP formulation. This flexibility in accommodating new primers is a significant advantage, allowing for the rapid expansion of the assay to target emerging or additional pathogens. Ideally, future studies would also include testing of actual clinical samples, as was done for SARS-CoV-2 in Chapter 3 and HSV in Chapter 6, to validate the real-world applicability of the LAMP assays.

Chapter 4 Development of a quantitative loop-mediated isothermal amplification (qLAMP) for the detection of SARS-CoV-2 and human genes

The content of this chapter has been published in *Microbial Biotechnology* as follows.

A quantitative RT-qLAMP for the detection of SARS-CoV-2 and human gene in clinical application. Yu, Y., Zhou, J.X.Y., Li, B., Ji, M., Wang, Y., Carnaby, E., Andersson, M.I., Huang, W.E., Cui, Z., 2022. A quantitative RT-qLAMP for the detection of SARS-CoV-2 and human gene in clinical application. Microb Biotechnol 15, 2619–2630. https://doi.org/10.1111/1751-7915.14112

My contribution includes the analysis of SARS-CoV-2 clinical samples, ensuring the robustness and reliability of the assays for real-world applications. I prepared and analyzed synthetic Twist RNA samples for all major COVID-19 variants using qLAMP, alongside human gene (ACTB) samples, which I evaluated with both qLAMP and qPCR methodologies. Additionally, I conducted RNA extraction from clinical samples and performed qPCR analysis for all synthetic RNA samples, ensuring comprehensive data coverage.

A key aspect of my contribution was integrating qLAMP TT-value data with qPCR CT-value data to establish correlations and enhance assay utility. Beyond experimental work, I also contributed to the writing and editing of the manuscript, ensuring clarity and precision in the presentation of our findings.

4.1 Introduction

The SARS-CoV-2 virus has infected over 700 million individuals around the world. [4]. The SARS-CoV-2 pandemic has had a significant impact on the whole of human society. [5,13,140,141], including through its adverse impact on the economies of many countries [142–146]. To control the spread of the virus, identifying asymptomatic carriers and infected individuals at an early stage, even before symptoms begin, is of utmost importance. [147,148]. Early diagnosis and rapid isolation of infected individuals and monitoring their contacts could prevent further transmission and assist governments in implementing effective public health measures. [147,149,150]. A Nucleic Acid Amplification Test (NAAT) based on reverse transcription real-time quantitative polymerase chain reaction (RT-qPCR) was promptly developed to detect the viral RNA of SARS-CoV-2 once the genetic sequence was published. [149]. Although RT-qPCR assays are characterised by high sensitivity and specificity, they require a long reaction time (around 2 hours), high-purity samples, sophisticated instruments for thermal cycling, and highly trained personnel. [151,152], limiting its application as a point-of-care test.

A Reverse Transcription Loop-mediated Isothermal Amplification (RT-LAMP) assay was developed to detect SARS-CoV-2 [27,153] . The RT-LAMP only needs a single temperature, for this assay, 65 °C, to detect the virus. In the RT-LAMP assay, a temperature-dependent 'molecular switch' was designed to prevent false positives caused by self- and off-target amplifications. [119]. This LAMP assay has been validated by 198 clinical samples and demonstrated the overall sensitivity of 90.2% (95% CI 83.8 – 94.7%) and specificity of 92.4% (95% CI 83.2 – 97.5%) [119].

However, the LAMP assay result can only indicate whether the tested individual has been infected or not. Unlike RT-qPCR, the result is presented as a cycle threshold (Ct) value, which

is correlated with the viral load of the sample [154,155]. The lower Ct values reflect a higher viral load. The individuals with Ct values less than 25 were independently associated with mortality in 875 clinical samples [156]. By contrast, samples with Ct values above 33-34 were regarded as non-infectious, as epidemiological data showed a low risk of transmission [157]. Therefore, the Ct values could be used as a parameter to identify patients at high risk for severe outcomes and may benefit the physician in making decisions on clinical treatment and patient management [156,158]. However, the previous RT-LAMP assay does not indicate the viral load, which might lead to ineffective treatment or unnecessary quarantine. Hence, it is described here the use of quantitative LAMP, termed as 'qLAMP' to achieve an evaluation of viral load.

In this work, the real-time amplification curve over the LAMP reaction was acquired by fluorescent and colorimetric signals. The time that is taken to reach the threshold was defined as the LAMP TT value, which has a linear relationship to the concentration of SARS-CoV-2. This quantitative LAMP (qLAMP) assay with viral primers was evaluated with synthetic full-length SARS-CoV-2 RNA, alongside its variants, inactivated viral particles, and clinical samples. Meanwhile, the qLAMP assay was extended to use a novel human primer set to quantify human genes in the samples.

4.2 Materials and methods

4.2.1 Primer Design and DNA Synthesis for RT-LAMP

Viral primer sets, QO117, N1, and N15 primer sets, were designed as previously described in Huang et al [27,119]. Each primer was synthesised by Integrated DNA Technologies (IDT, UK). The 10X N1 and N15 primer mix were prepared with RNase/DNase-free water (11538646,

Invitrogen) in the concentration of 16μM for FIP and BIP, 2 μM for F3 and B3, and 4 μM for LB and LF. The additional 24 µCμM switch was added for QO117 primers [119].

A set of ACTB-n primers, including loop primers, was designed to target the human ACTB gene. Primers were designed using LAMP primer designing software, PrimerExplorer (http://primerexplorer.jp/e/) [40]. The 10X ACTB primer mix was prepared with RNase/DNase-free water at a concentration of 16 μM for FIP and BIP, 2 μM for F3 and B3, and 4 μM For LB and LF. The sequences of each primer of ACTB-n are listed in Table 4.1.

Table 4.1 Gene Sequence of ACTB-n primers

ACTB-n	**Sequence 5'-3'**
F3	GGCATCCTCACCCTGAAGT
B3	AGGCCAGGAAGGAGGGAG
FIP	TCCTCGGGAGCCACACGCA-GCATCGTCACCAACTGGGAC
BIP	TGACCGAGGCCCCCCTGAA-CCACCAGAAGAGGTAGCGG
LF	GGTGCCAGATTTTCTCCATGT
LB	CGAGAAGATGACCCAGGTGAGTG

4.2.2 qLAMP Assay with SARS-CoV-2 RNA

All equipment, including the laminar-flow cabinet, pipettes, and working bench, was wiped with PCR clean (15-2001, Cambio) and 70% ethanol (Thermo-Fisher). For each RT-LAMP reaction, 12.5 μL Of LAMP 2X WarmStart master mix (M1800, New England BioLabs), containing Bst 2.0 polymerase and reverse transcriptase, was mixed with 2.5 μL of 10X primer mix in each well of 96-well PCR plates (Bio-Rad). A viral QO117 primer set was used if there was no specific indication. 5 μL of SYTO 9 fluorescent dye (S34854, ThermoFisher) in the concentration of 2.5 μM was added for fluorescent reading while 5 μl RNase/DNase-free water was added for colorimetric reading. 5 μL RNA or DNA template in different concentrations was added as a positive control, while RNase/DNase-free water was used as a negative control. Each test was repeated in triplicate.

The full-length RNA of all SARS-CoV-2 variants (Twist Bioscience) was serially diluted six-fold with RNase/DNase-free water. 5 μL of each concentration of RNA was mixed with the above reagents.

4.2.3 Fluorescent Reading and Colorimetric Reading

For RT-LAMP reaction, qPCR machines (Lepgen-96, Lepu & CFX-96, Bio-Rad) were applied for fluorescence acquisition while using the thermostatic photometer (Sinopharm) for colorimetric reading, details of which can be seen in Chapter 6.

After placing the PCR plate into the qPCR machine, the PCR cycle conditions were set to 20 seconds at 65 °C for 90 cycles with fluorescence acquisition. The LAMP TT values were given by qPCR machines based on Cq Values. The threshold for determining time-to-threshold (TT) values in the qLAMP assays was defined using Bio-Rad CFX software, following the same

approach typically used for qPCR Ct analysis. The software automatically sets a fluorescence threshold based on the baseline signal and amplification kinetics, identifying the point at which the fluorescence signal exceeds background levels with consistent exponential growth.

For colorimetric reading, the image of the samples was taken every 20 seconds by a thermostatic photometer (Sinopharm). The colour in the image was digitised based on RBG. The average of the first five readings was set to the initial average value. When the colour index, the difference between the real-time data and the initial average value was greater than 2, this time point was set to the LAMP TT values by colorimetric reading.

4.2.4 qPCR Assay and Digital PCR Assay

GoTaq Probe one-step RT-qPCR kit (A6121, Promega) was used with 1.5 μL primer mix to assess the Ct values of the samples. CDC N1 primer set (1006770, IDT) was used for SARS-CoV-2 detection, while CDC RNase P primer set was used for human gene detection. Both primer sets contain 100 μM forward and backward primers. After adding 5 μL of the eluted solution, the final reaction volume was increased to 20 μL by adding RNase/DNase-free water.

The PCR cycle conditions were set according to the manufacturer's instructions. The solutions were reverse transcribed for 15 minutes at 45 °C and initial denaturation for 2 minutes at 95 °C. Then, 45 cycles of 3 seconds at 95°C and 30 seconds at 55 °C were processed.

Digital PCR assay (QX200 Droplet Digital PCR System, Bio-Rad) was used to acquire the template copy number in the samples. The whole procedure was performed using the manufacturer's protocol. Briefly, 20 μL of the sample (RNA solution or CDC standard positive control plasmid) was mixed with 70 μL DG oil (Bio-Rad) and placed into a droplet generator.

After conducting PCR on a thermal cycler, droplets were analysed by QX200 Droplet Reader. Meanwhile, the sample was run qPCR assay simultaneously to obtain the Ct values.

4.2.5 qLAMP Assay with Viral Particles

An inactivated SARS-CoV-2 vaccine candidate, BBIBP-CorV [159], was used for spiking. BBIBP-CorV, also known as the Sinopharm COVID-19 vaccine, is an inactivated SARS-CoV-2 vaccine developed by the Beijing Institute of Biological Products. It contains chemically inactivated whole virus particles and was one of the first vaccines approved for emergency use in multiple countries. The viral particle was serially diluted with RNase/DNase-free water five-fold and split into 3 sets, which were measured directly, after heat inactivation and after RNA extraction.

For the first set, 5 μL of each concentration was added to each well of the PCR plate containing 12.5 μL of master mix, 2.5 μL of 10X primer mix, and 5 μL of SYTO 9 fluorescent dye at a concentration of 2.5 μM. The RT-LAMP reaction was run on the qPCR machine at 65 °C for 30 minutes, and the FAM channel was read every 20 seconds.

The second set went through heat inactivation on a Dry Bath incubator (MVS-200, Scottech Medical co.), set to 95 °C. After heating for 5 minutes and cooling back to room temperature, 5 μL of each concentration was added to the reaction well, containing the reagents described above.

The third set of tubes went through an RNA purification process outlined in later sections by Qiagen QIAamp Viral RNA Mini Kit (52904, Qiagen). 60 μL The eluted RNA solution was mixed with 80 μL RNase/DNase free water to maintain the concentration. 5 μL of the eluted

RNA was added to reaction tubes containing the reagents as mentioned above. Each test in this process was done in triplicate.

For viral particle experiments using clinical samples, the clinical samples were nasal swabs taken with disposable swabs (Jiangsu Kangjian Medical Apparatus) and placed into a sampling tube containing 1 mL saline solution. The swab solution was then used to serially dilute the viral particle five-fold. After heating at 95 °C for 5 minutes and cooling back to room temperature, 5 μL of each concentration was added to the RT-LAMP reaction. RNA was extracted from the heat-inactivated sample following the manufacturer's protocol and eluted into RNase/DNase-free water. 60 μL of the eluted RNA solution was mixed with 80 μL RNase/DNase Free water to maintain the concentration. 5 μL of the eluted RNA is mixed with qPCR reagents and run the qPCR assay. Each test in this process was repeated in triplicate.

4.2.6 RNA Extraction from Viral Particles and Clinical Samples

RNA was extracted from the samples by Qiagen QIAamp Viral RNA Mini Kit (52904, Qiagen) to minimise the impurity effect in the qPCR assay. All the RNA extraction processes followed the manufacturer's protocol.

After RNA extraction, 5 μL of the eluted RNA was added to LAMP reagents in the 96-well plate. After centrifugation, the 96-well plate was placed into the qPCR machine (Lepgen-96, Lepu & CFX-96, Bio-Rad) and heated at 65 °C for 30 minutes. The fluorescent signal was acquired every 20 seconds by the FAM channel. The LAMP TT values were given by qPCR machines based on Cq Values. At the same time, 5 μL of the eluted RNA was added to qPCR reagents. After following the qPCR assay protocol, the Ct values of the sample could be obtained.

4.2.7 qLAMP Assay with Human Genomic DNA and Cell lines

TaqMan Control Genomic DNA, purchased from Thermo Fisher, was used as the positive control. The human bronchial epithelium cell line (BEAS-2B) and the human A549 adenocarcinoma cell line obtained from Sigma-Aldrich were dissociated with Trypsin and resuspended in sterile sodium chloride solution (S8776, Sigma-Aldrich). The cells were counted and diluted into 2000, 1500,1000, 500, 100, 50, 10, 5, 1 $cell/\mu L$.

12.5 μL LAMP colorimetric 2X master mix (NEB) was mixed 2.5 μl 10X ACTB-n primer mix. 5 μL of SYTO 9 fluorescent dye (S34854, Thermo Fisher) in the concentration of 2.5 μM was added for fluorescent reading while 5 μL RNase/DNase-free water was added for colorimetric reading. Finally, 5 μL of the sample, DNA template or cell solution with different concentrations was added.

The same batch of cell samples was split into 2 groups, treated with and without heat inactivation (95 °C for 5 minutes). After cooling down to room temperature, the cell samples were transferred into wells of PCR plates. The PCR plate was heated on the qPCR machine at 65 °C for 30 minutes. Lepgen-96 qPCR machine (Lepu) was applied for fluorescent reading while using a thermostatic photometer (Sinopharm) for colorimetric reading.

4.2.8 Statistical Analysis

Statistical differences of the groups with various conditions were analysed by analysis of variance (ANOVA). The P values between groups less than 0.05 was considered as a significant difference. The statistical analysis was performed with GraphPad Prism 6.0. All numerical values are reported to four significant figures to ensure consistency in precision across a wide dynamic range. As a result, the number of decimal places may vary depending on the magnitude of the value.

4.3 Results

4.3.1 The Linear Relationship Between the Copy Number and Reaction Time in qLAMP assay

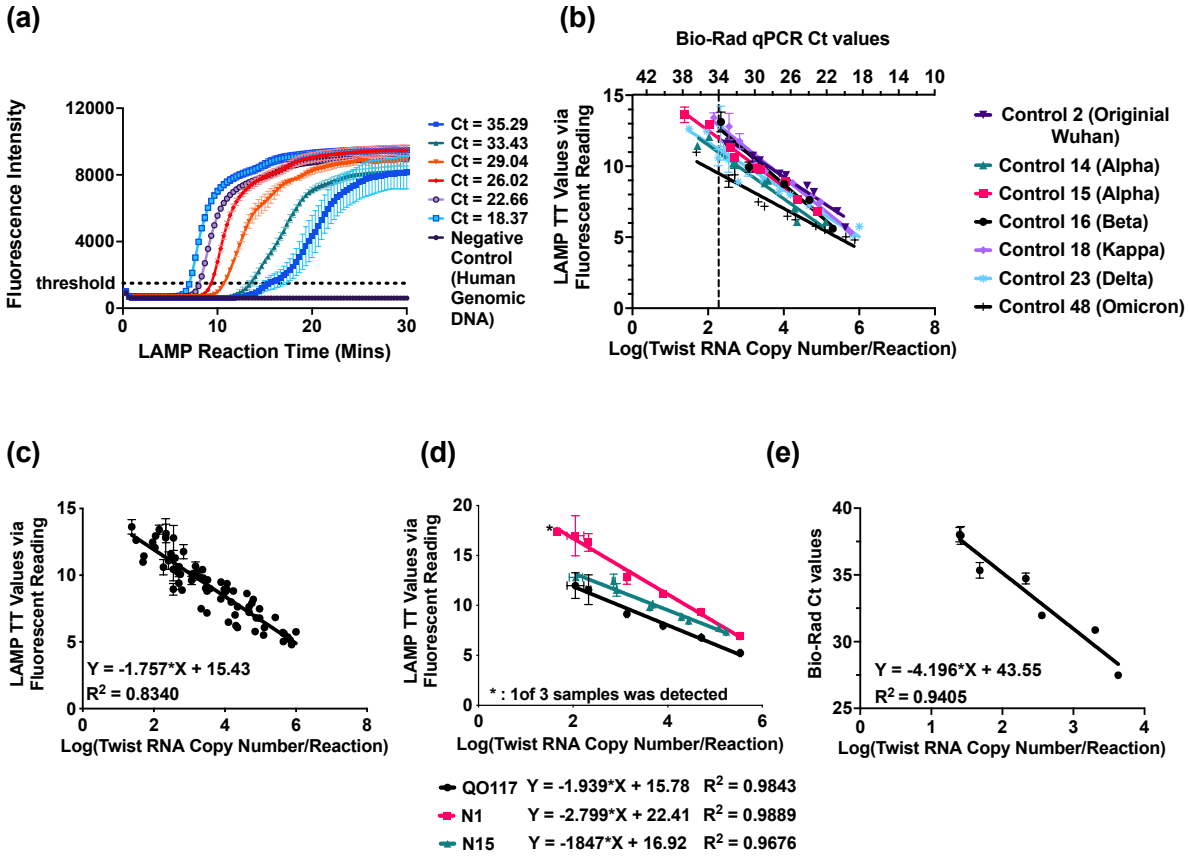

Figure 4.1 ***Standard curves for the qLAMP assay detecting SARS-CoV-2. (a)*** *LAMP amplification curves were based on the fluorescent intensity in 30 minutes with a full-length SARS-CoV-2 RNA template (Control 2). The RNA concentrations were measured by qPCR assay.* ***(b)*** *Standard curves for the LAMP TT value against the Twist RNA copy number. The copy number was converted from the qPCR Ct values (upper x-axis) based on the standard curve presented in (e). The Different variants of SARS-CoV-2 in full-length RNA were tested.* ***(c)*** *Standard curve for qLAMP assay after combining all the data in (b) from different SARS-CoV-2 variants.* ***(d)*** *Standard curves for qLAMP assay using different COVID-19 primer sets. Twist RNA control 2 was used as the positive control.* ***(e)*** *The standard curve between Bio-Rad qPCR Ct values and Twist RNA copy numbers. Twist RNA control 2 was used as a positive control. The copy number was determined by digital droplet PCR. All the results* ***(a-e)*** *are presented as* $MEAN \pm SEM$.

Using SYTO 9 as a fluorescent dye, the real-time amplification curves of RT-LAMP assays with the QO117 primer set[16,18] were obtained (Figure 4.1a). The RT-LAMP reaction shows a similar pattern to qPCR: the lower the concentration of SARS-CoV-2 RNA, the longer the time to reach the threshold. qPCR was run in parallel with RT-LAMP using the same batch of RNA solution to get Ct values of qPCR.

Two qPCR machines, Lepgen (Lepu Ltd, China) and Bio-Rad (Bio-Rad Ltd, UK), were used for the experiments. Since the threshold settings are different, the qPCR Ct values generated by the Lepgen-96 qPCR machine were slightly lower than those generated in the Bio-Rad machine when testing the same sample, and both calibration curves have very similar slopes. Figure 4.2 illustrates the conversion of Ct values between these two qPCR machines, $y_{Bio-Rad} = x_{Lepu} + 3.274$. All qPCR Ct values generated by the Lepgen qPCR machine were converted to Bio-Rad machine-based Ct values. To quantify the copy number of SARS-CoV-2, digital PCR and qPCR were used to establish a calibration curve of the copy number and Ct values of qPCR (Figure 4.1e).

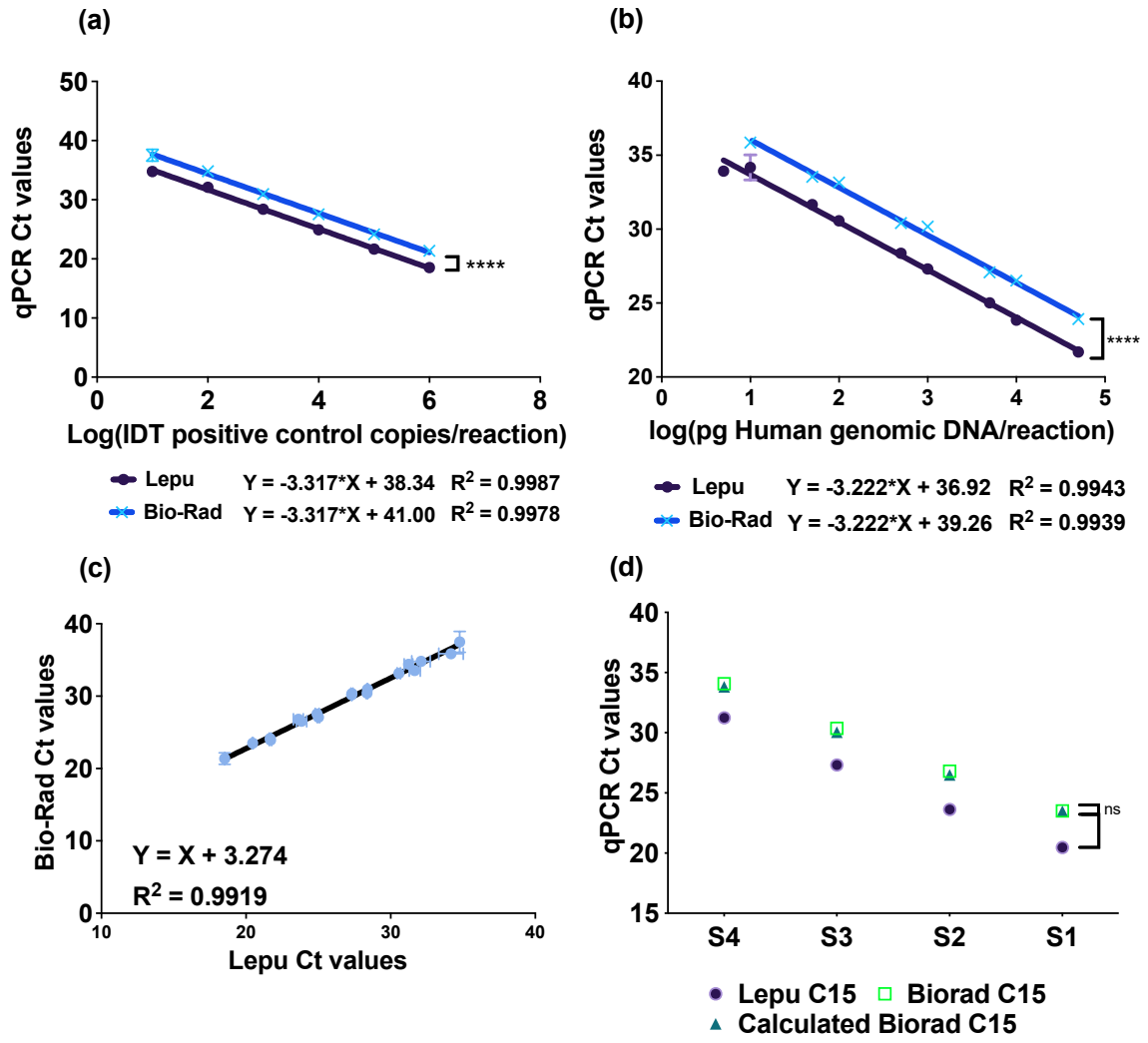

Figure 4.2 ***Standard curves of Lepgen qPCR machine (black) and Bio-Rad qPCR machine (Bule). (a)*** *Standard curves of two qPCR machines for qPCR Ct values against the copy number of positive controls. The qPCR assay was run by Promega's qPCR kit (A6121) with CDC N1 primers (1006770, IDT). IDT positive control (1006625, IDT) was used.* ***(b)*** *Standard curves of two qPCR machines for qPCR Ct values against the copy number of human genomic DNA. The qPCR assay was run by Promega's qPCR kit (A6121) with RNase P primers (1006770, IDT). Genomic DNA from Thermo Fisher (4312660) was used.* ***(c)****The correlation of qPCR Ct values from these two qPCR machines after combining the data from (a) and (b).* ***(d)*** *The validation of the standard curve, which was generated in (c). There was no statistically significant difference in the qPCR Ct values between generating from Bio-Rad and converting from the qPCR Ct values from the Lepgen qPCR machine. The results were presented as Mean ± SEM. ns: P>0.05, ****: P<0.0001.*

Unlike the qPCR assay, the RT-LAMP reaction uses a single temperature without thermocycling. The reaction of this RT-LAMP takes place at a constant temperature, in this case 65 °C. The time of the fluorescence signal exceeding the threshold is proposed to represent the LAMP threshold time value (LAMP TT value), which showed a linear relationship with the RNA concentrations (Figure 4.1b). This linear relationship was observed in the original SARS-CoV-2 strain, as well as SARS-CoV-2 variants, including Alpha, Beta, Kappa, Delta, and Omicron variants. The equations of calibration curves for these variants are listed in Table 4.2.

Table 4.2 ***The linear relationship between the copy number and LAMP Ct values****.*

Control	GISAID NAME	Regression Equation*	R^2
Control 2	Wuhan-Hu-1	Y = -1.758*X + 16.29	0.9658
Control 14 Alpha	England/205041766/2020	Y = -1.893*X + 15.28	0.9445
Control 15 Alpha	England/MILK-9E05B3/2020	Y = -1.987*X + 16.48	0.9803
Control 16 Beta (B.1.351)	South Africa/KRISP-EC-K005299/2020	Y = -2.303*X + 17.95	0.9564
Control 18 Kappa (B.1.617.1)	India/CT-ILSGS00361/2021	Y = -2.138*X + 17.75	0.9796
Control 23 Delta (B.1.617.2)	India/MH-NCCS P1162000182735/2021	Y = -1.657*X + 14.98	0.9171
Control 48 Omicron (B.1.1.529)	Hong Kong/HKU-211129-001/2021	Y = -1.432*X + 12.76	0.9499

**: Y represents the LAMP TT values, and X stands for the logarithm of the template copy number.*

In spite of many mutations in the variants, the results show that the QO117 primer set can detect all the above variants of SARS-CoV-2, consistent with the in-silico analysis which can be seen in Table 4.3 in the appendix. qLAMP assay is especially sensitive to Twist Control 15 (Alpha) and Twist Control 23 (Delta), which detect the samples with Ct=37.77 and Ct=37.75,

respectively. Remarkably, all the amplification of these variants was detected within 15 minutes via fluorescent reading.

All the data from different variants of SARS-CoV-2 were combined to give an overall standard curve (Figure 4.1c), which could estimate the viral loads of the samples. The deviation of LAMP TT values was increased with the decrease in the viral RNA concentrations. When Ct values of the RNA samples were greater than 32, the variation of LAMP TT values was greater than 1, which is about a 2-cycle-number difference of Ct value in qPCR.

Apart from the QO117 primer set, the other two primer sets, the N1 and N15 primer sets, were designed for detecting SARS-CoV-2 in the previous work[27]. According to Figure 4.1d and Table 4.3 in the appendix, these three primer sets were all capable of detecting the original SARS-CoV-2 strain (Twist RNA control 2) within 20 minutes and present a linear relationship between the LAMP TT values and qPCR Ct values. Among these three primer sets, using QO117 resulted in the shortest incubation for the same RNA concentration.

4.3.2 Fluorescent and Colorimetric qLAMP Assay

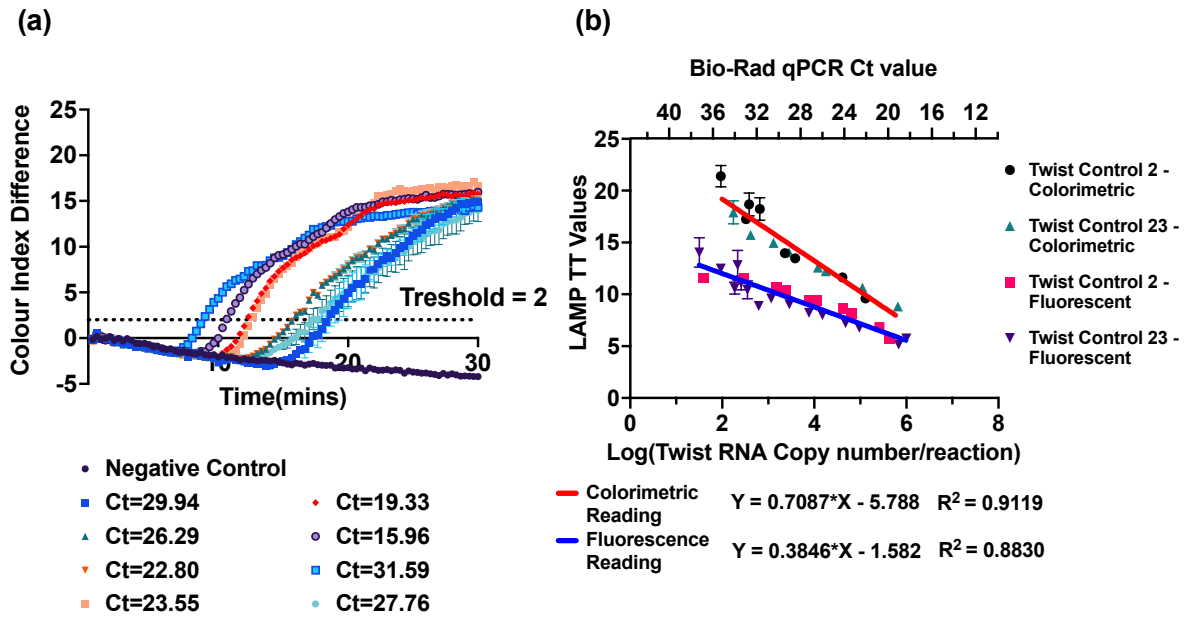

Figure 4.3 ***Standard curves for the qLAMP assay using Twist RNA in six-fold serial dilution via colorimetric reading.*** ***(a)*** *LAMP amplification curves were generated by colorimetric reading in 30 minutes with a full-length SARS-CoV-2 RNA template in different concentrations. The RNA concentrations were measured by qPCR assays.* ***(b)*** *Standard curves for the LAMP TT value against the template concentration via colorimetric and fluorescent readings. The copy number was converted from the qPCR Ct values (upper x-axis) based on the standard curve presented in Figure 4.1 (e). Twist RNA control 2 (original) and Twist RNA control 23 (Delta variant) were used as the positive control. The individual standard curves were presented in Supplementary Figure 4.4. All the results were presented as* $MEAN \pm SEM$.

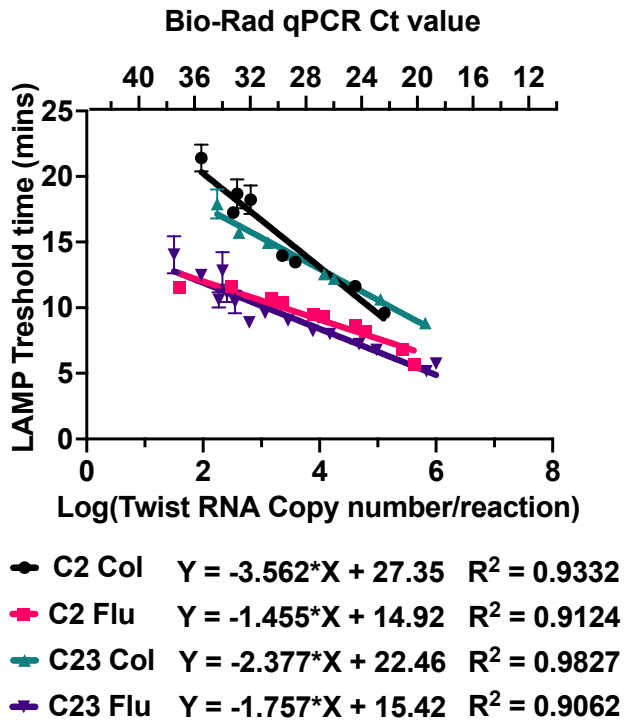

Figure 4.4 ***Standard curves for the LAMP TT value against the template concentration via colorimetric and fluorescent readings****. The copy number was converted from the qPCR Ct values (upper x-axis) based on the standard curve presented in Figure 4.1 (e). Twist RNA control 2 (original) and Twist RNA control 23 (Delta variant) were used as the positive control. The individual standard curves are presented below the figure. All the results were presented as* $\boldsymbol{MEAN \pm SEM}$.

In previous work [27,119], a colorimetric assay was employed for the detection of SARS-CoV-2. The test result could be read by the colour change, yellow for positive and pink for negative. The difference in colour between the real-time and initial data was plotted against the reaction time (Figure 4.3a). Similar to the curves of fluorescent reading, the colorimetric signal entered the exponential phase when the amplification accelerated, and the LAMP TT value is related to the viral RNA concentration.

After setting the threshold for colorimetric reading, the LAMP TT values for detecting Twist Control 2 (Original) and Twist Control 23 (Delta variant) were linear to the copy numbers of

the viral RNA, as well as the corresponding qPCR Ct values (Figure 4.3b). Compared to fluorescent reading, the colorimetric assay had a longer incubation time but could reach the same sensitivity (Ct <34) within 30 minutes. The flat slope of the colorimetric standard curve led to a minor error in Ct value estimation.

4.3.3 qLAMP Assay with Inactivated Viral Particles

Since RNA would be quickly degraded by the RNase in clinical samples, this work also evaluated qLAMP assays using serially diluted inactivated SARS-CoV-2 viral particles, BBIBP-CorV [159]. The inactivated viral particles were diluted in RNase/DNase-free water with three different conditions for RT-LAMP running, with and without heat inactivation, and extracted RNA.

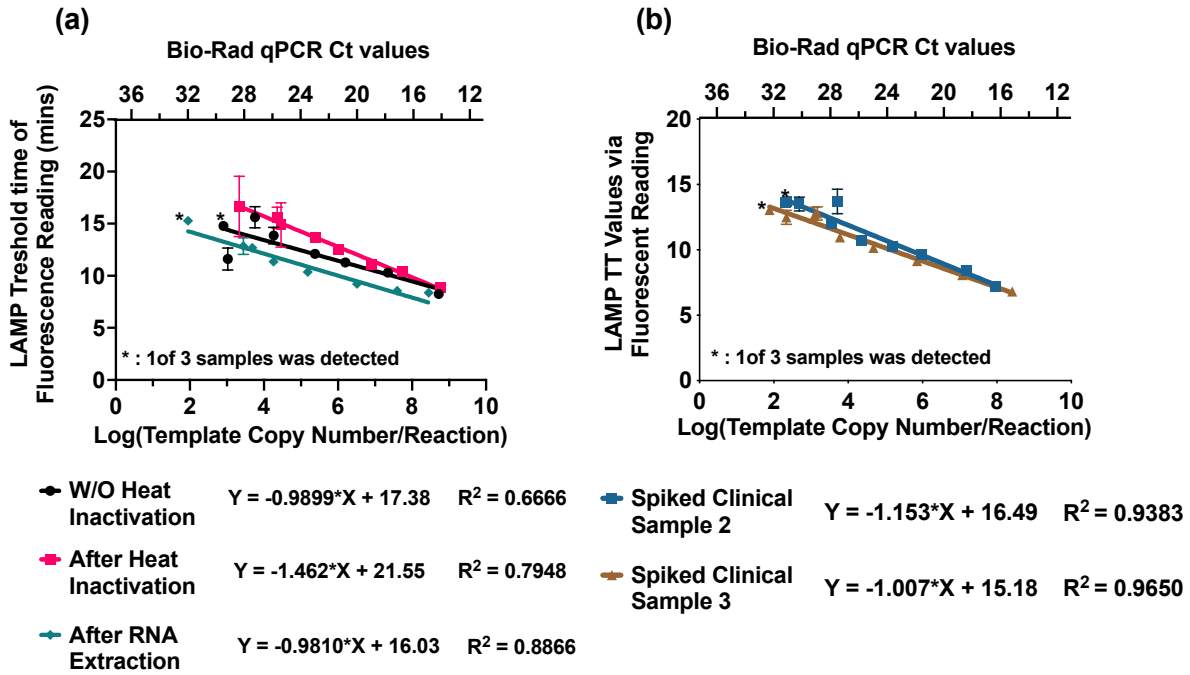

Figure 4.5 ***Standard curves for the qLAMP assay using viral particles in serial dilution in water (a) and clinical samples(b).*** *In* ***(a)****, the copy number in logarithm was calculated qPCR*

Ct values in the upper axis. The calibration between qPCR Ct values and copy number was presented in (c). The regression equations below the figure describe the relationship between LAMP TT values and template copy numbers in logarithms. In ***(b)****, inactivated viral particles were spiked into three clinical samples. The qLAMP assay was run after heat inactivation. The copy number was converted from Ct values of qPCR assays, shown in the upper axis.*

The linear relationship between LAMP TT values and the corresponding qPCR Ct values was established for these three different pre-treatments (Figure 4.5a). A greater deviation of LAMP TT values was found when testing the sample after heat inactivation, especially for the sample with high Ct values. Although RNA should be released from viral particles after heat inactivation, the RT-LAMP TT values were even higher than the same samples without heat inactivation. However, it is safer to heat the samples at 95 °C for 5 minutes to inactivate the virus before the RT-LAMP assay. Negative swab samples were spiked with BBIBP-CorV and heated to 95 °C for 5 minutes to assess the potential of qLAMP application to clinical samples (Figure 4.5b). The linearity between LAMP TT values and template concentrations was also observed in the spiked clinical samples.

RNA extraction could purify the samples and shorten the reaction time (Figure 4.5a). At the same time, using RNA extracted samples reached a comparatively higher sensitivity than the samples after the other two treatments. Moreover, the standard deviation in the LAMP TT values for each concentration was much smaller.

4.3.4 qLAMP Assay with Human Gene

In the COVID-19 screening, LAMP primers for the beta-actin gene (ACTB) in human samples were also used as an internal control to ensure sampling quality. A previously reported ACTB primer set for detecting the human housekeeping gene only had four primers [27,160]. The lack of loop primers prolongs the reaction. Therefore, a new set of primers was designed, ACTB-n, which also detected the ACTB sequence but with the additional loop primers.

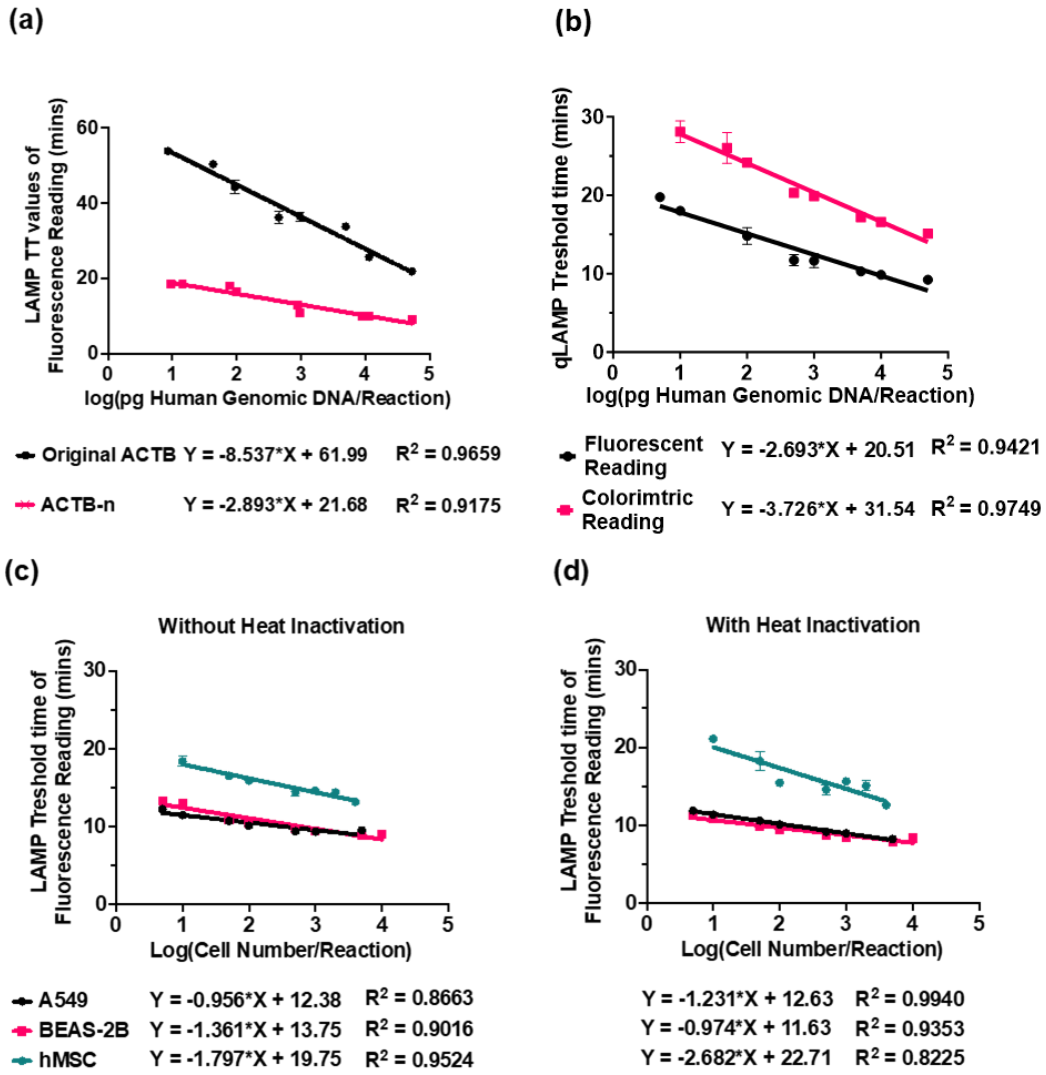

Figure 4.6 ***Standard curves for the qLAMP assay using human primers to detect human genome and cell lines. (a)****Standard curves for the LAMP TT values against human genomic DNA. Human genomic DNA was used as the positive control. The upper axis presents the corresponding Ct values of qPCR using RNase P primers. Different human primers were used.* ***(b)*** *Standard curves for the LAMP TT value via fluorescent and colorimetric reading against human genomic DNA.* ***(c)*** *Standard curve for qLAMP assay detecting human genomic DNA by human primers (ACTB set 3) via fluorescence and colorimetric readings.* ***(d)*** *Standard curve for qLAMP assay detecting human genomic DNA in human cells without heat inactivation. Human bronchial epithelium cell line (BEAS-2B), Human lung adenocarcinoma cell line (A549), and Human mesenchymal stem cells (hMSC) were tested.* ***(e)*** *Standard curve for qLAMP assay detecting human genomic DNA in human cells after heat inactivation. Human bronchial epithelium cell line (BEAS-2B), Human lung adenocarcinoma cell line (A549), and Human mesenchymal stem cells (hMSC) were tested. All the results are presented as* $MEAN \pm SEM$.

Using human genomic DNA as positive controls, the LAMP TT values by fluorescent reading were decreased linearly with the increase of the masses of human genomic DNA (Figure 4.6a). The original ACTB required a much longer incubation time and could only detect the samples with Ct values less than 25 within 30 minutes. By contrast, the ACTB-n primer set was able to detect samples with Ct value > 35 or 10 pg Human genomic DNA within 20 minutes based on the fluorescent reading (Figure 4.6a).

Figure 4.6b illustrates the difference in LAMP TT values between the fluorescence and colorimetric readings. ACTB-n primer set detected the human genomic DNA down to 10 pg per reaction within 30 minutes and had a relatively minor deviation in LAMP TT values. The time difference between these two readings was slightly decreased with the growth of the human gene concentration. However, even at the highest concentration, 50 ng human genomic DNA per reaction, there is still around a 6-minute gap between these two readings (Figure 4.6b).

To assess the potential of estimating the concentration of human genomic DNA in the clinical sample, the performance of ACTB-n was tested with three different human cell lines **(**4.6c and 4.6d), which were the Human bronchial epithelium cell line (BEAS-2B), Human lung adenocarcinoma cell line (A549), and Human mesenchymal stem cells (hMSC). The qLAMP assay was conducted with two different pre-treatments, with and without heat inactivation.

The LAMP TT values of fluorescent reading were linearly increased with the reducing cell numbers, irrespective of the pre-treatments. There was no significant difference in LAMP TT values for detecting the ACTB gene in the samples with and without heat inactivation. Meanwhile, the ACTB-n primer set could detect all three cell lines down to 10 cells per reaction within 20 minutes. The LAMP TT values for hMSC were relatively higher than the other two cell lines, BEAS-2B and A549. It might be caused by the different gene expression levels in different cell lines.

4.3.5 qLAMP Assay with Clinical Samples

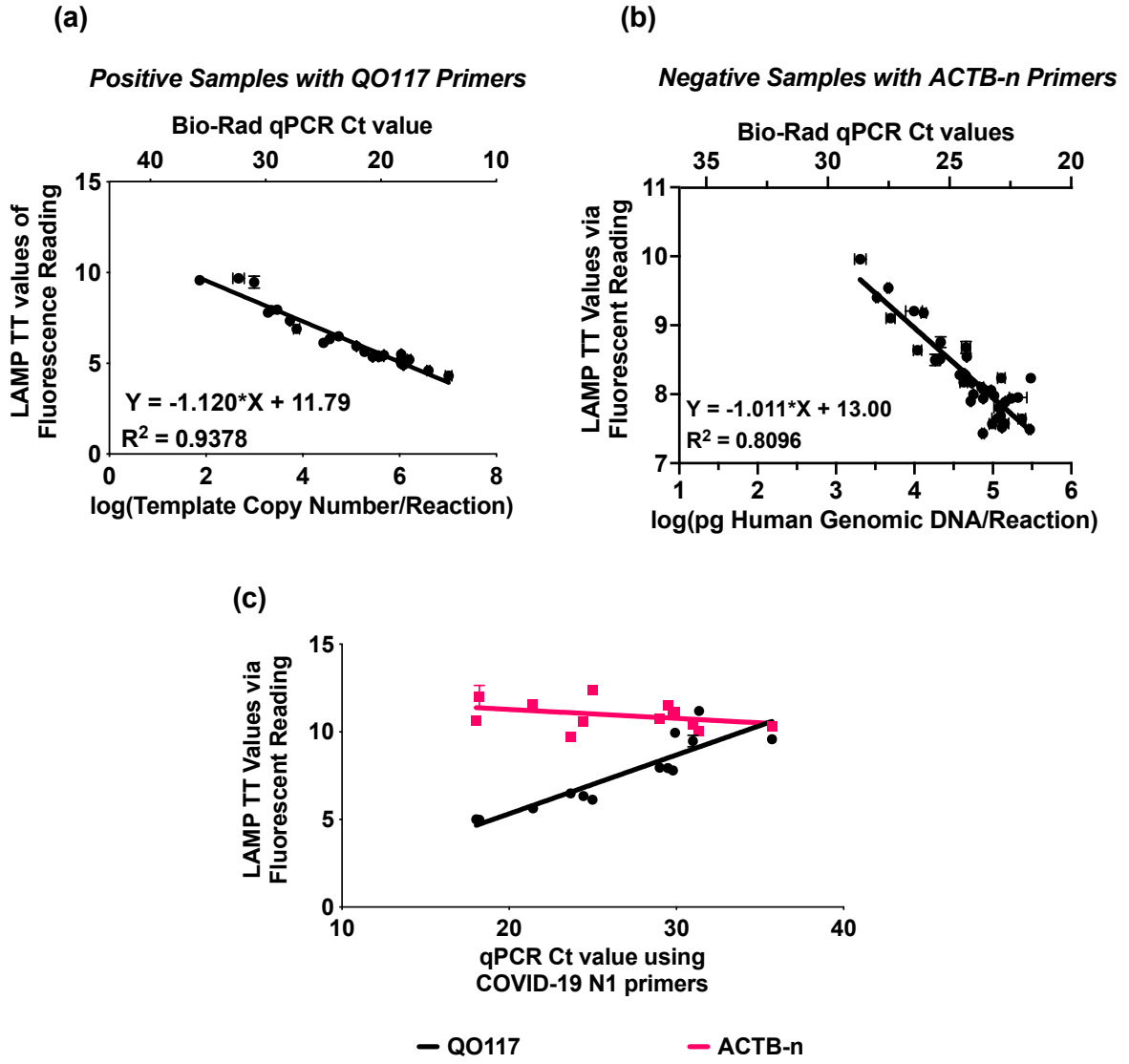

Figure 4.7 ***Standard curves for using qLAMP assay with clinical samples. (a)*** *Standard curves for qLAMP assay using QO117 primers to detect positive clinical samples. The LAMP TT values were plotted against template copy numbers in logarithm, calculated from qPCR Ct values based on the calibration curve in Figure 4.1 (e).* ***(b)*** *Standard curves for qLAMP assay using ACTB-n primers to detect negative clinical samples. The LAMP TT values were plotted against template copy numbers in logarithm, calculated from qPCR Ct values based on the calibration curve in Figure 4.2 (b).* ***(c)*** *qLAMP assays with QO117 and ACTB-n primers tested the viral load and the human gene of the same sample. The LAMP TT values of both qLAMP*

assays were plotted against the Ct values of qPCR using N1 primers to detect SARS-CoV-2. 13 samples were tested in total. All the results are presented as $MEAN \pm SEM$.

In a single-blind format, sixty-four RNA-extracted clinical samples, including 25 positives and 39 negatives, were applied to validate the qLAMP assays. As presented in Figure 4.7a, the RT-LAMP reaction detected all the positive samples by fluorescent reading within 10 minutes, even to the samples with Ct =35 by qPCR assay. The LAMP TT values of positive samples were linear to the logarithm of template copy number (Figure 4.7a). For negative samples, the ACTB gene was all detected with ACTB-n primers (Figure 4.7b). The LAMP TT values for ACTB primers also had a linear relationship with the mass of the human genomic gene, with higher variations than qLAMP assay with QO117 primers (Figure 4.7b).

To access the correlation of cell numbers in the sample against the viral load, 13 of 25 positive samples were run qLAMP assays with QO117 and ACTB primers simultaneously, but in different reaction wells of a 96-well plate (Figure 4.7c). The LAMP TT values of the sample from both the qLAMP assay using QO117 primers and ACTB-n primers were plotted against the Ct values from the qPCR assay using the same sample with N1 primers to detect SARS-CoV-2. The LAMP TT values for detecting SARS-CoV-2 were linear to the Ct values of qPCR, while the LAMP TT values for detecting human ACTB in the positive samples were maintained around 11.05. It indicates that the number of human cells in the swab samples was consistent, and the sampling process was reliable.

The number of clinical samples used in this study was determined by availability rather than prospective sample size calculation, as the primary aim was to demonstrate proof-of-concept using accessible materials. While this approach provided sufficient data for initial evaluation, future studies will incorporate formal sample size calculations to ensure adequate statistical power for diagnostic performance assessments.

4.4 Discussions and Conclusions

This work demonstrates that qLAMP can be applied to quantitatively evaluate the viral loads and assess the sampling quality. This work used fluorescent dye, SYTO 9, to acquire the real-time amplification curve. LAMP TT values were linear with the template concentrations, either in RNA or DNA. This linear relationship was validated by two different targeted sequences, SARS-CoV-2 and human ACTB gene, using the corresponding primer sets.

The qLAMP assay using QO117 primers was able to detect the samples containing the original SARS-CoV-2 strain as well as its variants (Alpha, Beta, Kappa, Delta and Omicron). The RNA concentration 200 copies per reaction, or Ct < 34 can be detected within 15 minutes by fluorescent reading in the qLAMP assay. The colorimetric reading has the same sensitivity but required a longer incubation time (Figure 4.1b & Figure 4.3b). Since the colorimetric assay was based on the colour changing of the pH indicator, the accumulation of hydrogen ions, released from the amplification, was required to overcome the low concentration pH buffer in the reagents [73].

The design of primers could affect the amplification efficiency. The addition of loop primers could significantly reduce the amplification time (Figure 4.6a). The targeting region's selection may also be essential for amplification (Figure 4.1d). With the same RNA template concentration, using QO117 primer set, targeting RNA encoding Orf1ab, exhibited lower LAMP TT values than using N1 and N15 primer sets, targeting two regions of nucleocapsid protein. Even within the same region, the LAMP TT values of N1 and N15 were slightly different. This variation may be caused by the secondary structure of the RNA template. The

primer binding could be much easier if the target region was exposed, shortening the amplification time.

Since RNase quickly digested full-length Twist RNA in the real samples, the inactivated SARS-CoV-2 viral particles, BBIBP-CorV, were spiked to evaluate the feasibility of applying qLAMP assay for clinical samples (Figure 4.5). Although detecting the heat-inactivated samples took even longer than those without heat treatment, and after RNA extraction, it is still the most practical way to inactivate the virus and release the RNA for testing. It might be accounting for the RNA degradation due to the heat inactivation [161] and the interaction between the RNA template and the protein shell [162].

The qLAMP assay was run for spiked clinical samples after heat inactivation and cooling back to room temperature. The LAMP TT values showed a linear relationship with the RNA concentrations in each clinical sample. The RT-LAMP reaction after RNA extraction gave a higher sensitivity and smaller LAMP TT values than the sample with and without heat inactivation. Even with RNA extraction, the overall detection time using qLAMP could be completed within 1 hour, much quicker than qPCR. The additional requirements associated with extraction may limit its application in the point-of-care setting.

A new set of ACTB primers was designed to quantify the human genes in the samples to assess the quality of sampling. For detecting the ACTB gene in cell lines, there was no significant difference in the LAMP TT values and sensitivity between the samples with and without heat treatment. The reason for that might be that the reagents do not maintain the osmotic pressure of cells. The cells burst after adding them to the reagents, which had the same result as heat inactivation.

The qLAMP assays with QO117 primers and ACTB-n primers were both validated by 64 RNA-extracted clinical samples, including 25 positive samples. The linearity of LAMP TT values

against template concentrations was maintained for both qLAMP assays. In addition, the human gene and SARS-CoV-2 in 13 positive clinical samples were detected simultaneously. It turned out that there was no relationship between cell numbers in the samples and viral loads.

The LAMP TT values are analogous to Ct values in a qPCR assay to quantify the concentration of RNA or DNA templates. Either fluorescence or colorimetric assay could be used to read these LAMP TT values. This quantitative LAMP (qLAMP) requires a much shorter reaction time (around 1 hour) compared to the qPCR assay (around 2.5 hours). In practice, the LAMP TT values of qLAMP assay with QO117 primers could also be used to estimate the COVID-19 viral load in clinical samples while also indicating the quality of sampling by using ACTB-n primers. Consequently, the LAMP TT values could be used to quantify the viral load, assess sampling quality, and aid clinical decision-making.

Chapter 5 Lyophilisation and MART Drying for LAMP Assays

5.1 Introduction

The development of molecular diagnostic techniques like Loop-Mediated Isothermal Amplification (LAMP) has made rapid pathogen detection feasible in point-of-care (POC) settings, addressing challenges posed by traditional PCR methods, such as the need for thermal cycling and complex sample handling. LAMP can produce results within 30 minutes at a constant temperature, making it particularly useful for settings where laboratory resources are limited [27,39]. However, key reagents for LAMP, especially enzymes like Bst polymerase and reverse transcriptase, are thermolabile and must typically be stored at -20°C, restricting the technique's portability and use in low-resource environments [48,49].

To circumvent the limitations associated with cold-chain logistics, Matrix-Assisted Room Temperature (MART) drying and lyophilisation were chosen as viable stabilization methods. MART drying offers a simpler, energy-efficient approach for storing sensitive reagents at ambient temperatures by embedding proteins within sugar glass films on a cellulose fibre matrix. Lyophilisation, or freeze-drying, similarly stabilizes sensitive reagents but achieves this by freezing and sublimating water under vacuum, leaving a dry matrix where proteins are embedded within a solid, protective structure. This chapter discusses the application of MART drying and lyophilisation for LAMP reagents, highlighting the efficacy of both in maintaining reagent stability and functionality even in non-refrigerated settings.

5.2 Materials and methods

5.2.1 MART drying

Matrix-Assisted Room Temperature (MART) drying is a drying method that uses a biocompatible matrix to encapsulate biomolecules in sugar films, allowing proteins to be stabilized at ambient conditions without refrigeration. The approach builds on the concept of "sugar film drying" traditionally used in biological labs, where proteins are immobilized within protective sugar agents like trehalose or dextran. The sugar protects the biomolecules by replacing water molecules, thus preventing denaturation [163,164]

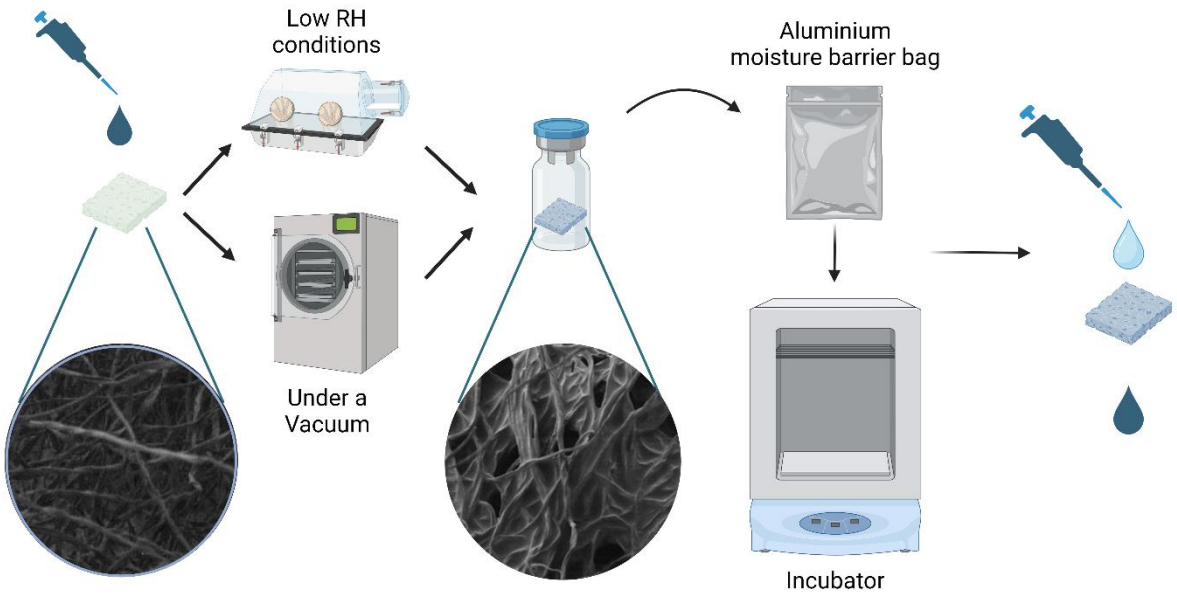

Figure 5.1 ***Visual Abstract of MART drying process****. Protective agents were formulated with functional proteins and the mixture was dried on a biocompatible cellulose fibre matrix. Drying was carried out at room temperature or elevated temperatures (~30 °C), either through dry air circulation (MART-DA drying) or under a vacuum (MART-V drying). After the drying process,*

the samples can be transferred to a moisture bag for stability tests or directly reconstituted with deionized water. Created with Biorender.com

There are two primary methods of MART drying, MART-DA (dry air) and MART-V (vacuum). While MART-DA employs air circulation, MART-V utilizes a vacuum to expedite the drying process. Each method has its operational advantages, with MART-V allowing for rapid drying within sealed containers to minimize contamination. For the LAMP reagents used in this study, MART-V was selected as the optimal method for its compatibility with POC settings, enabling reagents to be dried directly within PCR tubes.

The LAMP reagents included enzyme Bst 2.0, dNTPs, labelled primers, and essential salts. FAM and biotin were attached to the FIP and BIP primers, respectively, to allow for downstream detection via lateral flow assays (LFA). The reagents were loaded onto a cellulose fiber matrix, ensuring even distribution for effective MART drying within PCR-compatible tubes (Figure 5.2a). Reagent formulations were adjusted to optimize stability and reaction sensitivity following drying. The RT-LAMP reagents were dried using the MART-V method, where a vacuum was applied to reduce moisture without freezing. The reagents, loaded onto cellulose fiber matrices within PCR tubes, were placed into drying bottles connected to a freeze dryer's vacuum pump. The process involved drying for three hours under vacuum conditions, then transferring the dried reagents into moisture barrier bags with controlled humidity to prevent rehydration before testing. Samples were stored at 40 °C for one week to evaluate thermal stability. This temperature was chosen based on commonly used thresholds for accelerated stability testing in diagnostic reagent development, where 40 °C is considered a meaningful stress condition that reflects potential transport and storage challenges in warm climates [165]. The one-week duration provided an initial indication of formulation robustness without extending the experimental timeline.

5.2.2 Lyophilisation

Freeze-drying, or lyophilisation, is a more widely used approach for reagent stabilization and can be a critical technique for the long-term preservation of LAMP reagents. The process involves freezing reagents and subsequently applying a vacuum to sublimate the ice, leaving behind a dry, porous structure that can be rehydrated when needed. Key stabilizers, such as sugars (e.g., trehalose and dextran) and proteins like bovine serum albumin (BSA), are typically added to prevent collapse and structural degradation. In this study, the lyophilisation of LAMP reagents aimed to maintain assay sensitivity and structure integrity, even after storage at 4 °C for two months. HSV gDNA was used as samples to test the validity of the assays after drying. The lyophilised kits were tested after being stored at 4 °C for two months because this reflected the actual storage conditions used in the lab following freeze-drying. The shelf-life assessment was conducted near the end of the project, using available kits that had been kept in the refrigerator during that period. Due to time constraints, room temperature or elevated temperature stability tests were not conducted. This test was intended as a practical check of medium-term stability under refrigerated conditions, rather than a comprehensive stability study. HSV gDNA was used as samples to test the validity of the assays after drying.

LAMP master mixes were supplemented with 15% w/v trehalose and 15% w/v dextran. In addition, 0.5 µL of 10% BSA in DPBS was added to a 30 µL final reaction volume BSA. These additives provided cryoprotection by forming a glassy matrix around the enzymes and maintaining structural integrity through sublimation. The freeze-dryer was calibrated to incrementally lower the temperature to -40 °C, held under vacuum pressure below 50 mTorr for primary drying. This was followed by secondary drying at 20 °C to remove residual moisture. The freeze-dried reagents were then stored at 4 °C for stability testing.

5.3 Results

5.3.1 MART Drying

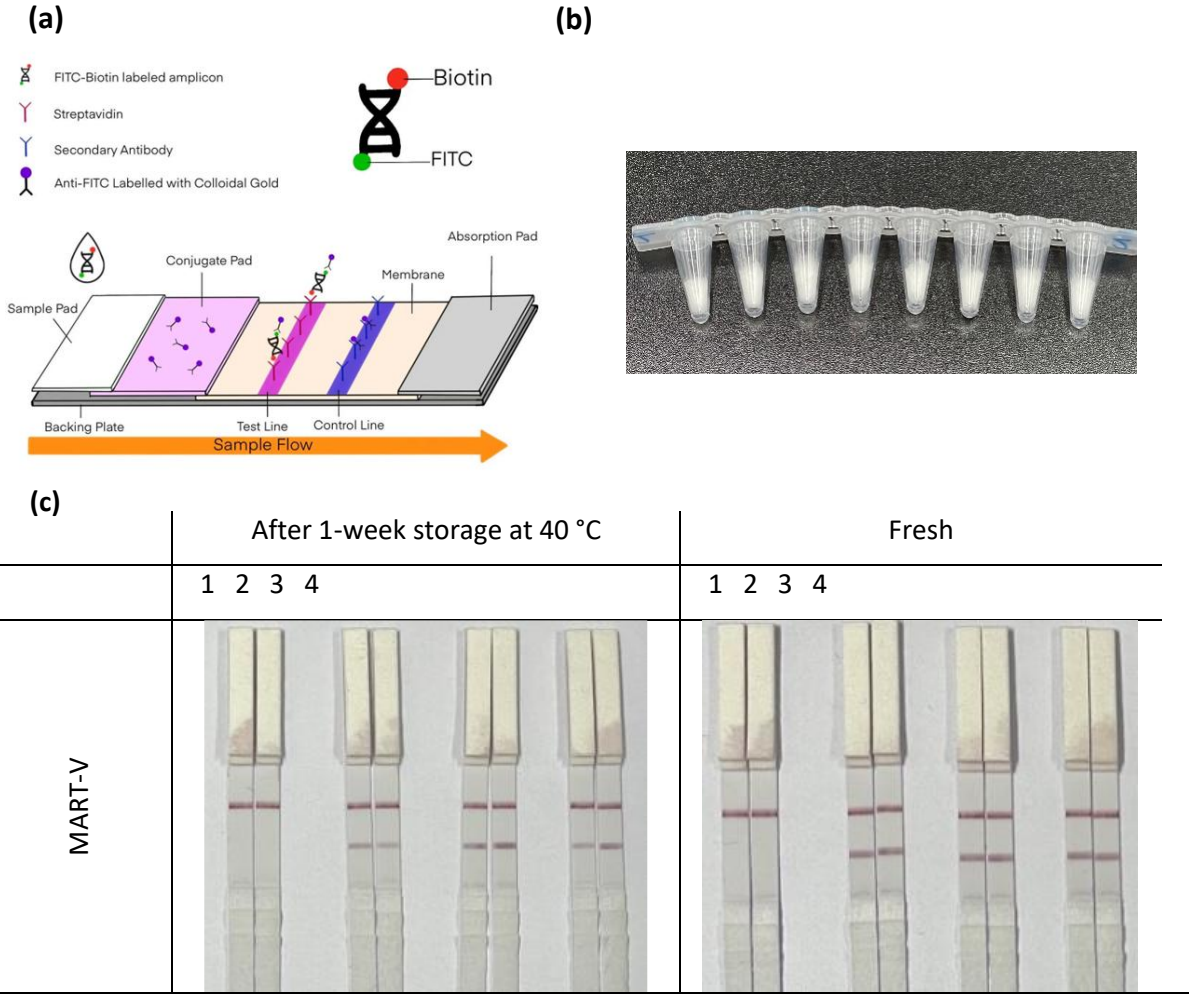

Figure 5.2 ***MART-V drying of LAMP-LFT reagents****. (a) Schematic diagram for LFT Test after RT-LAMP amplification. (b) The fibre matrix with dried RT-LAMP reagents. (c)The LFT results after RT-LAMP reactions with samples 1-4 of different template concentrations. The same batch of samples 1-4 was evaluated by qPCR assays as well and the concentration of templated was represented by CT values.*

From Figure 5.2c we can see that following one week of storage at 40 °C, the MART-V dried RT-LAMP reagents retained their detection sensitivity, as evidenced by qPCR cycle threshold (CT) values around 33.7 for test samples containing the SARS-CoV-2 full-length RNA template (Twist Control 2). MART-V drying preserved reagent functionality on par with freshly prepared counterparts, affirming MART's utility in high-temperature settings where cold-chain storage is unavailable. Moreover, Figure 5.2b shows that MART drying enabled reagents to be packaged in user-ready formats like PCR tubes, highlighting its practicality for POC deployment.

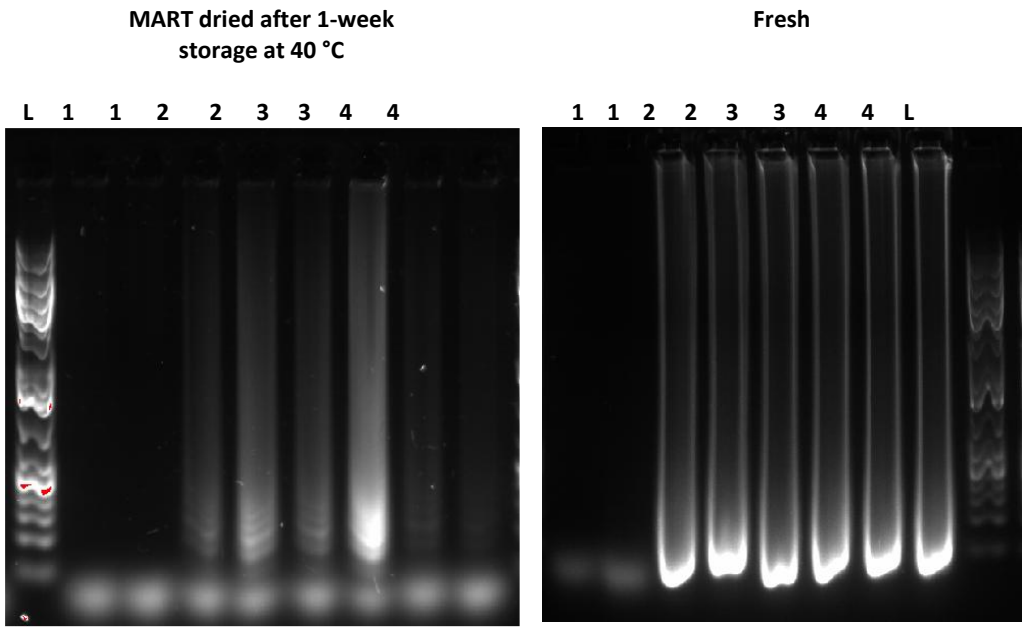

Figure 5.3 ***The gel electrophoresis result of the MART-dried LAMP reagents with samples in different RNA concentrations comparing them to a freshly prepared master mix****. The experiment involved four samples labelled 1-4, each containing different RNA concentrations. Simultaneously, the same batch of samples (1-4) underwent evaluation through qPCR assays, with the concentration of templated represented by CT values, as indicated above. Each sample testing was conducted in duplicate.*

Beyond the stability results observed through qPCR (Figure 5.2c), additional validation of MART-V dried RT-LAMP reagent functionality was achieved using gel electrophoresis, as shown in Figure 5.3. Here, MART-dried reagents were tested across varying RNA concentrations, comparing fresh and MART-V dried mixes for visible consistency in band intensity. Despite the slight fading of band intensity for the samples with very high CT values, the resulting gel images demonstrate similar amplification profiles for both the dried and fresh samples, further confirming the reagents' stability. This secondary analysis reinforces the qPCR findings and provides a clear, visual endorsement of the MART-V drying approach for preserving nucleic acid amplification capabilities across a range of sample concentrations, even after thermal exposure.

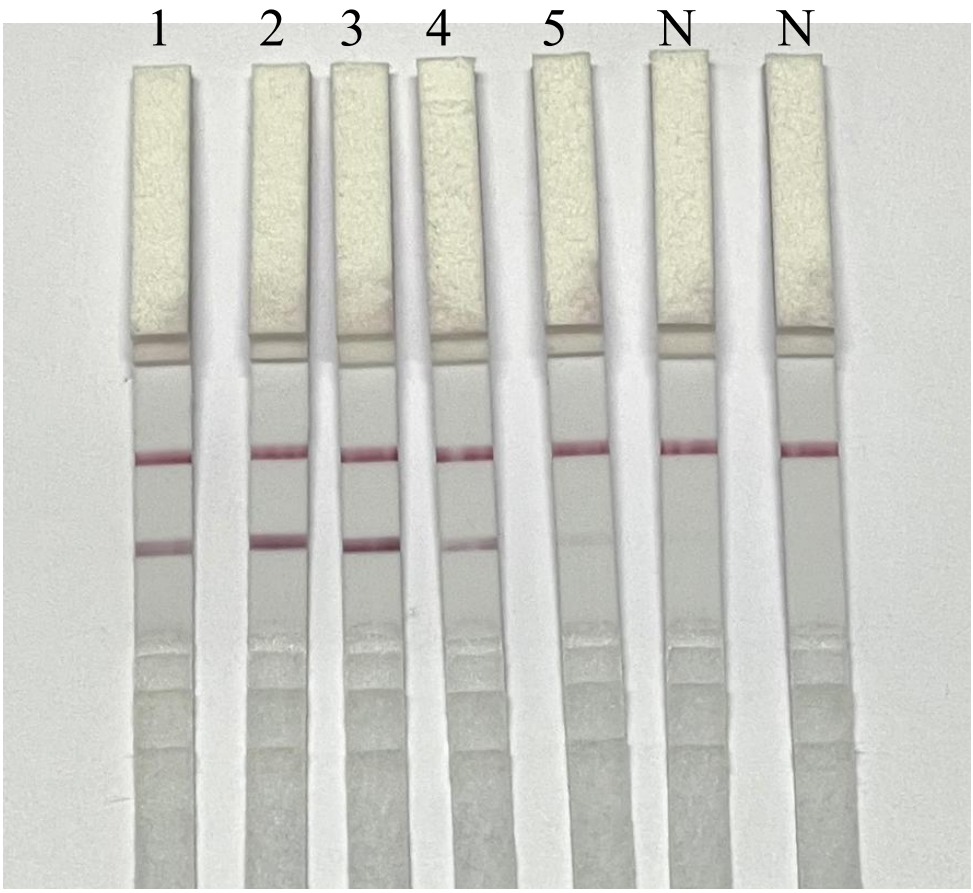

Figure 5.4 ***The serial dilution of amplicons after amplification were tested by lateral flow strip*** *for test sensitivity The mass of the RT-LAMP product was measured by a Qubit instrument (Thermo Fisher) with its relevant kit. 1: LAMP product ~543.6 µg/ml. 2: 10X diluted LAMP product ~54.36 µg/ml. 3: 100X diluted LAMP product ~5.436 µg/ml. 4: 1,000X diluted LAMP product ~0.5436 µg/ml. 5: 10,000X diluted LAMP product ~0.05436 µg/ml*

The Lateral Flow Assay (LFA) results provide another dimension of validation for MART-V drying by testing serial dilutions of the LAMP product. Figure 5.4 presents the sensitivity data, showing that MART-V dried reagents could detect LAMP amplicons at dilutions up to 1,000-fold, maintaining a detectable concentration down to approximately 0.5 µg/mL. This sensitivity matches conventional expectations for fresh LAMP assays and supports the capability of MART-V dried reagents to retain functional activity for pathogen detection across variable sample concentrations.

5.3.2 Lyophilisation

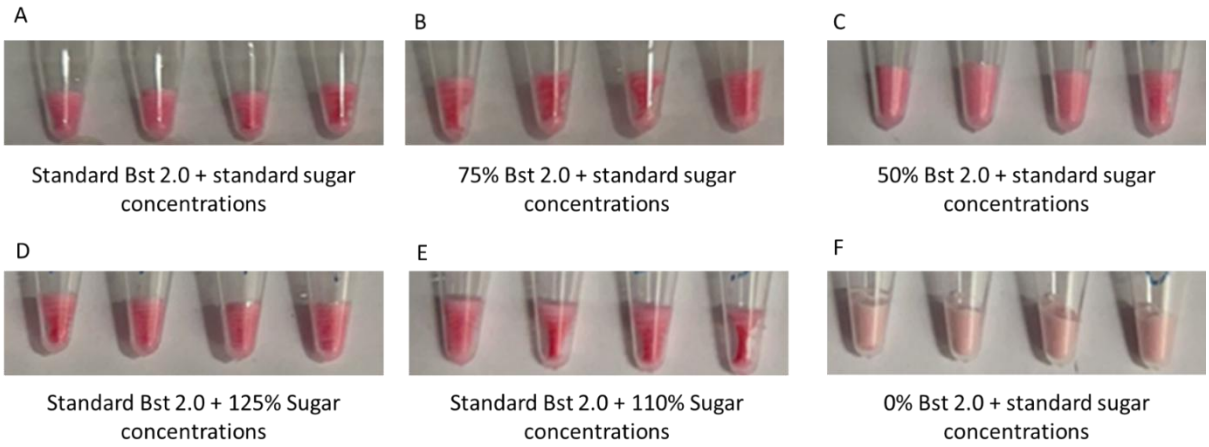

Figure 5.5 ***Lyophilised pH-independent LAMP product with varying levels of Bst 2.0 enzyme and sugar (Trehalose and Dextran) concentrations****. (A) – (C) have kept the standard sugar concentrations but have incremental changes in Bst 2.0 enzyme concentration. (D) and (E) have kept the standard Bst 2.0 enzyme concentration but have 25% and 10% more sugar concentration respectively. (F) lyophilised pH-independent LAMP with no Bst 2.0 enzyme solution within the reaction mix at all*

The initial reagent mixes of trehalose, dextran, and BSA consistently produced collapsed structures following freeze-drying, prompting a series of experiments aimed at addressing this issue. The initial assumptions were that we did not include enough sugar within our solution mix. This is due to their stabilizing qualities, as well as stress protection effects they have during the freeze-drying process[166,167]. However, from Figure 5.5, we can see that increasing sugar concentration had no effect on the outcome of the freeze-drying, and we would still get inconsistent collapsed structures. What was noticeable from the results was that lowering Bst 2.0 concentration was producing visible improvements on the state of the structure, to the point that when we removed Bst 2.0 enzyme completely, the structures were

perfect. It was suspected that this was due to the high concentrations of glycerol within the Bst 2.0 enzyme buffer.

A higher stock concentration of Bst 2.0 was then adopted in the reaction mixes, increasing from 8,000 U/mL to 120,000 U/mL. This adjustment reduced the total volume of Bst 2.0 enzyme buffer required in the pH-independent mix, subsequently lowering the glycerol content. As a result, stable lyophilised structures were successfully produced.

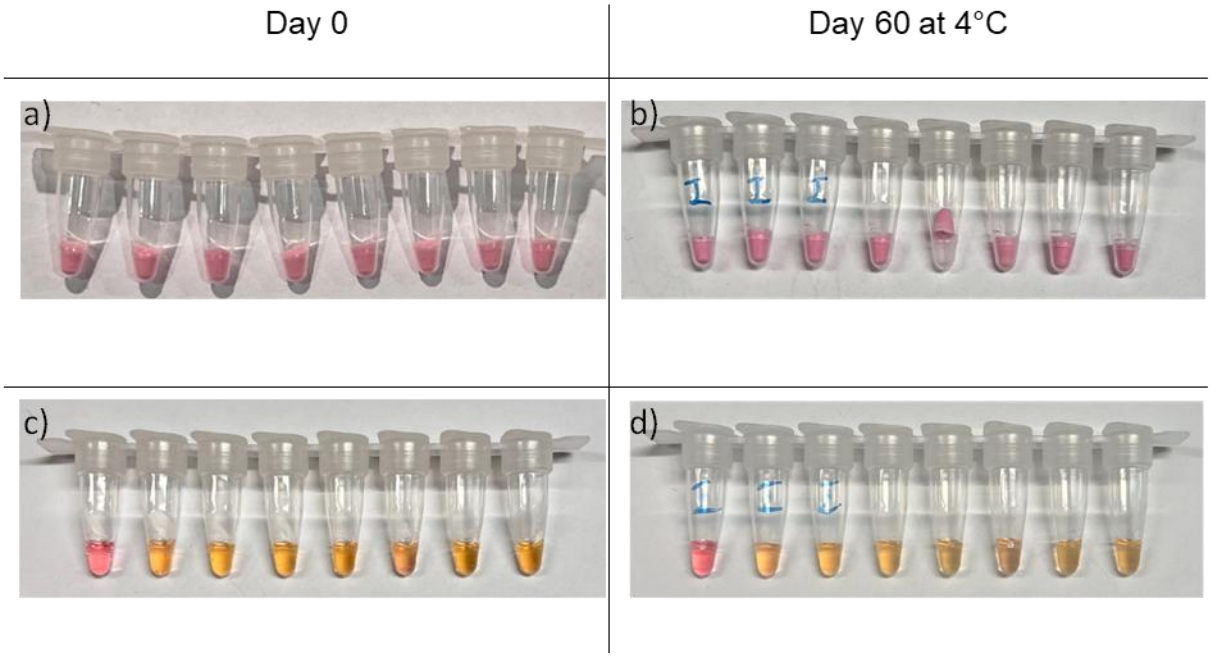

Figure 5.6 ***Analytical sensitivity of freeze-dried pH-independent LAMP assays and shelf-life verification.*** *A) Image of the initial batch of successfully made freeze-dried pH-independent LAMP assay. Fully solid with no collapsed structures. B) Freeze-dried assays kept in 4 °C conditions for just over two months straight after freeze-drying procedure. Fifth reaction tube from the left contains a dislodged product due to movement during transport. Has no effect on reaction performance. C) Colour change of freeze-dried assay set (A) after LAMP reaction run with HSV gDNA concentrations 0, 10, 20, 40, 80, 100, 250, 500. Verifying maintenance of sensitivity after freeze-drying using optimised formulation. D) Colour change after 40 minutes LAMP reaction using stability test freeze-dried assay. Concentrations of HSV gDNA tested are 0, 10, 20, 40, 80, 100, 250, 500 copies/reaction from left to right.*

After successfully optimising and implementing the freeze-drying formulation into pH-independent LAMP assays (same assay as detailed in Chapter 6), reactions were shown to maintain the same sensitivity of 10 copies per reaction and reaction time levels of 40 minutes for HSV gDNA when compared with non-freeze-dried assay counterparts. The stability of the lyophilised kit was evaluated again after leaving the kits at 4 °C for two months. Results from Figure 5.6 show us that our test assays were able to maintain validity after two months. Further shelf-life experiments, such as leaving lyophilised test assays for even longer and at higher temperatures, can be done in the future to ascertain the length of time it would take for our tests to begin losing effectiveness. The freeze-dried pH-independent LAMP assays were subsequently evaluated on HSV clinical swab samples to test their efficacy in real-world conditions. The results of these tests, along with further details, are presented in the following chapter.

5.4 Discussion

The stability achieved through MART drying addresses significant barriers in molecular diagnostics. MART drying allows for the preparation of reagents that can be stored and used in non-refrigerated settings, enabling broader POC applications. The success of the LFA with MART dried RT-LAMP reagents demonstrates that diagnostic tools can achieve sensitivity and specificity without the need for cold storage. Although lyophilisation offers a longer shelf life under refrigerated conditions, MART drying proves advantageous for environments where refrigeration is unreliable or unavailable. MART-V drying, in particular, facilitates rapid drying without exposing reagents to freezing stresses, which can destabilize certain proteins. By avoiding complex freeze-drying infrastructure, MART drying also presents a cost-effective alternative that aligns with the economic constraints of POC testing.

Current diagnostic workflows often depend on lyophilised reagents or cold-chain-stored liquid formulations, both of which pose challenges for transport, storage, and cost. Diagnostic manufacturing is largely concentrated in specialised contract manufacturing organisations, which tend to require high minimum order quantities and are not always suited to small-scale or local production needs. Much of the existing market remains reliant on traditional platforms that are not easily scalable or adaptable for low-resource environments [168]. In contrast, MART drying provides a more flexible and streamlined process that could enable the on-site or near-site manufacture of ambient-stable diagnostic kits without the need for high-end instrumentation.

Importantly, the MART technique is not limited to LAMP-based assays. With appropriate formulation optimisation, it holds potential for stabilising reagents used in qPCR, CRISPR-based diagnostics, and even immunoassays such as ELISAs. This versatility is particularly relevant given the global push toward developing ready-to-use, thermostable diagnostic platforms, especially in regions where consistent refrigeration cannot be guaranteed.

For MART drying to become widely adopted, further development is required in several key areas. These include establishing robust formulations that work reliably across a range of enzymes and assay types, conducting both accelerated and real-time stability testing under international stability conditions (such as 25 °C at 60% relative humidity and 40 °C at 75% relative humidity), and standardising the drying process to ensure reproducibility between batches. In addition, it will be important to evaluate the compatibility of MART-dried reagents with commercial-scale dispensing and packaging equipment, as this would affect their viability for broader production. Finally, regulatory validation will be essential, especially if MART-based kits are to enter clinical markets that require CE-IVD marking, WHO prequalification, or FDA approval.

Further research could explore the effects of varying matrix compositions and drying conditions on reagent stability. Additionally, investigations into the molecular mechanisms underlying MART drying's stabilization effects could refine formulations for diverse LAMP applications, enhancing the diagnostic utility across different disease markers.

Drying extends the usability of molecular diagnostics, making tools like RT-LAMP accessible to resource-limited settings. Development of these techniques is crucial for deploying LAMP in remote or under-resourced areas, where POC testing is most needed.

Chapter 6 Development of lyophilised pH-Independent colorimetric LAMP assays and integration into multiplex testing device

6.1 Introduction

LAMP results could be readout by fluorescence by adding fluorescent dye, turbidity, or electrophoresis. However, these methods all required specialized reading equipment, posing a barrier in resource-limited settings due to cost and availability [169–171].

In contrast, colorimetric LAMP assays are visible to the naked eye, making them ideal for POCT. They offer simplicity, cost-effectiveness, and rapid results, crucial in low-resource areas and situations needing quick decision-making [120,172–175].Traditional colorimetric LAMP assays, however, have a significant limitation due to their reliance on pH changes, usually indicated through colour shifts by pH indicators [176,177]. This reliance on pH shifts limits the applicability of the LAMP assay in different clinical sample types, as the assay's accuracy can be compromised by the sample's inherent pH or pH of the transport medium [178,179].

In this work, an innovative approach that employs a Zinc and 5-Br-PAPS (ZBP) system is used as a simple readout in the colorimetric LAMP assay [76,77,180]. The ZBP colorimetric system is based on the interaction between zinc ions and a colorimetric indicator, such as 5-Br-PAPS (5-bromo-2-pyridylazo-5-diethylaminophenol sulfonate), which is a metallochromic indicator. This system was previously used for the detection and quantification of zinc and other metal ions in various samples [75,181–183]. In the presence of zinc ions, 5-Br-PAPS forms a complex with zinc, which results in a pink colour. When LAMP DNA amplification cycles commence, pyrophosphate molecules are released into solution [76,184] that have a higher affinity to zinc ions than the 5-Br-PAPS [76,185], the 5-Br-PAPS returns to its original state, showing yellow colour. Therefore, the colour changing was no longer related to the pH.

In addition to addressing the pH-dependency issue, this research further enhances the LAMP assay's practicality by incorporating freeze-drying techniques. Freeze-drying, or lyophilization, is a technique extensively used in the pharmaceutical and biotechnological industries to increase the stability and shelf life of products [186–191]. This process involves the removal of water from a frozen sample through sublimation, converting ice directly into vapor without passing through a liquid phase [190,192,193]. Freeze-drying has numerous applications, including the stabilization of pharmaceuticals, preservation of food, and preparation of biological samples for transport and long-term storage [194–199]. In the context of diagnostic assays, freeze-drying offers several advantages. It enhances the stability of biological reagents, facilitates the transportation and storage of diagnostic kits at ambient temperatures, and minimizes the risk of contamination [200–203]. This method is particularly advantageous for diagnostic tests that need to be distributed and used in various geographical locations, including those with limited access to refrigeration and sophisticated laboratory equipment [204–207].

Herpes Simplex Virus (HSV), encompassing HSV-1 and HSV-2, is a pervasive human pathogen known for causing oral and genital lesions, along with other serious medical conditions such as encephalitis and neonatal herpes [208–212]. The global prevalence of HSV infection underscores the need for efficient, rapid, and accurate diagnostic techniques [213,214]. HSV diagnosis traditionally relies on methods like viral culture, serological testing, and polymerase chain reaction (PCR) [215–219]. However, these methods often require sophisticated laboratory facilities and prolonged processing times, posing challenges in resource-limited settings [220,221]. Early and accurate diagnosis of HSV is important not only for initiating timely antiviral therapy but also for preventing transmission, especially in cases of neonatal herpes, which can be fatal or cause serious long-term health issues in infants [222–226]. The development of this pH-independent LAMP assay for HSV can be of critical help in the field of virology and public health [51,204,227–229].

In this work, rigorous optimisation for various buffer, enzyme, and salt concentrations had to be done to ensure rapid and efficient test results. Then, a pH-independent assay for detecting HSV samples was developed and was further lyophilised for enhancing the thermostability. The lyophilised kits were validated by genomic DNA and clinical samples.

In this chapter, I also explored the integration of OxLAMP, the culmination of improvements from the previous chapters, into a multiplex diagnostic platform. OxLAMP is now employed in a device that can simultaneously test for multiple pathogens from a single patient sample. This is achieved using a colorimetric reader, specifically the Sinopharm thermostatic photometer, which monitors real-time colour changes in each reaction well, providing a quantitative analysis every 20 seconds. This device was custom-built for Oxsed [230], an Oxford University spin-out company, and is currently not on the market.

Figure 6.1 ***Sinopharm Colorimetric Reader****. The Sinopharm thermostatic photometer is used to track real-time colour changes in LAMP reactions. This model was custom-built for Oxsed Limited* [230] *to facilitate high-throughput diagnostics, capturing images every 20 seconds for*

RGB digital analysis. The machine enables precise determination of time-to-threshold values for pathogen detection across a full 96-well plate.

The Sinopharm reader functions by capturing images of the samples at these 20-second intervals using a temperature-controlled photometer. These images are converted into RGB digital format, where the mean of the initial five measurements is established as the baseline average. Subsequently, the colour metric, calculated as the variance between the instantaneous measurement and the baseline average, is documented throughout the reaction process. A colour metric exceeding 2.5 marks the determination of the LAMP TT (time-to-threshold) values, providing precise colorimetric assessment. This method allows for earlier and more reliable detection of positive results by eliminating the subjectivity associated with naked-eye interpretation, especially in cases where colour change is ambiguous, such as when the test appears orange rather than fully yellow.

By tracking the colour index over time and pinpointing when the colour change surpasses a pre-set threshold, the Sinopharm reader accurately marks a positive result. With a capacity to monitor up to 96 wells at once, this system enables high-throughput diagnostics, allowing for simultaneous detection of multiple pathogens or varying concentrations of a single pathogen across wells. This capability is especially valuable for rapid and comprehensive testing, providing both sensitivity and specificity in pathogen detection while reducing human error.

Through this integration, OxLAMP becomes a powerful tool for multiplex diagnostics, expanding its potential in clinical and resource-limited settings alike.

6.2 Materials and methods

6.2.1 Materials

Deoxyribonucleotide triphosphate (dNTP) (N0447L), Bst2.0 WarmStart Enzyme [M0537M], and Magnesium Sulphate solution (B1003S) were purchased from New England Bioscience, UK. Potassium Chloride (P3911), 5-Br-PAPS (93832), Zinc Sulphate solution (Z2876), Tris hydrochloride (10812846001) were obtained from Sigma-Aldrich, UK. SYTO™ 9 Green Fluorescent Nucleic Acid Stain (S34854) and UltraPure™ DNase/RNase-Free Distilled Water (11538646) were acquired from Thermo Fisher, UK. GoTaq® qPCR Master Mix (A6001) was purchased from Promega, UK.

6.2.2 Primer design

LAMP primers have been designed to target the DNA polymerization gene (NCBI, X14112.1:62807-66514) for the detection of HSV. Utilizing PrimerExplorer V5 (https://primerexplorer.jp/e/), primer sets for LAMP were developed, each comprising six primers: F3, B3, FIP (F1c-F2), BIP (B1c-B2), LF, and LB.

The primers were synthesized by Integrated DNA Technology, EU, and reconstituted with DNase/RNase-free water. 10x HSV primer mix was prepared in the concentration of 16 μM for FIP and BIP, 2 μM for F3 and B3, and 4 μM for LB and LF. The sequences of each primer are listed in the table below [231].

Table 6.1 HSV LAMP primer sequences

FIP	**GCGGTGAGGACAAAGTCCTGG ATTTTTCGTCCTCGTAGACGCCCA**
BIP	CGCGTACACCAACAAGCGCCTTTTTA TGGACGGGACCTGCG
F3	TGCCCGAGGGACTGCA

B3	TCACGTACGGGATCCGG
LF	CTCTCCGGGTCGGTGATGCG
LB	GGT GTA TTA CAA GCT CAT GGCC

6.2.3 Reaction conditions

The reaction conditions were optimised upon previous work done with phenol red colorimetric LAMP [27]. Seven separate pH-independent LAMP master mixes were made each containing a different concentration of Zinc and 5-Br-PAPs. Different concentrations of HSV gDNA, as well as nuclease-free water negative controls, were tested for all seven master mix reactions. The LAMP tests were run in a qPCR machine (CFX-OPUS 96, Bio-Rad) for one hour at 65°C. After establishing the optimum combined concentration, the ratio between zinc and 5-Br-PAPs was then adjusted and tested in triplicate repeats of 250 copies/reaction HSV gDNA, 500 copies/reaction HSV gDNA, and duplicate negative controls for each assay.

We tested 20 mM, 40 mM, 60 mM, 80 mM, 100 mM, and 120 mM concentrations of Potassium chloride (KCl), as well as 0mM KCl negative controls, within the standard pH-independent LAMP reaction mix. A master mix for each KCl concentration in pH-independent LAMP was made, and each was divided into 24 reaction wells, allowing for testing triplicates of eight different concentrations of HSV gDNA: 0, 25, 50, 75, 100, 200, 250, 500 copies/reaction. All reactions were run in a BioRad-qPCR machine at 65 °C for one hour.

Once an optimal KCl concentration was selected, it was then used as a set KCl concentration within the pH-independent LAMP reaction mix as the effects of different Tris-Hydrochloride (Tris-HCl) concentrations were tested. 8 mM, 16 mM, 25 mM, 32 mM, and 40 mM concentrations of Tris-HCl, as well as 0 mM negative controls, were tested within pH-

independent LAMP reaction mixes. Master mixes with each respective concentration of Tris-HCl were divided into reaction wells to test triplicate of 0, 25 and 50 copies/reaction of HSV gDNA. All reactions were run in a BioRad-qPCR machine at 65 °C for one hour.

To optimise the reaction, the concentrations of components were tuned against the LAMP Time to threshold (TT) values based on the fluorescent signal. Lower TT values indicate a faster reaction. The optimised components of colorimetric LAMP assay are listed in Table 6.2.

Table 6.2 The optimised components for pH-independent colorimetric LAMP assay.

Components	Concentration	Volume (μL) per 25 μL reaction volume
Deoxyribonucleotide triphosphate (dNTP)	10 mM	4.5
Bst 2.0 WarmStart Enzyme	8 U/μL	2
Potassium Chloride (KCl)	2.5 M	0.6
Zinc Sulphate ($ZnSO_4$)	2.5 mM	0.25
5-Br-PAPS	5 mM	0.25
Tris-Hydrochloride (Tris-HCl)	1 M	0.8
Magnesium Sulphate ($MgSO_4$)	100 mM	2
1X Primer mix	44 μM	2.5
SYTO™ 9 Green Fluorescent Nucleic Acid Stain	25 μM	0.5

Quantified HSV full-length gDNA (LGC, UK) was serially diluted to their appropriate concentrations with DNase/RNase-free water. DNase/RNase-free water or human whole genomic DNA was added to reactions for negative controls.

Reactions were run at isothermal 65°C for one hour. pH-independent LAMP was run in parallel on a qPCR machine (CFX-OPUS96, Bio-Rad) as well as a colorimetric reader (Sinopharm). The fluorescent stain Syto 9 was added for the fluorescent signal, which was recorded by the FAM channel every 20 seconds on the qPCR machine.

6.2.4 Manganese Sulphate / 5-Br-PAPS experiments

100 μM of Manganese Sulphate ($MnSO_4$) and 75 μM of 5-Br-PAPs were incorporated into pH-independent LAMP assays in replacement of the Zinc Sulphate/5-Br-PAPS colorimetric system. Nuclease-free water negative controls as well as different concentrations of HSV gDNA were then tested to see the efficacy of this colorimetric system in LAMP. Optimisation experiments followed that included testing higher concentrations of $MnSO_4$ by increments of 20 μM up to 200 μM. Lowering the 5-Br-PAPS concentration down to 50 μM was also attempted to try and improve colour outcomes. All reactions were run in a BioRad-qPCR machine at 65°C for one hour.

6.2.5 Experiments on the effects of pH on colorimetric pH-independent LAMP assays versus phenol red LAMP assays

Various concentrations of Tris-HCl and HCl were diluted and tested with pH meter machines (MT30266626, Sigma-Aldrich) to achieve a range of solutions with pHs ranging from two to nine.

Triplicates of nuclease-free water negative control alongside 125 and 250 copies/reaction HSV gDNA positive control were tested on colorimetric pH-independent LAMP as well as traditional phenol red pH-indicator colorimetric LAMP. Reaction mixes were divided into eight separate columns of a qPCR plate for both types of LAMP reaction in order to test the eight prepared pH solutions. When mixing the reagents together, during the process of adding nuclease-free water and sample to make up a 25 μL reaction, 5 μL of each pH solution were added to their respective reaction mixes. Negative and positive controls were also diluted to the required quantity using the prepared pH solutions to mimic acidic and alkaline samples being added to LAMP reactions. All reactions were run in BioRad-qPCR machine at 65°C for 40 minutes.

6.2.6 Freeze-dry procedure

The pH-independent LAMP master mix containing HSV primers was supplemented with sugars and bovine serum albumin (A7906, Sigma. UK). Once all components were dissolved, the solution was aliquoted into PCR tubes (Thermo Fischer, UK), and the liquid was centrifuged to remove any air bubbles. The PCR tubes were then placed on ice before being transferred to a freeze dryer.

The freeze dryer (Christ Epsilon 1-4) was cleaned with PCR clean and 70% ethanol, and then wiped with DNase/RNase-Free water. Subsequently, all PCR tubes were loaded into the freeze dryer. The shelf temperature was gradually cooled at 1°C/min until reaching -40 °C, where it was held for 2 hours before initiating the vacuum pump. Ice crystals underwent sublimation at -40 °C under a vacuum with a pressure lower than 50 mTorr. After an 8-hour primary drying, the shelf temperature was increased at 0.5 °C/min up to 20 °C and maintained at 20 °C for 1 hour before shutting down the freeze dryer. To release the vacuum, ambient air was purged

into the freeze dryer. The PCR tubes were capped immediately after removal from the freeze dryer.

6.2.7 Optimisation of lyophilisation formulation

A lyophilisation reaction mix for pH-independent LAMP refers to the total reagent combinations within the solution optimised for freeze-drying. Different combinations of Trehalose and Dextran sugar concentrations were mixed and incorporated in the lyophilisation mix of pH-independent LAMP. Different combinations of Bst 2.0 enzyme, as well as sugar, were prepared and embedded into separate pH-independent LAMP mixes. Each reaction mix was loaded into a freeze-dryer. The freeze dryer (Christ Epsilon 1-4) was cleaned with PCR clean and 70% ethanol, and then wiped with DNase/RNase-Free water. Subsequently, all PCR tubes were loaded into the freeze dryer and run in the same reaction conditions as above.

6.2.8 Clinical sample preparation and test

Ethics: The protocol for the use of residual clinical samples at OUH John Radcliffe Hospital, as described in this manuscript, was reviewed by the Research Governance Team of OUH and determined to constitute service evaluation and development. As such, this study was deemed to not require research ethics review.

Previously de-identified clinical samples, human lesion swabs in BD universal transport medium, were heat-inactivated at 95 °C for 10 minutes. After cooling down to room temperature, the samples were diluted by using nuclease-free water to the appropriate quantity.

1 μL of each clinical sample was added to freeze-dried pH-independent assays, and then run at 65 °C for one hour.

6.2.9 qPCR assay

DNA extractions of clinical samples were carried out using QIAamp DNA Micro Kit (QIAGEN, 56304) following manufacturer's protocol. Samples are lysed in a buffer that ensures the thorough breakdown of cellular structures, releasing the DNA into solution. Proteinase K is used in this step to digest proteins and enhance DNA yield. After binding and washing steps, purified DNA is eluted in a small volume of nuclease-free water.

We used the GoTaq qPCR master mix (A6001, Promega) with a 1.5 μL primer mix to assess the Ct values of the samples. HSV primer set (IDT) was used for HSV detection. Primer sets contain 100 μM forward and backward primers. After adding 5 μL of the sample solution, the final reaction volume was increased to 20 μL by adding RNase/DNase Free water. The PCR cycle conditions were set according to the manufacturer's instructions. The solutions were initially denatured for 2 min at 95°C. Then, 45 cycles of 3 sec at 95 °C and 30 s at 55 °C were processed. PCR primers targeting the DNA polymerase gene reported by Kessler et al were adopted to detect both HSV subtypes [232].

6.2.10 Multiplex colorimetric data for HSV gDNA and HSV clinical sample using Sinopharm reader

To implement this protocol, a pH-independent LAMP mix with HSV-specific primers was prepared and then freeze-dried following the procedures outlined above. After freeze-drying, the assay was rehydrated with water, carefully adjusted to achieve the appropriate

concentration for optimal LAMP reaction conditions. Once the assay was reconstituted, a controlled concentration of HSV gDNA at 100 copies per reaction was added to the reaction mix, setting up the sample for colorimetric analysis. The mix was then placed in the Sinopharm colorimetric reader and monitored over a 40-minute period. Using the Sinopharm thermostatic photometer, real-time colour changes were captured at 20-second intervals, converting the visual colour shift into an RGB colour index. To ensure robust and reproducible data, each reaction was conducted in triplicate, with negative controls included to establish a baseline and verify assay specificity. The colour index data gathered over time was subsequently plotted as a line graph, visually representing the progression of colour change in the HSV sample and highlighting the precise time points where amplification led to detectable shifts in colour. This initial test served as a proof-of-concept, demonstrating the reader's capacity to detect HSV DNA reliably via a standardized colorimetric threshold.

Following the success of initial tests, the assay was applied to clinical samples to further validate compatibility for real-world diagnostics. Informed by findings from clinical validation, where compatibility with clinical samples was established, clinical swab samples were prepared by diluting each one at a 1:10 ratio to standardize the input concentration, ensuring a consistent addition of 1 μL per assay. These clinical samples were run in triplicate, with duplicate negative controls, and placed in the Sinopharm colorimetric reader for a 40-minute run. The colorimetric data from these clinical samples further confirmed the assay's applicability in clinical diagnostics, supporting its use in detecting pathogens directly from patient-derived samples without extensive preparation.

To showcase the multiplex capabilities of the OxLAMP system with the Sinopharm colorimetric reader, testing was expanded to include multiple pathogens within a single run. gDNA samples for *E. coli*, *S. haemolyticus*, and HSV, along with bacterial cell suspensions of *E. faecalis* and *S. epidermidis*, from Chapter 3 were prepared. Each pathogen-specific sample

was loaded into the reader with its respective OxLAMP assay, demonstrating the system's versatility and high-throughput diagnostic capability by running all samples concurrently. The Sinopharm reader tracked the colour change for each well individually, allowing documentation of the time-to-threshold (TT) values for each sample. These TT values, marked by a specific colour index threshold, were recorded and plotted to enable a comparative analysis across the different pathogens and concentrations. The concentrations of each pathogen were chosen based on their colorimetric LAMP LODs established in previous chapters.

6.3 Results and Discussion

6.3.1 pH-independent LAMP Assay

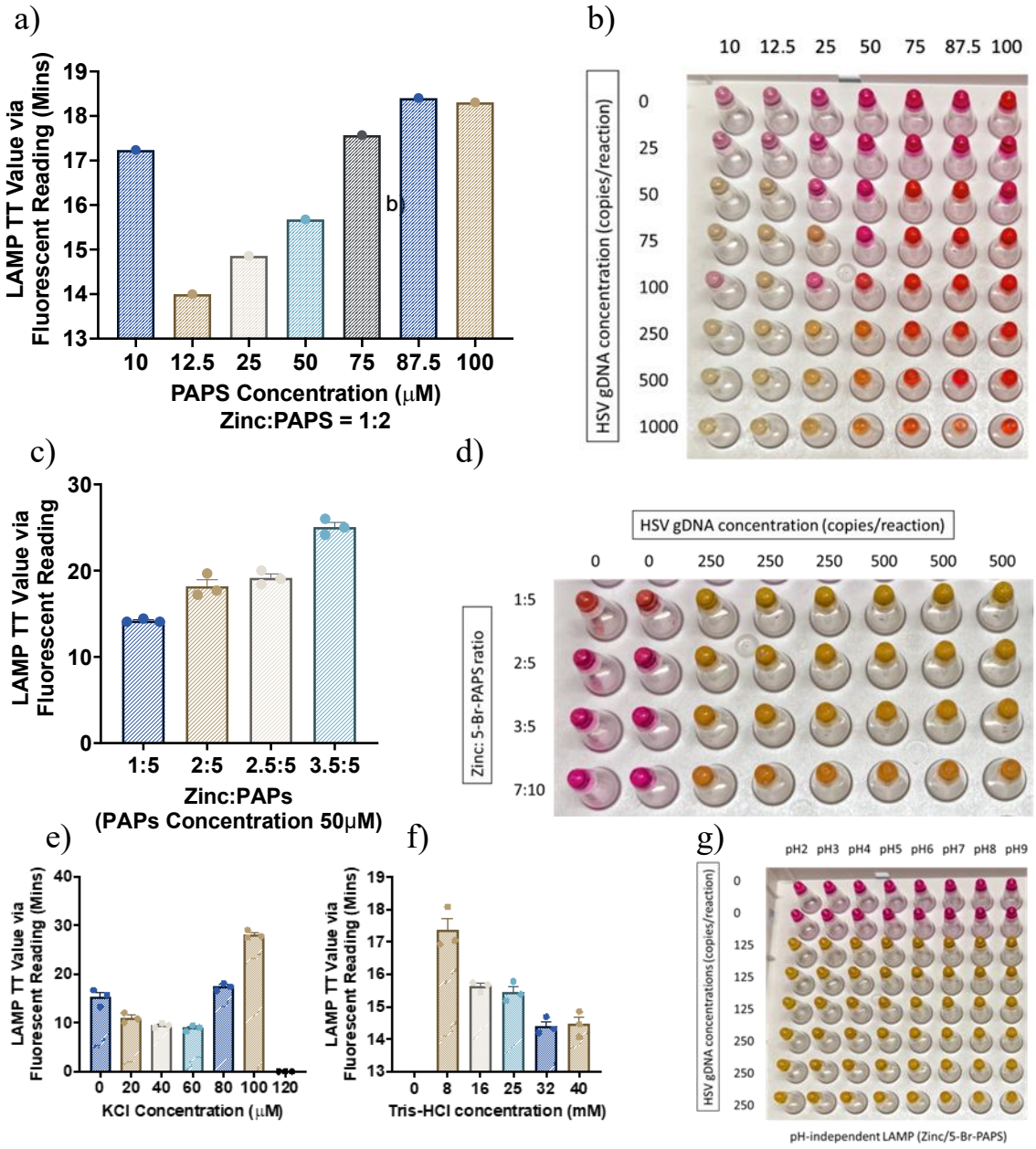

Figure 6.2 ***Optimisation of pH-independent colorimetric LAMP assay.*** *A) Fluorescence data showing reaction time performance of LAMP assays containing different concentrations of Zinc and 5-Br-PAPS. B) Colour change results of LAMP assays containing different concentrations of Zinc and 5-Br-PAPS after one hour LAMP reaction. Zinc:PAPS ratio is 1:2 C) Fluorescence data showing reaction time performance of LAMP assays containing different concentration ratios of Zinc and 5-Br-PAPS. D) Colour change results of LAMP assays containing different concentration ratios of Zinc and 5-Br-PAPS after 40 minutes LAMP reaction. E) Fluorescence data showing reaction time performance of LAMP assays containing different concentrations of KCl. F) Fluorescence data showing reaction time performance of LAMP assays containing different concentrations of Tris-HCl. G) Colour change results of pH independent LAMP in the context of different pH levels ranging from 2-9, testing 125 and 250 copies/reaction concentrations of HSV gDNA as well as nuclease free water negative control. Results are presented as MEAN ± SEM.*

Colorimetric Loop-Mediated Isothermal Amplification (LAMP) is well-suited for point-of-care (POC) testing, where the visibility of colour change indicating positive target amplification is crucial. The addition of zinc and PAPS could facilitate the pH-independent colour change [77]. However, directly adding Zinc and PAPS to the commercialized kit did not produce clear colour changes. Therefore, a formulation was developed to achieve valid colour changes. The reagents comprised Bst 2.0 polymerase, dNTPs, Tris-HCl, KCl, $MgSO_4$, $ZnSO_4$, and PAPs. The concentration of each component was optimized based on reaction rate and colour change visibility. Betaine, a common stabilizer in nucleic acid amplification, was removed due to its low glass transition temperature. The inclusion of betaine in the master mix lowered the glass transition temperature to about -60°C, significantly increasing the difficulty of freeze-drying.

Stoichiometrically, two parts of zinc ions would bind to one part of PAPS to generate the complex, resulting in a pink colour. After maintaining the same ratio, total amounts of Zinc-

PAPS complex were added to the reagents. Since zinc ion could replace Mg^{2+} to bind polymerase and reduce its activity[233,234], lowering the Zinc concentration in the reagents increases enzyme activity and leads to lower threshold time (TT) values (Figure 6.2a). Conversely, when the complex concentration is too low, such as 10 μM in the master mix, the reaction is considerably hindered. This hindrance may be due to the low ion strength, which decreases the solubility of the polymerase, thereby reducing the efficiency of amplification.

Although the 12.5 μM Zinc-PAPS complex provides the highest reaction rate, the visibility of the pink negative control colour is compromised. The pink colour is not deep enough, resulting in a lighter and more transparent appearance. Therefore, a more balanced concentration of 25 μM Zinc Sulphate and 50 μM 5-Br-PAPS was selected initially for the bright pink negative control colour, with hopes that calibrating the Zinc to 5-Br-PAPS ratio would brighten the positive control yellow colour.

After optimising the amount of Zinc-PAPS complex, the ratio of zinc and PAPS was further refined. Compared to the original 25 μM Zinc, if we lower the Zinc concentration to 10μM, we get the fastest reaction speeds; however, from the colour change pictures we can see that the negative control pink colour becomes compromised. A slightly lowered Zinc Sulphate concentration, 20 μM, was selected as optimum instead, due to its maintenance of a bright pink colour for negative and least impact on slowing reaction time in comparison to higher concentrations. Zinc was favoured over other metal ions such as Manganese. Experiments conducted using Manganese did not work as an indicator, as can be seen in Figure 6.3.

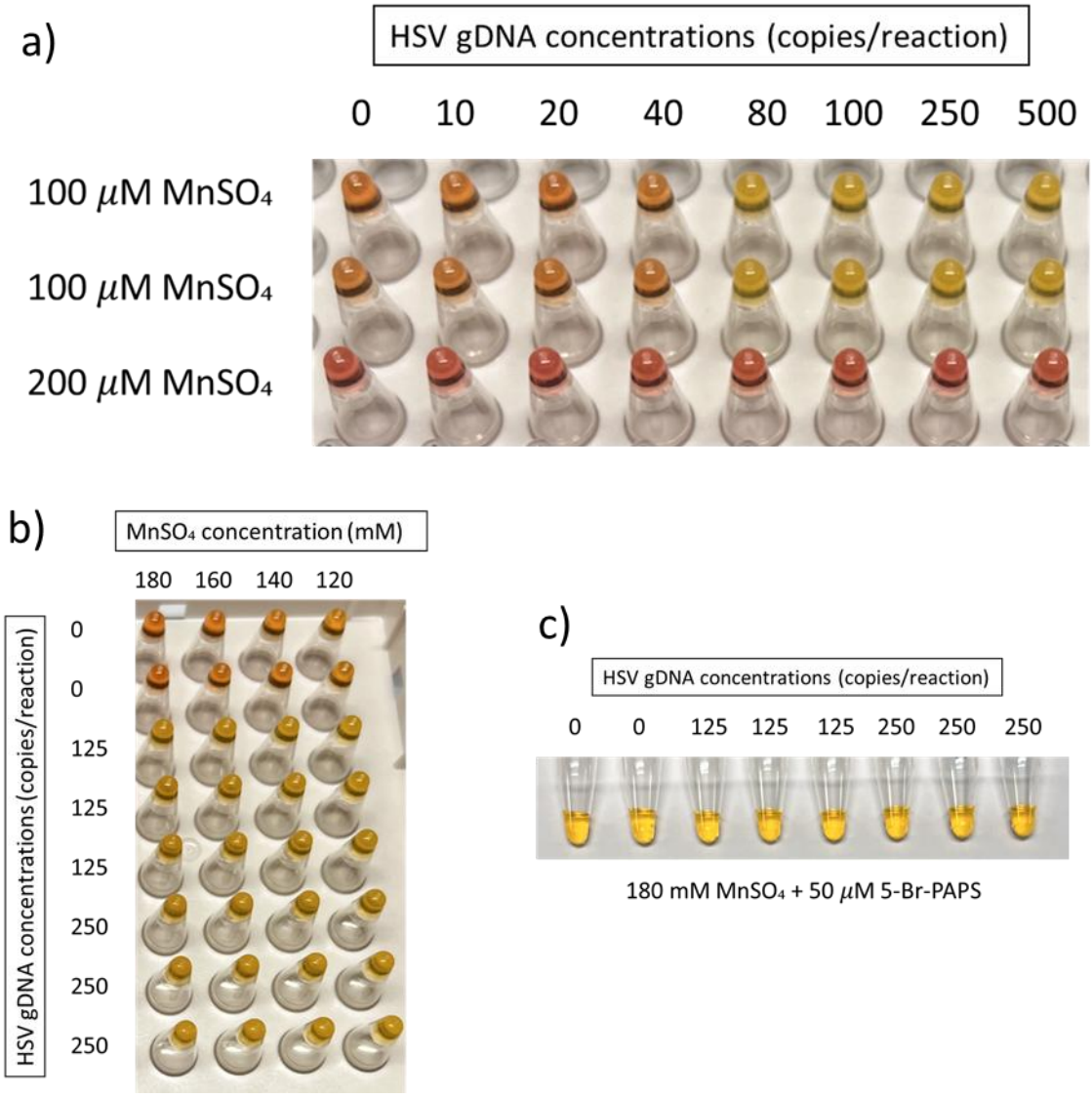

Figure 6.3 ***Colour change results of $MnSO_4$ + 5-Br-PAPS colorimetric system embedded within pH-independent LAMP reaction mix****. A) colour change results of duplicate repeat pH-independent LAMP reaction runs using 100 μM $MnSO_4$ + 75 μM 5-Br-PAPS and a singular reaction run using 200 mM $MnSO_4$ + 75μM 5-Br-PAPS, tested with various concentrations of HSV gDNA positive control and nuclease-free negative control. B) Colour change results of pH-independent LAMP using different concentrations of $MnSO_4$ ranging from 120-180 mM + 75 μM 5-Br-PAPS. Tested in triplicate repeats using 125 and 250 copies/reaction HSV gDNA and duplicate nuclease-free water negative control. C) Colour change results of pH-independent LAMP using 180 mM $MnSO_4$ and 50 μM PAPS. Tested in triplicate repeats using 125 and 250 copies/reaction HSV gDNA and duplicate nuclease-free water negative control.*

Initial results with $MnSO_4$ and 5-Br-PAPS showed us that although we can achieve a bright yellow positive result colour after a reaction run, the negative colour is very orange, as can be seen in Figure 6.3. In an attempt to turn the negative colour a more distinct pink, 200 mM of $MnSO_4$ was used, which was double the usual amount of 100 mM, and that proved to be too high a concentration. Resulting in positive control reactions with high quantities of HSV gDNA not being able to turn yellow after a reaction run. In order to find if there is a medium level of $MnSO_4$ that can make the reaction mix pinker without being too high a concentration, it delays the reaction time, a series of different $MnSO_4$ concentrations was tried between 100 mM and 200 mM. What we can see from Figure 6.3 is that the negative controls remained too orange. Another alternative was to lower the 5-Br-PAPS amount, but results show that even lower by 25 μM would turn the negative controls a bright yellow colour.

In the end, the $MnSO_4$ was not selected as the metal ion to combine with 5-Br-PAPS for our colorimetric system as it was not able to produce as distinct colours between positive and negative results as $ZnSO_4$ can.

Tris-HCl and KCl play crucial roles in maintaining the optimal reaction conditions necessary for efficient DNA amplification. Tris-HCl helps stabilize the DNA polymerase and protects nucleic acids from degradation, ensuring that the enzyme remains active throughout the isothermal amplification process [235]. Tris-HCl is also typically used to maintain the pH of a solution mix, important for stabilising enzymes and other reagents in a reaction mix [236]. KCl is used to adjust the ionic strength of the reaction mixture. The concentration of potassium ions can significantly affect the activity of DNA polymerases. Potassium ions are known to facilitate the binding of the polymerase to the DNA template, improving the efficiency of the amplification [237,238]. Therefore, optimising these reagents to maximise pH-independent LAMP outcomes is important.

Colour change results depicted in Figure 6.2 show us that ion levels within the assay do not affect the intensity of colour change, up until the rate of reaction is impacted so heavily at 120 μM KCl concentration that the reactions do not change colour within the set reaction time of one hour. The high KCl concentration was enough to inhibit amplification and colour change.

In terms of colour change sensitivity, all concentrations of KCl from 0-100uM achieve a 25 copies/reaction limit of detection within one hour. Colour change data of KCl optimisation experiments can be seen in Figure 6.4.

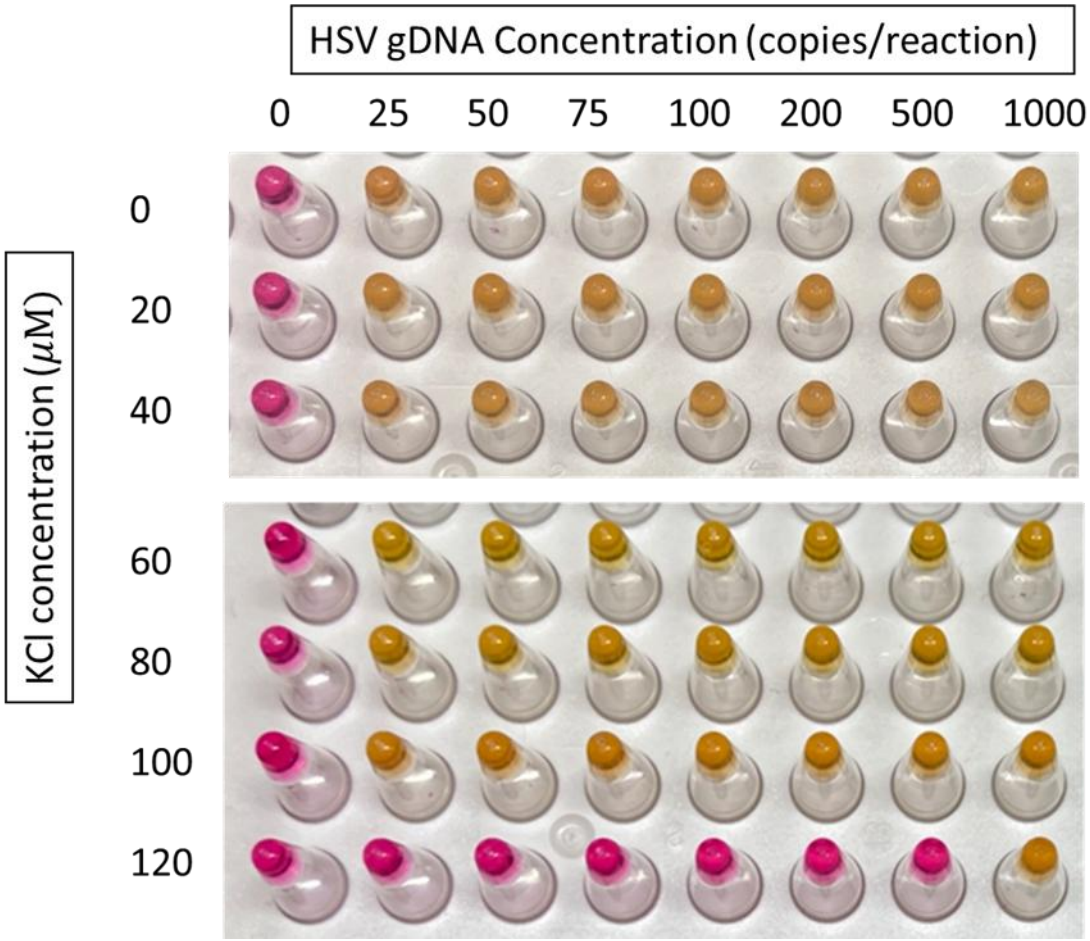

Figure 6.4 ***Colour change and fluorescence results of KCl concentration optimisation experiments for pH-independent LAMP****. Sensitivity test and colour change results of pH-independent LAMP with different concentrations of KCl after one hour reaction.*

When comparing the fluorescence results in Figure 6.2e, we can see that there are differences in reaction rate, with 40 μM and 60 μM KCl concentrations performing significantly better than the others. 60 μM was selected as the optimum KCl concentration, as a slight improvement in performance in reaction time by a minute or two was seen over 40 μM.

Using a 60 μM KCl concentration within the standard pH-independent LAMP reaction mix, Tris-HCl concentrations were compared to analyse reaction time performance. From the fluorescence data in Figure 6.2f, we can see that 32 mM outperforms 25 mM Tris-HCl concentrations, with 40 mM having a similarly short reaction time. 32 mM was selected as the optimum concentration in this instance

The main purpose of introducing a new Zinc/5-Br-PAPS colorimetric system into these LAMP reactions is for the testing to be resilient to samples and reagents with varying degrees of pH levels in samples. 5 μL sample was added. To verify the effectiveness of this system, we embedded these assays into different samples with varied levels of pH and analysed the results. From Figure 6.2g, we can see that all negative controls across the different pH levels for Zinc/5-Br-PAPS LAMP have remained consistently pink. The colour change performance for the HSV gDNA positive controls is also not hindered at any pH level.

6.3.2 Analytic sensitivity in fluorescent and colorimetric reading

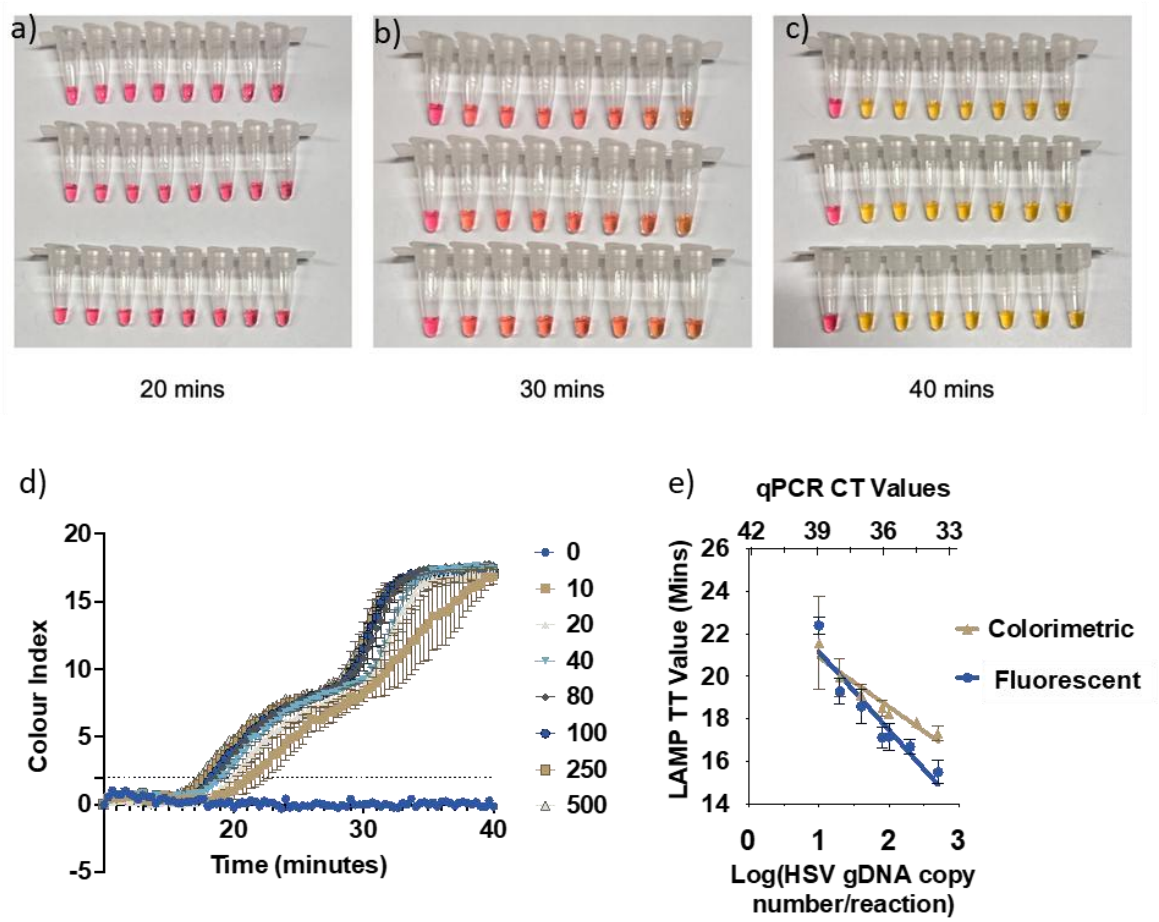

Figure 6.5 **Optimised ph-independent colorimetric LAMP.** *Images (A), (B), and (C) represent the same triplicate repeats of assays containing eight different concentrations of HSV gDNA: 0, 10, 20, 40, 80, 100, 200, 500 copies/reaction after 20, 30 and 40 minutes reaction times in dry incubators. D) Thermostatic photometer (Sinopharm) analysing colour change over 40 minutes of LAMP assays containing various concentrations of HSV gDNA each repeated in triplicate ranging from 10-500 copies/reaction. Each data point is the average reading of three repeats with MEAN ± SEM error bars. E) Fluorescence threshold time (TT) values derived from the principles of quantitative LAMP (qLAMP) correlated with HSV gDNA concentration per reaction. (F) The standard curve between Bio-rad qPCR Ct values and HSV gDNA copy numbers. Results were presented as MEAN ± SEM.*

The analytic sensitivity of the assay was evaluated by full-length genomic DNA of HSV-1. As shown in Figure 6.5, colour change can occur for all tested concentrations of HSV gDNA, 10 copies to 500 copies, after 40 minutes. The yellow colour indicating positive for sample amplification is very visible and distinct from the negative result of pink, meaning that the

colour optimisation for Zinc and 5-Br-PAPs was effective. Prior to reagent optimisations, reaction times would require close to one hour for visible colour change results, as can be seen in these Tris-HCl and Zinc Sulphate-PAPS optimisation experiments in Figure 6.2. Being able to hit a sensitivty of 10 copies per reaction (2 copies/μL) in 40 minutes represents a significant improvement.

To access the real-time colour change, a thermostatic photometer was used for acquiring the colour index of the samples during the incubation. As shown in Figure 6.5c, all HSV gDNA concentrations, ranging from 10 copies to 500 copies per reaction, can be detected before 40 minutes. For concentrations below 500 copies per reaction before 20 minutes, it would be impractical to ascertain slight differences in colour hue (pink vs slightly orange) with the naked eye after such little time as can be seen in Figure 6.5b, but a photometer indicates an uptick in colour index rating around that time (Figure 6.6d).

After setting the threshold (colour index=2), the time to threshold (TT) values based on colorimetric reading were obtained, which showed a high linearity against the concentration. In addition, each pH-independent LAMP assay is equipped with SYTO9 DNA intercalating fluorescent dye. Same dye that was used previously for this phenol-red colorimetric LAMP reactions when quantitative LAMP (qLAMP) was established for this assay. The same batch of samples was used for both colourmetric and fluorescent reading. Figure 6.5 highlights that qLAMP is able to detect positive sample results with a sensitivity of 10 copies per reaction, which was equivalent to CT= 38 in the qPCR assay, as early as 22 minutes.

The correlation of TT values based on fluorescent signal against concentration was also obtained for both colorimetric assays as well as qLAMP assays without the Zinc-PAPS colour change system. Figure 6.5 shows us that at lower HSV gDNA concentrations, there is no difference between the two, but as the gDNA template concentrations are higher, we see that

TT values for the pure qLAMP assays are much lower, meaning they have faster reaction speeds. The colorimetric index data presented in Figure 6.5d indicate that for HSV gDNA concentrations ranging from 0 to 500 copies per reaction, the times required for observable colour change are consistently within the 15 to 20-minute interval. This phenomenon may be attributed to the mechanism whereby the dissociation of zinc ions from 5-Br-PAP complexes is contingent upon surpassing a critical concentration threshold of pyrophosphate substrates. Such a threshold is likely achieved subsequent to sufficient cycles of loop-mediated isothermal amplification (LAMP), thereby precluding any observable acceleration in colour transition prior to the 20-minute mark despite the exponential increase in amplification rates. Consequently, a rapid alteration in colorimetric response is observed only after the in-solution concentration of pyrophosphate reaches this predefined threshold.

6.3.3 Freeze-drying of pH-independent colorimetric LAMP assay and test sensitivity

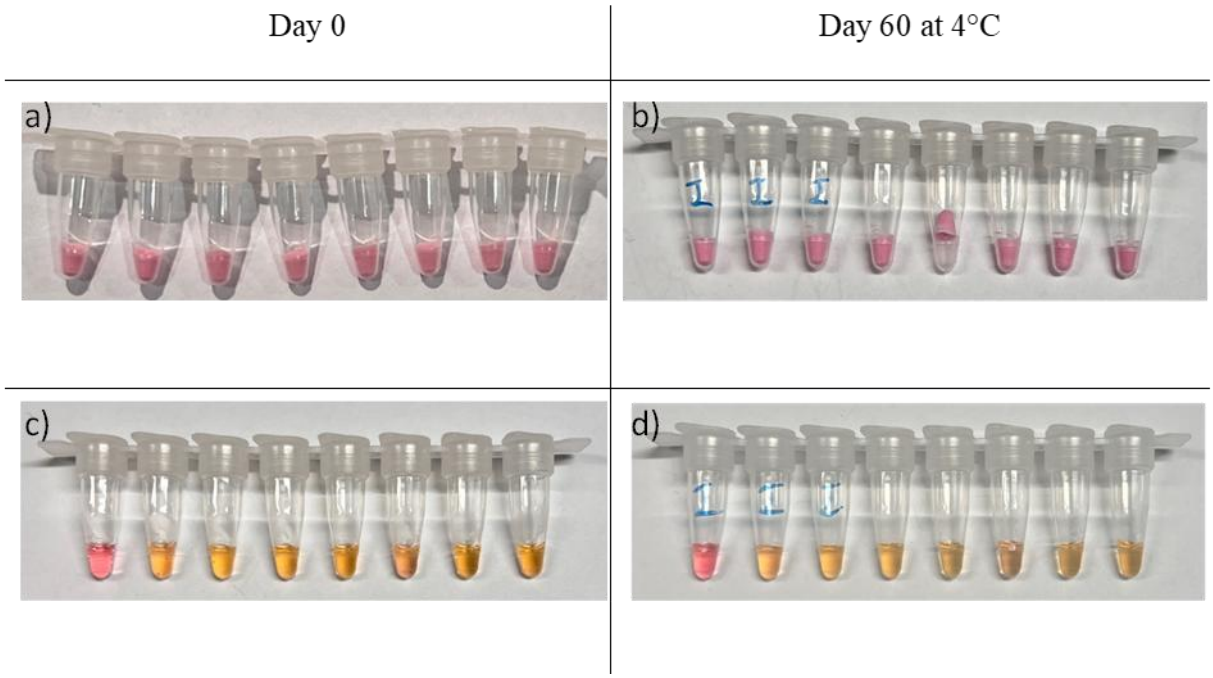

Figure 6.6 ***Analytical sensitivity of freeze-dried pH-independent LAMP assays and shelf-life verification****. A) Image of the initial batch of successfully made freeze-dried pH-independent LAMP assay. Fully solid with no collapsed structures. B) Freeze-dried assays kept in 4 °C conditions for just over two months straight after freeze-drying procedure. Fifth reaction tube from the left contains a dislodged product due to movement during transport. C) Colour change of freeze-dried assay set (A) after LAMP reaction run with HSV gDNA concentrations 0, 10, 20, 40, 80, 100, 250, 500. Verifying maintenance of sensitivity after freeze-drying using optimised formulation. D) Colour change after 40 minutes LAMP reaction using stability test freeze-dried assay. Concentrations of HSV gDNA tested are 0, 10, 20, 40, 80, 100, 250, 500 copies/reaction from left to right.*

The optimised HSV LAMP detection kit could reach the analytical sensitivity of 10 copies per reaction within 40 minutes. However, since reagents are temperature sensitive, the temperature for transportation needs to be maintained at -20 °C from manufacturing to the customer, which increases the cost and also limits the applications in POCT as fridge storage can be limited

[53]. To extend the shelf life, the reagents were supplemented with sugars and thermostabilised by freeze-drying. Results of the freeze-drying optimisation can be seen in data relating to Figure 5.5 of Chapter 5.

After freeze-drying, LAMP reactions were shown to maintain the same LOD of 10 copies per reaction and reaction time levels of 40 minutes when compared with non-freeze-dried assay counterparts.

The stability of the lyophilised kit was evaluated after leaving the kits at 4 °C for two months. Results from Figure 6.6 show us that these test assays were able to maintain validity after two months. Further shelf-life experiments, such as leaving lyophilised test assays for even longer and at higher temperatures, can be done in the future to ascertain the length of time it would take for these tests to begin losing effectiveness.

6.3.4 HSV clinical sample validation

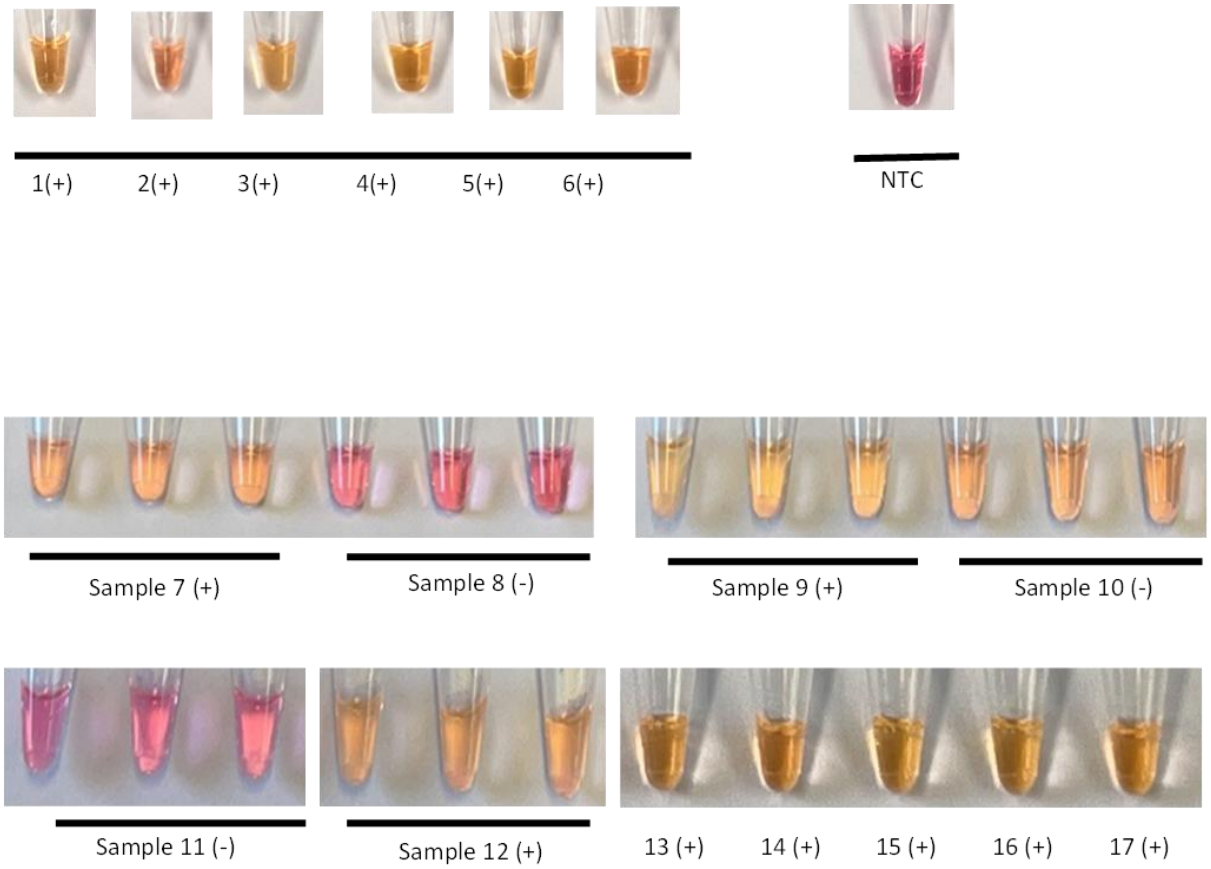

Figure 6.7 ***HSV Clinical Samples in Lyophilised pH-Independent LAMP and Colour Change Results****. Samples 1-6 were initial trial runs, all clinically diagnosed as HSV-positive, used to verify the effectiveness of the test with a 0.5 µL sample volume. These samples showed consistent colorimetric changes, confirming the test's functionality. Samples 7-12 were tested in triplicate, with samples 8 and 11 being HSV-negative and showing no colour change (remaining pink), while the other samples demonstrated positive results with a distinct colour change to yellow. Due to limited availability, samples 13-17 were tested individually but also produced positive results.*

After developing the thermostabilised HSV detection kits, a total of 17 clinical swab samples, including 15 HSV-positive and 2 HSV-negative samples, were used to validate the assays. The clinical results for these samples were predetermined using the BD ProbeTec™ Herpes

Simplex Viruses (HSV1&2) Qx Amplified DNA Assays, where DNA was extracted from the samples prior to nucleic acid amplification.

The application of the ZBP-LAMP assay in real clinical settings In a single-blind format would significantly validate the practical utility of these diagnostic tests. As shown in Figure 6.7, the direct addition of 0.5 µL from clinical samples 1-6, during the initial trial runs, consistently produced a clear positive colorimetric response for HSV-positive specimens. Following the success of these trials, samples 8-17 were tested in triplicate. Samples 8 and 11, which were negative for HSV, remained pink, indicating no colour change in this pH-independent colorimetric LAMP test. In contrast, the HSV-positive samples, 7 through 17, showed a distinct colour change to yellow, confirming positive results.

We plan to continue testing additional clinical samples as they become available. Additionally, future comparisons of the DNA extracted from these clinical samples, using both qLAMP and qPCR, will provide further insights into the test's accuracy and overall performance. To determine the number of clinical samples needed for a statistically robust validation of the test's specificity, an online sample size calculator for diagnostic studies was used (https://sample-size-calculator-69531.firebaseapp.com/). Based on prior expectations for the test, a specificity of 95% was input to the calculator, a disease prevalence of 30%, a maximum marginal error of 5%, and a confidence level of 95%. The required likelihood ratio Q was calculated as (1 – sensitivity) / specificity, which, using an expected sensitivity of 90%, resulted in a Q value of approximately 0.11. When these parameters were entered, the calculator estimated that a total sample size of 165 would be required to achieve the desired statistical precision. This sample size would allow for meaningful estimation of diagnostic specificity and support downstream analyses comparing the performance of the assay with qPCR.

6.3.5 Multiplex colorimetric Sinopharm reader results and discussion

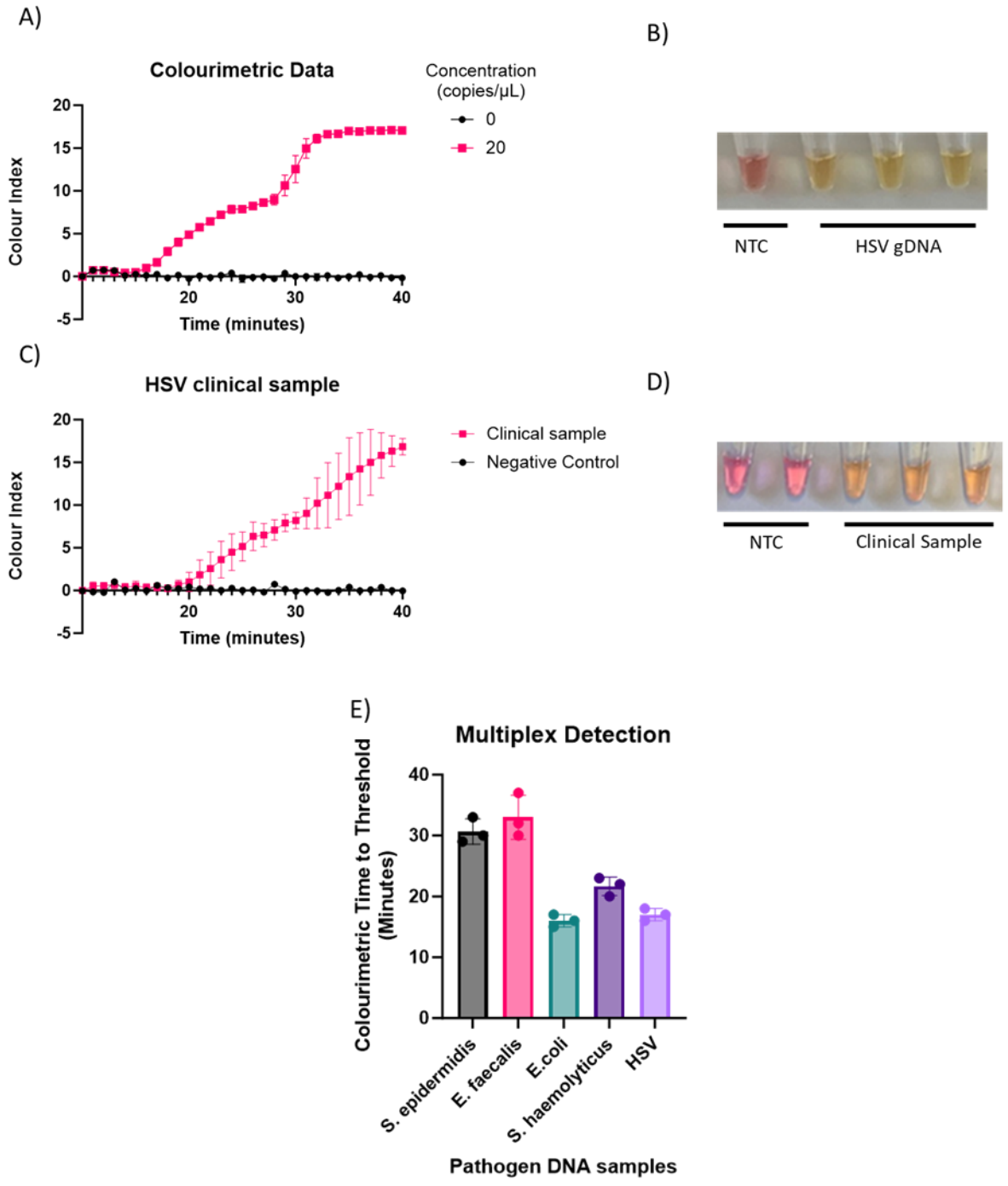

Figure 6.8 ***Colour index data of pH-independent colorimetric LAMP assay via colorimetric reading.*** *Each data point is the average reading of three repeats with images A and C having MEAN ± SD error bars and image E having MEAN + SEM error bars. A) Thermostatic photometer analysing colour change over 40 minutes of LAMP assays containing 100*

copies/reaction concentrations of HSV gDNA. B) Photos of LAMP reaction wells from image A after a 40-minute run in colorimetric reader. C) Thermostatic photometer analysing colour change over 40 minutes of LAMP assays containing HSV clinical sample repeated in triplicate alongside duplicate negative controls. D) Photos of LAMP reaction wells from image C after 40-minute run in colorimetric reader. E) Time-to-threshold results for five pathogen DNA samples run simultaneously on the colorimetric reader. This graph shows the time required to reach the colorimetric threshold for each pathogen, all run concurrently to demonstrate the reader's multiplex capability: S. epidermidis and E. faecalis at 2000 cells/reaction, E. coli and S. haemolyticus at 5 pg/reaction gDNA, and HSV at 100 copies/reaction gDNA.

The selected concentrations of bacterial and HSV DNA were based on the lowest concentrations that had previously yielded consistently positive results in earlier sensitivity tests. Upon comparing Figures 6.8a and 6.8c, despite potential differences in DNA concentration between the HSV gDNA and the clinical sample, their time-to-threshold (TT) values were remarkably similar. This observation supports the concept explored in Figure 6.5d, where the colorimetric response time is influenced by the mechanism of zinc ion dissociation from 5-Br-PAP complexes.

The larger standard deviation error bars observed in Figure 6.8c, representing clinical samples, likely result from inherent sample impurities and variability. Unlike purified gDNA, which is designed to yield highly consistent results, clinical samples contain a mix of extraneous materials (e.g., host DNA, proteins, and potential contaminants) that can influence amplification speed and consistency, introducing greater variance in the observed colour change.

Figures 6.8b and 6.8d demonstrate that post-run samples can still be effectively diagnosed by the naked eye, providing an additional diagnostic option beyond the colour index data. This could be particularly useful in field settings where immediate access to a colorimetric reader

may not be available, allowing for flexible diagnostic applications without compromising reliability.

Figure 6.8e highlights the successful generation of colour index data for all five pathogens, affirming OxLAMP's capability to diagnose multiple pathogens within a single reaction run. This multiplex diagnostic setup, tested under a range of conditions, offers a substantial advantage in scenarios where rapid and simultaneous pathogen identification is essential. Analysis of the TT values across the panel reveals that bacterial colony samples reached the threshold more slowly than the purified gDNA samples, with S. haemolyticus being the slowest among the group. This was followed by E. coli and HSV gDNA, which had nearly identical TT values, indicating faster amplification in these purified samples. The slower response times in bacterial colony samples likely stem from sample impurities and the additional cellular material present, which could disrupt the efficiency of the amplification process and delay threshold achievement by approximately 10 minutes.

This multiplex run successfully demonstrates the potential of OxLAMP in simultaneous multi-pathogen diagnostics, showcasing its efficiency and adaptability. Through this experiment, OxLAMP, in conjunction with the Sinopharm colorimetric reader, was shown to provide reliable, specific, and sensitive results for a diverse set of pathogens. The ability to simultaneously test a panel of diseases in one reaction run presents a significant step forward for OxLAMP's application in clinical and field settings, particularly where high-throughput and broad-spectrum diagnostics are required. Furthermore, the results underscore the system's adaptability for both pure and clinical sample types, emphasizing its robustness even in the face of sample variability and the inherent complexities of clinical diagnostics. Moving forward, the development of a plate specifically designed for OxLAMP would enhance the utility and accessibility of this diagnostic tool. Ideally, such a plate could have reagents freeze-dried directly into individual wells, each containing primers for a distinct pathogen, facilitating

simultaneous testing for a panel of pathogens from a single sample. For instance, primers for a variety of STDs could be set adjacent to HSV primers, while the top pathogens responsible for bloodstream infections, such as E. faecalis and S. epidermidis, could be placed alongside each other to create a comprehensive diagnostic suite. This pre-configured plate design would streamline setup and minimize handling, especially useful in high-throughput settings and emergency cases.

Additionally, although the device can currently process up to 96 reactions in one run, this capacity may exceed what is necessary for many point-of-care (POC) diagnostic applications, where space and simplicity are critical. Sacrificing some reaction wells in favour of a smaller, more portable machine could make OxLAMP even more accessible for rapid POC diagnostics, particularly in resource-limited or mobile settings. A leaner, more compact version of the device would align closely with the goals of rapid and versatile diagnostics, furthering OxLAMP's mission to deliver effective, on-the-spot testing in diverse clinical and field environments.

6.4 Summary

Our novel LAMP assay has proven to be effective in amplifying and detecting HSV gDNA whilst not relying on pH change for observable colour change detection. this optimised pH-independent colourimteric LAMP assay experiments have shown an analytic sensitivity of 10 copies/reaction can be achieved within 40 minutes, and 17 clinical samples total have been successfully tested thus far. Extensive rounds of reagent optimisation have allowed us to achieve comparable test sensitivity and reaction times to traditional pH-indicator-based LAMP reactions whilst foregoing the potential downsides of pH-dependent LAMP. Different aspects of this test were investigated using a thermostatic photometer to generate data based on changes

in colour index, and we validated the LAMP amplification and test results using qLAMP, qPCR, and gel electrophoresis. Furthermore, being able to package this assay into a freeze-dried solid state greatly improves its shelf-life and ease of transport. Being able to make these additions to colorimetric LAMP whilst maintaining its functionality with different reading methodologies, such as by fluorescence in qLAMP, means this pH-independent colorimetric LAMP assay can be used for a multitude of uses. Most significantly, being able to directly test HSV clinical samples after optimisation of sample dilutions validates the practicality of this test for its most important use; as a POC test. The hope is for this test to be used and transported globally, to aid in the rapid diagnostics of pathogens such as HSV, regardless of economic condition.

Chapter 7 Discussion and Conclusion

This thesis presents a series of innovations in Loop-Mediated Isothermal Amplification (LAMP) technology, ultimately resulting in OxLAMP, a diagnostic tool designed for POC applications. OxLAMP was developed to address significant limitations in existing LAMP and nucleic acid amplification technologies, providing a multiplexed diagnostic system with quantitative, rapid, and pH-independent pathogen detection capabilities. Each component of the project contributed to the advancement of OxLAMP, with objectives focused on enhancing specificity, sensitivity, stability, and adaptability across varied diagnostic contexts. This chapter will conclude all the major sections as well as bring up potential next steps for the development of the technology.

Adapting and optimising qLAMP for practical diagnostic use in OxLAMP assay was a key part of this thesis. In this work, fluorescence-based detection methods were used to implement a qLAMP workflow, enabling the calculation of threshold time (TT) values that correlate with target DNA concentration. These TT values serve a similar function to Ct values in qPCR, allowing for semi-quantitative analysis within a LAMP framework. The integration of this approach into the OxLAMP system adds an important dimension of clinical relevance. The introduction of a portable fluorescent reading device would enhance qLAMP's accessibility in resource-limited settings, where standard lab equipment may be unavailable. Furthermore, developing a smartphone-based fluorescent reader could enable rapid, on-site quantification with minimal infrastructure, allowing qLAMP to be implemented in point-of-care (POC) diagnostics more seamlessly and effectively.

Beyond quantification, primer design and multiplexing were essential to expanding OxLAMP's utility for multi-pathogen detection. Designing and validating primer sets for various pathogens, including SARS-CoV-2 variants, Herpes Simplex Virus (HSV), and sepsis-

related bacteria, this thesis demonstrated high specificity and minimized off-target amplification. Primer validation was achieved through in silico and experimental testing, reinforcing OxLAMP's adaptability and flexibility. This precision in primer design facilitates high-throughput diagnostics in OxLAMP, where the ability to detect multiple pathogens in parallel is invaluable for syndromic testing and situations where rapid identification of several potential agents is necessary. Further validation of these pathogen primers with additional clinical samples, as was done with HSV, would enhance their reliability and broaden OxLAMP's clinical applicability, strengthening its role in diverse diagnostic settings where accuracy and scope are critical.

A key development in this project was addressing LAMP's reliance on cold-chain logistics. Diagnostic reagents, especially those involving enzymes and temperature-sensitive compounds, typically require cold storage to maintain stability. This need presents logistical challenges, particularly in resource-limited settings where refrigeration and consistent power supply are not feasible. OxLAMP's cold-chain independence was achieved by utilizing lyophilization and Matrix-Assisted Room Temperature (MART) drying techniques, which preserved enzyme activity and reagent integrity at room temperature. This stability greatly enhances OxLAMP's portability and accessibility, making it feasible for use in decentralized POC diagnostics, emergency response, and remote healthcare settings where storage conditions cannot be tightly controlled. Consequently, OxLAMP aligns with global health priorities by improving diagnostic reach in underserved areas, especially during pandemics when rapid, scalable testing is critical.

Another critical improvement in OxLAMP is the development of a pH-independent colorimetric assay. Traditional colorimetric LAMP assays often rely on pH-sensitive dyes, which can be unreliable when testing samples with varying acidity levels. Such variability can produce ambiguous results, especially in POC settings where samples may not undergo

extensive pretreatment. By formulating a pH-stable dye, this work enabled consistent colorimetric changes independent of sample pH, reducing the complexity of interpreting results and making OxLAMP more robust in field applications. This pH-independent approach enhances OxLAMP's suitability for diverse diagnostic environments, where sample conditions are unpredictable, and visual clarity is crucial for quick, reliable diagnosis.

The culmination of these advancements was the integration of OxLAMP into a multiplex diagnostic platform, specifically adapted for the Sinopharm colorimetric photometer. This integration allowed for high-throughput diagnostics across a 96-well plate, enabling simultaneous testing of multiple pathogens from a single patient sample. The colorimetric photometer provides automated interpretation of results through real-time colorimetric readings, minimizing subjectivity and human error. This device configuration amplifies OxLAMP's potential as both a centralized and decentralized diagnostic tool, capable of streamlining high-volume diagnostics while retaining its accessibility and efficiency. However, the current reliance on the Sinopharm photometer, while effective in laboratory settings, may limit OxLAMP's utility in remote locations. Developing a more portable, battery-operated photometer would improve OxLAMP's accessibility, allowing real-time quantitative analysis in resource-constrained settings and further extending its usability in decentralized, field-based diagnostics.

In conclusion, OxLAMP represents a significant advancement in the field of isothermal amplification, addressing core limitations that have been associated with LAMP's clinical applicability. The innovations presented in this thesis position it as a flexible, scalable, and reliable diagnostic solution capable of meeting diverse healthcare needs. Its development marks a step forward in pandemic preparedness, equipping healthcare systems with a tool that supports effective, accessible, and rapid diagnostics across varied clinical and resource-limited settings. As the global landscape of infectious diseases continues to evolve, OxLAMP's

adaptability and reliability make it as an invaluable asset for future diagnostic challenges. Through continued innovation and validation, we can set new standards in POC diagnostics, contributing to a future where high-quality diagnostic access and effective disease control are within reach for all.

Appendix

Table 0.1 ***In silico study.*** *Mutations and deletions in B.1.1.7 (alpha variant), B.1.351 (beta variant) and B.1.671 (delta variant) lineages.*

Gene	**OxLAMP target**	**Genome sequence positions**			**Amino acid**
		B.1.1.7 (alpha)	B.1.351 (beta)	B.1.671 (delta)	
ORF1ab			C1059T		T265I
	1346-1547 (O117)				
				C241T	
				C3037T	
				C3457T	
		C3267T			T1001I
				C4965T	T1567I
			G5230T		K1655N
		C5388A			A1708D
		T6954C			I2230T
					A2306V
					H2583R

			A10323G		K3353R
				A11201G	T3646A
				C14408T	P4715L
				G17523T	M5753I
				A20396G	K6711R
		11288-11296 deletion			SGF 3675-3677 deletion
S gene			C21614T		L18F
	21653-21885 (S17)*		A21801C		D80A
		21765-21770 deletion			HV 69-70 deletion
				T21895C	
				G21987A	G142D
		21991-21993 deletion			Y144 deletion
				G22022A	E154K
			A22206G		D215G
			T22287A		L242H
			22286-22294 deletion		L242-244L deletion
			G22299T		R246I
			G22813T		K417N
				T22917G	L452R
				G23012C	E484Q
			G23012A		E484K
		A23063T	**A23063T**		**N501Y**
		C23271A			A570D

			A23403G	**D614G**
	C23604A			**P681H**
			C23604G	P681R
	C23664T			A701V
	C23709T			T716I
	T24506G			S982A
			A24775T	Q1072R
	G24914C			D1118H
Orf3a			C25469T	S26L
		G25563T		Q57H
				96 deletion
		C25904C		S171L
Orf7a			T27638C	V82A
M gene			T26767G	I82S
Orf8	C27972T			Q27stop
				P93S
				E106Q
	G28048T			R52I
	A28111G			Y73C
E gene		C26456T		P71L
N gene	28280 GAT->CTA			D3L
	28285-28486 (N1)			
			G28881T	R203M
	28702-28914 (N15)	C28887T		T205I
				215 deletion

	C28977T		S235F
		G29402	D377Y

References

[1] Belser JA, Tumpey TM. The 1918 flu, 100 years later. Science 2018;359:255. https://doi.org/10.1126/science.aas9565.

[2] Wu F, Zhao S, Yu B, Chen Y-M, Wang W, Song Z-G, et al. A new coronavirus associated with human respiratory disease in China. Nature 2020;579:265–9. https://doi.org/10.1038/s41586-020-2008-3.

[3] Cucinotta D, Vanelli M. WHO Declares COVID-19 a Pandemic. Acta Biomed 2020;91:157–60. https://doi.org/10.23750/abm.v91i1.9397.

[4] COVID-19 cases | WHO COVID-19 dashboard. Datadot n.d. https://data.who.int/dashboards/covid19/cases (accessed October 16, 2024).

[5] Tangcharoensathien V, Bassett MT, Meng Q, Mills A. Are overwhelmed health systems an inevitable consequence of covid-19? Experiences from China, Thailand, and New York State. BMJ 2021;372:n83. https://doi.org/10.1136/bmj.n83.

[6] Cohen J, Rodgers Y van der M. Contributing factors to personal protective equipment shortages during the COVID-19 pandemic. Prev Med 2020;141:106263. https://doi.org/10.1016/j.ypmed.2020.106263.

[7] Meyer A, Walter W, Seuring S. The Impact of the Coronavirus Pandemic on Supply Chains and Their Sustainability: A Text Mining Approach. Front Sustain 2021;2. https://doi.org/10.3389/frsus.2021.631182.

[8] Bartik AW, Bertrand M, Cullen Z, Glaeser EL, Luca M, Stanton C. The impact of COVID-19 on small business outcomes and expectations. Proceedings of the National Academy of Sciences of the United States of America 2020;117:17656. https://doi.org/10.1073/pnas.2006991117.

[9] Wang J, Yang J, Iverson BC, Kluender R. Bankruptcy and the COVID-19 Crisis 2020. https://doi.org/10.2139/ssrn.3690398.

[10] Kawohl W, Nordt C. COVID-19, unemployment, and suicide. Lancet Psychiatry 2020;7:389–90. https://doi.org/10.1016/S2215-0366(20)30141-3.

[11] Ainslie KEC, Walters CE, Fu H, Bhatia S, Wang H, Xi X, et al. Evidence of initial success for China exiting COVID-19 social distancing policy after achieving containment. Wellcome Open Res 2020;5:81. https://doi.org/10.12688/wellcomeopenres.15843.2.

[12] Pietrabissa G, Simpson SG. Psychological Consequences of Social Isolation During COVID-19 Outbreak. Front Psychol 2020;11. https://doi.org/10.3389/fpsyg.2020.02201.

[13] Rogers JP, Chesney E, Oliver D, Pollak TA, McGuire P, Fusar-Poli P, et al. Psychiatric and neuropsychiatric presentations associated with severe coronavirus infections: a systematic review and meta-analysis with comparison to the COVID-19 pandemic. The Lancet Psychiatry 2020;7:611. https://doi.org/10.1016/S2215-0366(20)30203-0.

[14] Fancourt D, Aughterson H, Finn S, Walker E, Steptoe A. How leisure activities affect health: a narrative review and multi-level theoretical framework of mechanisms of action. Lancet Psychiatry 2021;8:329–39. https://doi.org/10.1016/S2215-0366(20)30384-9.

[15] Shields C, Bernard J, Mirza OI, Reeves D, Wells A, Heagerty A. Covid-19, Lockdown and Self-Isolation: Evaluation of Deliberate Self-Harm Admissions. Frontiers in Psychiatry 2021;12:662885. https://doi.org/10.3389/fpsyt.2021.662885.

[16] Boylan BM, McBeath J, Wang B. US–China Relations: Nationalism, the Trade War, and COVID-19. Fudan J Hum Soc Sci 2021;14:23–40. https://doi.org/10.1007/s40647-020-00302-6.
[17] Zimmermann KF, Karabulut G, Bilgin MH, Doker AC. Inter-country distancing, globalisation and the coronavirus pandemic. The World Economy 2020;43:1484. https://doi.org/10.1111/twec.12969.
[18] Callaway E. Coronavirus variants get Greek names — but will scientists use them? Nature 2021;594:162–162. https://doi.org/10.1038/d41586-021-01483-0.
[19] Mian A, Khan S. Coronavirus: the spread of misinformation. BMC Medicine 2020;18:89. https://doi.org/10.1186/s12916-020-01556-3.
[20] Hughes JM, Drotman DP. In Memoriam: Joshua Lederberg (1925–2008) - Volume 14, Number 6—June 2008 - Emerging Infectious Diseases journal - CDC n.d. https://doi.org/10.3201/eid1406.080413.
[21] Carroll D, Watson B, Togami E, Daszak P, Mazet JA, Chrisman CJ, et al. Building a global atlas of zoonotic viruses. Bulletin of the World Health Organization 2018;96:292. https://doi.org/10.2471/BLT.17.205005.
[22] Alvarez E, Bielska IA, Hopkins S, Belal AA, Goldstein DM, Slick J, et al. Limitations of COVID-19 testing and case data for evidence-informed health policy and practice. Health Research Policy and Systems 2023;21:11. https://doi.org/10.1186/s12961-023-00963-1.
[23] Knoll MD, Wonodi C. Oxford–AstraZeneca COVID-19 vaccine efficacy. The Lancet 2021;397:72–4. https://doi.org/10.1016/S0140-6736(20)32623-4.
[24] Chagla Z. The BNT162b2 (BioNTech/Pfizer) vaccine had 95% efficacy against COVID-19 ≥7 days after the 2nd dose. Ann Intern Med 2021;174:JC15. https://doi.org/10.7326/ACPJ202102160-015.
[25] Riemersma KK, Haddock LA, Wilson NA, Minor N, Eickhoff J, Grogan BE, et al. Shedding of infectious SARS-CoV-2 despite vaccination. PLoS Pathog 2022;18:e1010876. https://doi.org/10.1371/journal.ppat.1010876.
[26] Larremore DB, Wilder B, Lester E, Shehata S, Burke JM, Hay JA, et al. Test sensitivity is secondary to frequency and turnaround time for COVID-19 screening. Science Advances 2021;7:eabd5393. https://doi.org/10.1126/sciadv.abd5393.
[27] Huang WE, Lim B, Hsu C-C, Xiong D, Wu W, Yu Y, et al. RT-LAMP for rapid diagnosis of coronavirus SARS-CoV-2. Microbial Biotechnology 2020;13:950–61. https://doi.org/10.1111/1751-7915.13586.
[28] Yoo HM, Kim I-H, Kim S. Nucleic Acid Testing of SARS-CoV-2. International Journal of Molecular Sciences 2021;22:6150. https://doi.org/10.3390/ijms22116150.
[29] Maia R, Carvalho V, Faria B, Miranda I, Catarino S, Teixeira S, et al. Diagnosis Methods for COVID-19: A Systematic Review. Micromachines 2022;13:1349. https://doi.org/10.3390/mi13081349.
[30] Ngom B, Guo Y, Wang X, Bi D. Development and application of lateral flow test strip technology for detection of infectious agents and chemical contaminants: a review. Anal Bioanal Chem 2010;397:1113–35. https://doi.org/10.1007/s00216-010-3661-4.
[31] Wise J. Covid-19: Lateral flow tests miss over half of cases, Liverpool pilot data show. BMJ 2020;371:m4848. https://doi.org/10.1136/bmj.m4848.
[32] Tourism's Contribution To UK Economy | VisitBritain.org n.d. https://www.visitbritain.org/research-insights/value-tourism-england (accessed October 16, 2024).
[33] Geraci-Yee S, Allam B, Collier JL. A Nested Quantitative Pcr Assay For Detection Of The Hard Clam Pathogen Mucochytrium Quahogii (=Qpx) In Environmental Samples n.d.

[34] Karon BS, Donato LJ, Bridgeman AR, Blommel JH, Kipp B, Maus A, et al. Analytical Sensitivity and Specificity of Four Point of Care Rapid Antigen Diagnostic Tests for SARS-CoV-2 Using Real-Time Quantitative PCR, Quantitative Droplet Digital PCR, and a Mass Spectrometric Antigen Assay as Comparator Methods. Clinical Chemistry 2021;67:1545–53. https://doi.org/10.1093/clinchem/hvab138.
[35] Kralik P, Ricchi M. A Basic Guide to Real Time PCR in Microbial Diagnostics: Definitions, Parameters, and Everything. Front Microbiol 2017;8. https://doi.org/10.3389/fmicb.2017.00108.
[36] Udvardi MK, Czechowski T, Scheible W-R. Eleven Golden Rules of Quantitative RT-PCR. The Plant Cell 2008;20:1736. https://doi.org/10.1105/tpc.108.061143.
[37] Roux G, Ravel C, Varlet-Marie E, Jendrowiak R, Bastien P, Sterkers Y. Inhibition of polymerase chain reaction: Pathogen-specific controls are better than human gene amplification. PLoS ONE 2019;14:e0219276. https://doi.org/10.1371/journal.pone.0219276.
[38] Notomi T, Okayama H, Masubuchi H, Yonekawa T, Watanabe K, Amino N, et al. Loop-mediated isothermal amplification of DNA. Nucleic Acids Res 2000;28:E63. https://doi.org/10.1093/nar/28.12.e63.
[39] Nagamine K, Hase T, Notomi T. Accelerated reaction by loop-mediated isothermal amplification using loop primers. Mol Cell Probes 2002;16:223–9. https://doi.org/10.1006/mcpr.2002.0415.
[40] Tomita N, Mori Y, Kanda H, Notomi T. Loop-mediated isothermal amplification (LAMP) of gene sequences and simple visual detection of products. Nat Protoc 2008;3:877–82. https://doi.org/10.1038/nprot.2008.57.
[41] Kitajima H, Tamura Y, Yoshida H, Kinoshita H, Katsuta H, Matsui C, et al. Clinical COVID-19 diagnostic methods: Comparison of reverse transcription loop-mediated isothermal amplification (RT-LAMP) and quantitative RT-PCR (qRT-PCR). Journal of Clinical Virology 2021;139:104813. https://doi.org/10.1016/j.jcv.2021.104813.
[42] Wang Y, Li J, Li S, Zhu X, Wang X, Huang J, et al. LAMP-CRISPR-Cas12-based diagnostic platform for detection of Mycobacterium tuberculosis complex using real-time fluorescence or lateral flow test. Microchimica Acta 2021;188. https://doi.org/10.1007/s00604-021-04985-w.
[43] Ahmadi Y, Yu Y, Cui Z, Huang WE, Andersson MI. Loop-Mediated Isothermal Amplification (LAMP) for the Diagnosis of Sexually Transmitted Infections: A Review. Microbial Biotechnology 2025;18:e70153. https://doi.org/10.1111/1751-7915.70153.
[44] Duan Y-B, Ge C-Y, Zhang X-K, Wang J-X, Zhou M-G. Development and Evaluation of a Novel and Rapid Detection Assay for Botrytis cinerea Based on Loop-Mediated Isothermal Amplification. PLOS ONE 2014;9:e111094. https://doi.org/10.1371/journal.pone.0111094.
[45] Techathuvanan C, Draughon FA, D'souza DH. Real-Time Reverse Transcriptase PCR for the Rapid and Sensiti Detection of *Salmonella* Typhimurium from Pork. Journal of Food Protection 2010;73:507–14. https://doi.org/10.4315/0362-028x-73.3.507.
[46] Port to patient: Improving country cold chains for COVID-19 vaccines | McKinsey n.d. https://www.mckinsey.com/industries/social-sector/our-insights/port-to-patient-improving-country-cold-chains-for-covid-19-vaccines (accessed October 16, 2024).
[47] Why optimized cold-chains could save a billion COVID vaccines 2020. https://www.unep.org/news-and-stories/story/why-optimized-cold-chains-could-save-billion-covid-vaccines (accessed October 16, 2024).

[48] Wang Y, Chen J, Yang Z, Wang X, Zhang Y, Chen M, et al. Advances in Nucleic Acid Assays for Infectious Disease: The Role of Microfluidic Technology. Molecules 2024;29:2417. https://doi.org/10.3390/molecules29112417.
[49] Crego-Vicente B, del Olmo MD, Muro A, Fernández-Soto P. Multiplexing LAMP Assays: A Methodological Review and Diagnostic Application. International Journal of Molecular Sciences 2024;25:6374. https://doi.org/10.3390/ijms25126374.
[50] Drain PK. Point-of-Care Diagnostics (POCD) in Resource-Limited Settings. Diagnostics 2024;14:1926. https://doi.org/10.3390/diagnostics14171926.
[51] Ansumana R, Jacobsen KH, Bockarie MJ, Stenger DA. Point-of-care tests: where is the point? Lancet Infect Dis 2014;14:922–3. https://doi.org/10.1016/S1473-3099(14)70915-6.
[52] Kadja T, Liu C, Sun Y, Chodavarapu VP. Low-Cost, Real-Time Polymerase Chain Reaction System for Point-of-Care Medical Diagnosis. Sensors 2022;22:2320. https://doi.org/10.3390/s22062320.
[53] Garcia PJ, You P, Fridley G, Mabey D, Peeling R. Point-of-care diagnostic tests for low-resource settings. Lancet Glob Health 2015;3:e257-258. https://doi.org/10.1016/S2214-109X(15)70089-6.
[54] Chen S, Ge B. Development of a toxR-based loop-mediated isothermal amplification assay for detecting Vibrio parahaemolyticus. BMC Microbiology 2010;10:41. https://doi.org/10.1186/1471-2180-10-41.
[55] Patel JC, Oberstaller J, Xayavong M, Narayanan J, DeBarry JD, Srinivasamoorthy G, et al. Real-time loop-mediated isothermal amplification (RealAmp) for the species-specific identification of Plasmodium vivax. PLoS One 2013;8:e54986. https://doi.org/10.1371/journal.pone.0054986.
[56] Quyen TL, Ngo TA, Bang DD, Madsen M, Wolff A. Classification of Multiple DNA Dyes Based on Inhibition Effects on Real-Time Loop-Mediated Isothermal Amplification (LAMP): Prospect for Point of Care Setting. Front Microbiol 2019;10. https://doi.org/10.3389/fmicb.2019.02234.
[57] Sun Y, Quyen TL, Hung TQ, Chin WH, Wolff A, Bang DD. A lab-on-a-chip system with integrated sample preparation and loop-mediated isothermal amplification for rapid and quantitative detection of Salmonella spp. in food samples. Lab Chip 2015;15:1898–904. https://doi.org/10.1039/C4LC01459F.
[58] Moehling TJ, Choi G, Dugan LC, Salit M, Meagher RJ. LAMP Diagnostics at the Point-of-Care: Emerging Trends and Perspectives for the Developer Community. Expert Rev Mol Diagn 2021;21:43–61. https://doi.org/10.1080/14737159.2021.1873769.
[59] Lai MY, Ooi CH, Lau YL. Validation of SYBR green I based closed-tube loop-mediated isothermal amplification (LAMP) assay for diagnosis of knowlesi malaria. Malaria Journal 2021;20:166. https://doi.org/10.1186/s12936-021-03707-0.
[60] Zhou D, Guo J, Xu L, Gao S, Lin Q, Wu Q, et al. Establishment and application of a loop-mediated isothermal amplification (LAMP) system for detection of cry1Ac transgenic sugarcane. Sci Rep 2014;4:4912. https://doi.org/10.1038/srep04912.
[61] Karthik K, Rathore R, Thomas P, Arun TR, Viswas KN, Dhama K, et al. New closed tube loop mediated isothermal amplification assay for prevention of product cross-contamination. MethodsX 2014;1:137. https://doi.org/10.1016/j.mex.2014.08.009.
[62] Jelocnik M, Nyari S, Anstey S, Playford N, Fraser TA, Mitchell K, et al. Real-time fluorometric and end-point colorimetric isothermal assays for detection of equine pathogens C. psittaci and equine herpes virus 1: validation, comparison and application at the point of care. BMC Veterinary Research 2021;17:279. https://doi.org/10.1186/s12917-021-02986-8.

[63] Nie K, Qi S-X, Zhang Y, Luo L, Xie Y, Yang M-J, et al. Evaluation of a direct reverse transcription loop-mediated isothermal amplification method without RNA extraction for the detection of human enterovirus 71 subgenotype C4 in nasopharyngeal swab specimens. PLoS One 2012;7:e52486. https://doi.org/10.1371/journal.pone.0052486.
[64] Atçeken N, Yigci D, Ozdalgic B, Tasoglu S. CRISPR-Cas-Integrated LAMP. Biosensors 2022;12:1035. https://doi.org/10.3390/bios12111035.
[65] Bhatt A, Fatima Z, Ruwali M, Misra CS, Rangu SS, Rath D, et al. CLEVER assay: A visual and rapid RNA extraction-free detection of SARS-CoV-2 based on CRISPR-Cas integrated RT-LAMP technology. J Appl Microbiol 2022;133:410–21. https://doi.org/10.1111/jam.15571.
[66] Bao Y, Jiang Y, Xiong E, Tian T, Zhang Z, Lv J, et al. CUT-LAMP: Contamination-Free Loop-Mediated Isothermal Amplification Based on the CRISPR/Cas9 Cleavage. ACS Sens 2020;5:1082–91. https://doi.org/10.1021/acssensors.0c00034.
[67] Allgöwer SM, Hartmann CA, Lipinski C, Mahler V, Randow S, Völker E, et al. LAMP-LFD Based on Isothermal Amplification of Multicopy Gene ORF160b: Applicability for Highly Sensitive Low-Tech Screening of Allergenic Soybean (Glycine max) in Food. Foods 2020;9:1741. https://doi.org/10.3390/foods9121741.
[68] Jaroenram W, Kampeera J, Arunrut N, Sirithammajak S, Jaitrong S, Boonnak K, et al. Ultrasensitive detection of Mycobacterium tuberculosis by a rapid and specific probe-triggered one-step, simultaneous DNA hybridization and isothermal amplification combined with a lateral flow dipstick. Sci Rep 2020;10:16976. https://doi.org/10.1038/s41598-020-73981-6.
[69] Sukumolanan P, Demeekul K, Petchdee S. Development of a Loop-Mediated Isothermal Amplification Assay Coupled With a Lateral Flow Dipstick Test for Detection of Myosin Binding Protein C3 A31P Mutation in Maine Coon Cats. Front Vet Sci 2022;9. https://doi.org/10.3389/fvets.2022.819694.
[70] Mytzka N, Arbaciauskaite S, Sandetskaya N, Mattern K, Kuhlmeier D. A fully integrated duplex RT-LAMP device for the detection of viral infections. Biomed Microdevices 2023;25:36. https://doi.org/10.1007/s10544-023-00676-w.
[71] Dao Thi VL, Herbst K, Boerner K, Meurer M, Kremer LP, Kirrmaier D, et al. A colorimetric RT-LAMP assay and LAMP-sequencing for detecting SARS-CoV-2 RNA in clinical samples. Sci Transl Med 2020;12:eabc7075. https://doi.org/10.1126/scitranslmed.abc7075.
[72] Goto M, Honda E, Ogura A, Nomoto A, Hanaki K-I. Colorimetric detection of loop-mediated isothermal amplification reaction by using hydroxy naphthol blue. Biotechniques 2009;46:167–72. https://doi.org/10.2144/000113072.
[73] Tanner N, Zhang Y, Evans TC. Visual detection of isothermal nucleic acid amplification using pH-sensitive dyes. BioTechniques 2015;58 2:59–68. https://doi.org/10.2144/000114253.
[74] Aoki MN, de Oliveira Coelho B, Góes LGB, Minoprio P, Durigon EL, Morello LG, et al. Colorimetric RT-LAMP SARS-CoV-2 diagnostic sensitivity relies on color interpretation and viral load. Sci Rep 2021;11:9026. https://doi.org/10.1038/s41598-021-88506-y.
[75] Wang J, Niu Y, Zhang C, Chen Y. A micro-plate colorimetric assay for rapid determination of trace zinc in animal feed, pet food and drinking water by ion masking and statistical partitioning correction. Food Chemistry 2018;245:337–45. https://doi.org/10.1016/j.foodchem.2017.10.054.
[76] Hokazono E, Fukumoto S, Uchiumi T, Osawa S. Pyrophosphate detection method using 5-Br-PAPS to detect nucleic acid amplification - Application to LAMP method. Analytical Biochemistry 2024;684:115371. https://doi.org/10.1016/j.ab.2023.115371.

[77] Szobi A, Buranovská K, Vojtaššáková N, Lovíšek D, Özbaşak HÖ, Szeibeczederová S, et al. Vivid COVID-19 LAMP is an ultrasensitive, quadruplexed test using LNA-modified primers and a zinc ion and 5-Br-PAPS colorimetric detection system. Commun Biol 2023;6:233. https://doi.org/10.1038/s42003-023-04612-9.
[78] Mori Y, Nagamine K, Tomita N, Notomi T. Detection of loop-mediated isothermal amplification reaction by turbidity derived from magnesium pyrophosphate formation. Biochem Biophys Res Commun 2001;289:150–4. https://doi.org/10.1006/bbrc.2001.5921.
[79] Mori Y, Kitao M, Tomita N, Notomi T. Real-time turbidimetry of LAMP reaction for quantifying template DNA. J Biochem Biophys Methods 2004;59:145–57. https://doi.org/10.1016/j.jbbm.2003.12.005.
[80] Sappat A, Jaroenram W, Puthawibool T, Lomas T, Tuantranont A, Kiatpathomchai W. Detection of shrimp Taura syndrome virus by loop-mediated isothermal amplification using a designed portable multi-channel turbidimeter. J Virol Methods 2011;175:141–8. https://doi.org/10.1016/j.jviromet.2011.05.013.
[81] Yuan X-Y, Wang Y-L, Meng K, Zhang Y-X, Xu H-Y, Ai W. LAMP real-time turbidity detection for fowl adenovirus. BMC Veterinary Research 2019;15:256. https://doi.org/10.1186/s12917-019-2015-5.
[82] Wastling SL, Picozzi K, Kakembo ASL, Welburn SC. LAMP for Human African Trypanosomiasis: A Comparative Study of Detection Formats. PLOS Neglected Tropical Diseases 2010;4:e865. https://doi.org/10.1371/journal.pntd.0000865.
[83] Enomoto Y, Yoshikawa T, Ihira M, Akimoto S, Miyake F, Usui C, et al. Rapid Diagnosis of Herpes Simplex Virus Infection by a Loop-Mediated Isothermal Amplification Method. Journal of Clinical Microbiology 2005;43:951. https://doi.org/10.1128/JCM.43.2.951-955.2005.
[84] Wong Y-P, Othman S, Lau Y-L, Radu S, Chee H-Y. Loop-mediated isothermal amplification (LAMP): a versatile technique for detection of micro-organisms. J Appl Microbiol 2018;124:626–43. https://doi.org/10.1111/jam.13647.
[85] Xie S, Yuan Y, Song Y, Zhuo Y, Li T, Chai Y, et al. Using the ubiquitous pH meter combined with a loop mediated isothermal amplification method for facile and sensitive detection of Nosema bombycis genomic DNA PTP1. Chemical Communications 2014;50 100:15932–5. https://doi.org/10.1039/c4cc06449f.
[86] Hua X, Yang E, Yang W, Yuan R, Xu W. LAMP-generated H+ ions-induced dimer i-motif as signal transducer for ultrasensitive electrochemical detection of DNA. Chem Commun (Camb) 2019;55:12463–6. https://doi.org/10.1039/c9cc06738h.
[87] Zhao J, Gao J, Zheng T, Yang Z, Chai Y, Chen S, et al. Highly sensitive electrochemical assay for *Nosema bombycis* gene DNA PTP1 via conformational switch of DNA nanostructures regulated by H+ from LAMP. Biosensors and Bioelectronics 2018;106:186–92. https://doi.org/10.1016/j.bios.2018.02.003.
[88] Bonney LC, Watson RJ, Slack GS, Bosworth A, Wand NIV, Hewson R. A flexible format LAMP assay for rapid detection of Ebola virus. PLOS Neglected Tropical Diseases 2020;14:e0008496. https://doi.org/10.1371/journal.pntd.0008496.
[89] Fukuta S, Iida T, Mizukami Y, Ishida A, Ueda J, Kanbe M, et al. Detection of Japanese yam mosaic virus by RT-LAMP. Arch Virol 2003;148:1713–20. https://doi.org/10.1007/s00705-003-0134-5.
[90] Kaneko H, Iida T, Aoki K, Ohno S, Suzutani T. Sensitive and rapid detection of herpes simplex virus and varicella-zoster virus DNA by loop-mediated isothermal amplification. J Clin Microbiol 2005;43:3290–6. https://doi.org/10.1128/JCM.43.7.3290-3296.2005.

[91] Sano S, Fukushi S, Yamada S, Harada S, Kinoshita H, Sugimoto S, et al. Development of an RT-LAMP Assay for the Rapid Detection of SFTS Virus. Viruses 2021;13:693. https://doi.org/10.3390/v13040693.
[92] Chen Z-D, Kang H-J, Chai A-L, Shi Y-X, Xie X-W, Li L, et al. Development of a loop-mediated isothermal amplification (LAMP) assay for rapid detection of Pseudomonas syringae pv. tomato in planta. European Journal of Plant Pathology 2020;156. https://doi.org/10.1007/s10658-019-01923-8.
[93] Safavieh M, Ahmed MU, Ng A, Zourob M. High-throughput real-time electrochemical monitoring of LAMP for pathogenic bacteria detection. Biosens Bioelectron 2014;58:101–6. https://doi.org/10.1016/j.bios.2014.02.002.
[94] Wu D, Kang J, Li B, Sun D. Evaluation of the RT-LAMP and LAMP methods for detection of Mycobacterium tuberculosis. J Clin Lab Anal 2018;32:e22326. https://doi.org/10.1002/jcla.22326.
[95] Li L, Zhang SY, Zhang C-Q. Establishment of a Rapid Detection Method for Rice Blast Fungus Based on One-Step Loop-Mediated Isothermal Amplification (LAMP). Plant Dis 2019;103:1967–73. https://doi.org/10.1094/PDIS-11-18-1964-RE.
[96] Nakayama T, Yamazaki T, Yo A, Tone K, Mahdi Alshahni M, Fujisaki R, et al. Detection of Fungi from an Indoor Environment using Loop-mediated Isothermal Amplification (LAMP) Method. Biocontrol Sci 2017;22:97–104. https://doi.org/10.4265/bio.22.97.
[97] Niessen L. The application of loop-mediated isothermal amplification (LAMP) assays for the rapid diagnosis of food-borne mycotoxigenic fungi. Current Opinion in Food Science 2018;23:11–22. https://doi.org/10.1016/j.cofs.2018.02.007.
[98] Adao DEV, Rivera WL. Loop-mediated isothermal amplification (LAMP) assay for the rapid detection of the sexually-transmitted parasite, Trichomonas vaginalis. Ann Parasitol 2016;62:25–31. https://doi.org/10.17420/ap6201.28.
[99] Njiru ZK, Mikosza ASJ, Armstrong T, Enyaru JC, Ndung'u JM, Thompson ARC. Loop-Mediated Isothermal Amplification (LAMP) Method for Rapid Detection of Trypanosoma brucei rhodesiense. PLOS Neglected Tropical Diseases 2008;2:e147. https://doi.org/10.1371/journal.pntd.0000147.
[100] Nzelu CO, Kato H, Peters NC. Loop-mediated isothermal amplification (LAMP): An advanced molecular point-of-care technique for the detection of Leishmania infection. PLoS Negl Trop Dis 2019;13:e0007698. https://doi.org/10.1371/journal.pntd.0007698.
[101] Zhang H, Thekisoe OMM, Aboge GO, Kyan H, Yamagishi J, Inoue N, et al. *Toxoplasma gondii*: Sensitive and rapid detection of infection by loop-mediated isothermal amplification (LAMP) method. Experimental Parasitology 2009;122:47–50. https://doi.org/10.1016/j.exppara.2009.01.012.
[102] Health C for D and R. Nucleic Acid Based Tests. FDA 2024.
[103] Chen X, Zhang J, Pan M, Qin Y, Zhao H, Qin P, et al. Loop-mediated isothermal amplification (LAMP) assays targeting 18S ribosomal RNA genes for identifying P. vivax and P. ovale species and mitochondrial DNA for detecting the genus Plasmodium. Parasit Vectors 2021;14:278. https://doi.org/10.1186/s13071-021-04764-9.
[104] The use of a commercial loop-mediated isothermal amplification assay (TB-lamp) for the detection of tuberculosis: expert group meeting report n.d. https://www.who.int/publications/i/item/WHO-HTM-TB-2013.05 (accessed October 18, 2024).
[105] Rapid evaluation of OptiGene RT-LAMP assay (direct and RNA formats). GOVUK n.d. https://www.gov.uk/government/publications/rapid-evaluation-of-optigene-rt-

lamp-assay-direct-and-rna-formats/rapid-evaluation-of-optigene-rt-lamp-assay-direct-and-rna-formats (accessed October 18, 2024).
[106] Gupta N. DNA Extraction and Polymerase Chain Reaction. Journal of Cytology 2019;36:116. https://doi.org/10.4103/JOC.JOC_110_18.
[107] Lu W, Wang J, Wu Q, Sun J, Chen Y, Zhang L, et al. High-throughput sample-to-answer detection of DNA/RNA in crude samples within functionalized micro-pipette tips. Biosens Bioelectron 2016;75:28–33. https://doi.org/10.1016/j.bios.2015.08.016.
[108] Ganguli A, Ornob A, Yu H, Damhorst GL, Chen W, Sun F, et al. Hands-free smartphone-based diagnostics for simultaneous detection of Zika, Chikungunya, and Dengue at point-of-care. Biomed Microdevices 2017;19:73. https://doi.org/10.1007/s10544-017-0209-9.
[109] Aydin-Schmidt B, Xu W, González IJ, Polley SD, Bell D, Shakely D, et al. Loop mediated isothermal amplification (LAMP) accurately detects malaria DNA from filter paper blood samples of low density parasitaemias. PLoS One 2014;9:e103905. https://doi.org/10.1371/journal.pone.0103905.
[110] Kim J-H, Oh S-W. Development of a filtration-based LAMP-LFA method as sensitive and rapid detection of E. coli O157:H7. J Food Sci Technol 2019;56:2576–83. https://doi.org/10.1007/s13197-019-03740-7.
[111] Nzelu CO, Cáceres AG, Guerrero-Quincho S, Tineo-Villafuerte E, Rodriquez-Delfin L, Mimori T, et al. A rapid molecular diagnosis of cutaneous leishmaniasis by colorimetric malachite green-loop-mediated isothermal amplification (LAMP) combined with an FTA card as a direct sampling tool. Acta Tropica 2016;153:116–9. https://doi.org/10.1016/j.actatropica.2015.10.013.
[112] Yan W, Shen Z, Tang X, Xu L, Li Q, Yue Y, et al. Detection of Nosema bombycis by FTA cards and loop-mediated isothermal amplification (LAMP). Curr Microbiol 2014;69:532–40. https://doi.org/10.1007/s00284-014-0619-3.
[113] de Puig H, Lee RA, Najjar D, Tan X, Soenksen LR, Angenent-Mari NM, et al. Minimally instrumented SHERLOCK (miSHERLOCK) for CRISPR-based point-of-care diagnosis of SARS-CoV-2 and emerging variants. Science Advances 2021;7:eabh2944. https://doi.org/10.1126/sciadv.abh2944.
[114] Najjar D, Rainbow J, Sharma Timilsina S, Jolly P, de Puig H, Yafia M, et al. A lab-on-a-chip for the concurrent electrochemical detection of SARS-CoV-2 RNA and anti-SARS-CoV-2 antibodies in saliva and plasma. Nat Biomed Eng 2022;6:968–78. https://doi.org/10.1038/s41551-022-00919-w.
[115] Zou Y, Mason MG, Wang Y, Wee E, Turni C, Blackall PJ, et al. Nucleic acid purification from plants, animals and microbes in under 30 seconds. PLOS Biology 2017;15:e2003916. https://doi.org/10.1371/journal.pbio.2003916.
[116] Wang D, Brewster J, Paul M, Tomasula P. Two Methods for Increased Specificity and Sensitivity in Loop-Mediated Isothermal Amplification. Molecules 2015;20:6048–59. https://doi.org/10.3390/molecules20046048.
[117] Meagher R, Priye A, Light YK, Huang C, Wang E. Impact of primer dimers and self-amplifying hairpins on reverse transcription loop-mediated isothermal amplification detection of viral RNA. The Analyst 2018;143 8:1924–33. https://doi.org/10.1039/c7an01897e.
[118] Rolando JC, Jue E, Barlow JT, Ismagilov RF. Real-time kinetics and high-resolution melt curves in single-molecule digital LAMP to differentiate and study specific and non-specific amplification. Nucleic Acids Res 2020;48:e42. https://doi.org/10.1093/nar/gkaa099.

[119] Lim B, Ratcliff J, Nawrot DA, Yu Y, Sanghani HR, Hsu C-C, et al. Clinical validation of optimised RT-LAMP for the diagnosis of SARS-CoV-2 infection. Sci Rep 2021;11:16193. https://doi.org/10.1038/s41598-021-95607-1.
[120] Nichols JH. Quality in point-of-care testing. Expert Rev Mol Diagn 2003;3:563–72. https://doi.org/10.1586/14737159.3.5.563.
[121] Niessen L, Luo J, Denschlag C, Vogel RF. The application of loop-mediated isothermal amplification (LAMP) in food testing for bacterial pathogens and fungal contaminants. Food Microbiol 2013;36:191–206. https://doi.org/10.1016/j.fm.2013.04.017.
[122] Natoli ME, Kundrod KA, Chang MM, Smith CA, Paul S, Coole JB, et al. Improving Performance of a SARS-CoV-2 RT-LAMP Assay for Use With a Portable Isothermal Fluorimeter: Towards a Point-of-Care Molecular Testing Strategy. J Biomol Tech 2021;32:180–5. https://doi.org/10.7171/jbt.21-3203-013.
[123] Bektaş A, Covington MF, Aidelberg G, Arce A, Matute T, Núñez I, et al. Accessible LAMP-Enabled Rapid Test (ALERT) for Detecting SARS-CoV-2. Viruses 2021;13:742. https://doi.org/10.3390/v13050742.
[124] Lin P-H, Li B-R. Passively driven microfluidic device with simple operation in the development of nanolitre droplet assay in nucleic acid detection. Sci Rep 2021;11:21019. https://doi.org/10.1038/s41598-021-00470-9.
[125] Tao Z-Y, Zhou H-Y, Xia H, Xu S, Zhu H-W, Culleton RL, et al. Adaptation of a visualized loop-mediated isothermal amplification technique for field detection of Plasmodium vivax infection. Parasit Vectors 2011;4:115. https://doi.org/10.1186/1756-3305-4-115.
[126] Zen LPY, Lai MY, Lau YL. Elimination of contamination in loop-mediated isothermal amplification assay for detection of human malaria. Trop Biomed 2020;37:1124–8. https://doi.org/10.47665/tb.37.4.1124.
[127] Quyen TL, Vinayaka AC, Golabi M, Ngoc HV, Bang DD, Wolff A. Elimination of Carryover Contamination in Real-Time Reverse Transcriptase Loop-Mediated Isothermal Amplification for Rapid Detection of the SARS-CoV-2 Virus in Point-of-Care Testing. Front Cell Infect Microbiol 2022;12. https://doi.org/10.3389/fcimb.2022.856553.
[128] Chander Y, Koelbl J, Puckett J, Moser MJ, Klingele AJ, Liles MR, et al. A novel thermostable polymerase for RNA and DNA loop-mediated isothermal amplification (LAMP). Front Microbiol 2014;5. https://doi.org/10.3389/fmicb.2014.00395.
[129] Hayashida K, Kajino K, Hachaambwa L, Namangala B, Sugimoto C. Direct Blood Dry LAMP: A Rapid, Stable, and Easy Diagnostic Tool for Human African Trypanosomiasis. PLOS Neglected Tropical Diseases 2015;9:e0003578. https://doi.org/10.1371/journal.pntd.0003578.
[130] Gavina K, Franco LC, Khan H, Lavik J-P, Relich RF. Molecular point-of-care devices for the diagnosis of infectious diseases in resource-limited settings - A review of the current landscape, technical challenges, and clinical impact. J Clin Virol 2023;169:105613. https://doi.org/10.1016/j.jcv.2023.105613.
[131] Carter C, Akrami K, Hall D, Smith D, Aronoff-Spencer E. Lyophilized visually readable loop-mediated isothermal reverse transcriptase nucleic acid amplification test for detection Ebola Zaire RNA. J Virol Methods 2017;244:32–8. https://doi.org/10.1016/j.jviromet.2017.02.013.
[132] Prado NO, Marin AM, Lalli LA, Sanchuki HBS, Wosniaki DK, Nardin JM, et al. Development and evaluation of a lyophilization protocol for colorimetric RT-LAMP diagnostic assay for COVID-19. Sci Rep 2024;14:10612. https://doi.org/10.1038/s41598-024-61163-7.

[133] Song X, Coulter FJ, Yang M, Smith JL, Tafesse FG, Messer WB, et al. A lyophilized colorimetric RT-LAMP test kit for rapid, low-cost, at-home molecular testing of SARS-CoV-2 and other pathogens. Sci Rep 2022;12:7043. https://doi.org/10.1038/s41598-022-11144-5.
[134] Khattak A, Sever C, Nelson P, Cooper R, Congdon T, Demartino J, et al. Cartridges, collectors, kits, and methods for enhanced detection and quantification of analytes in collected fluid samples. US20170043335A1, 2017.
[135] Lin Y-J, Nie H. A novel approach to mechanical characterization of pharmaceutical lyospheres. Powder Technology 2022;410:117868. https://doi.org/10.1016/j.powtec.2022.117868.
[136] Stratta L, Capozzi LC, Franzino S, Pisano R. Economic Analysis of a Freeze-Drying Cycle. Processes 2020;8:1399. https://doi.org/10.3390/pr8111399.
[137] Edmond MB, Wallace SE, McClish DK, Pfaller MA, Jones RN, Wenzel RP. Nosocomial Bloodstream Infections in United States Hospitals: A Three-Year Analysis. Clinical Infectious Diseases 1999;29:239–44. https://doi.org/10.1086/520192.
[138] Naber CK. Staphylococcus aureus Bacteremia: Epidemiology, Pathophysiology, and Management Strategies. Clinical Infectious Diseases 2009;48:S231–7. https://doi.org/10.1086/598189.
[139] Zhang J, Yang F, Sun Z, Fang Y, Zhu H, Zhang D, et al. Rapid and precise identification of bloodstream infections using a pre-treatment protocol combined with high-throughput multiplex genetic detection system. BMC Infectious Diseases 2022;22:823. https://doi.org/10.1186/s12879-022-07793-6.
[140] Canas LS, Sudre CH, Pujol JC, Polidori L, Murray B, Molteni E. Early detection of COVID-19 in the UKusing self-reported symptoms: a large-scale, prospective, epidemiological surveillance study. The Lancet Digital Health 2021;3:587–98. https://doi.org/10.1016/S2589-7500(21)00131-X.
[141] Yang J, Chen H, Wang Z, Yu X, Niu X, Tang Y. Development of a quantitative loop-mediated isothermal amplification assay for the rapid detection of novel goose parvovirus. Frontiers in Microbiology 2017;8:2472. https://doi.org/10.3389/fmicb.2017.02472.
[142] Borio C. The Covid-19 economic crisis: dangerously unique. Business Economics 2020;55:181–90. https://doi.org/10.1057/s11369-020-00184-2.
[143] Gu C, Zhu J, Sun Y, Zhou K, Gu J. The inflection point about COVID-19 may have passed. Sci Bull (Beijing) 2020;65:865–7. https://doi.org/10.1016/j.scib.2020.02.025.
[144] Ozili PK. COVID-19 pandemic and economic crisis: the Nigerian experience and structural causes. Journal of Economic and Administrative Sciences 2020;37:401–18. https://doi.org/10.1108/JEAS-05-2020-0074.
[145] Swinnen J, McDermott J. Covid-19 and global food security 2020. https://doi.org/10.1111/1746-692X.12288.
[146] Ye J, Ji P, Barthelemy M. Scenarios for a post-COVID-19 world airline network. Chaos 2023;33:043140. https://doi.org/10.1063/5.0146575.
[147] Huff HV. Controlling the COVID-19 pandemic blindly: silent spread in absence of rapid viral screening. Clinical Infectious Diseases 2021;73:3053–4. https://doi.org/10.1093/cid/ciaa1251.
[148] Olalekan A, Iwalokun B, Akinloye OM, Popoola O, Samuel TA, Akinloye O. COVID-19 rapid diagnostic test could contain transmission in low- and middle-income countries. Afr J Lab Med 2020;9:1255. https://doi.org/10.4102/ajlm.v9i1.1255.
[149] Peck KR. Early diagnosis and rapid isolation: response to COVID-19 outbreak in Korea. Clinical Microbiology and Infection: The Official Publication of the European

Society of Clinical Microbiology and Infectious Diseases 2020;26:805–7. https://doi.org/10.1016/j.cmi.2020.04.025.
[150] Brouard S, Vasilopoulos P, Becher M. Sociodemographic and Psychological Correlates of Compliance with the COVID-19 Public Health Measures in France. Can J Polit Sci n.d.:1–6. https://doi.org/10.1017/S0008423920000335.
[151] Yu L, Shanshan W, Hao X, Dong X, Mao L, Pelechano V. Rapid detection of COVID-19 coronavirus using a reverse transcriptional loop-mediated isothermal amplification (RT-LAMP) diagnostic platform. Clinical Chemistry 2020;66:975–7. https://doi.org/10.1093/clinchem/hvaa102.
[152] Babiker A, Myers CW, Hill CE, Guarner J. SARS-CoV-2 Testing. Am J Clin Pathol 2020;153:706–8. https://doi.org/10.1093/ajcp/aqaa052.
[153] Cui Z, Chang H, Wang H, Lim B, Hsu C-C, Yejiong Y. Development of a rapid test kit for SARS-CoV-2: an example of product design. Bio-Design and Manufacturing 2020;3:83–6. https://doi.org/10.1007/s42242-020-00075-7.
[154] Vogels CBF, Brito AF, Wyllie AL, Fauver JR, Ott IM, Kalinich CC. Analytical sensitivity and efficiency comparisons of SARS-CoV-2 RT–QPCR primer–probe sets. Nature Microbiology 2020;5:1299–305. https://doi.org/10.1038/s41564-020-0761-6.
[155] Han MS, Byun J-H, Cho Y, Rim JH. RT-PCR for SARS-CoV-2: quantitative versus qualitative. Lancet Infect Dis 2021;21:165. https://doi.org/10.1016/S1473-3099(20)30424-2.
[156] Faíco-Filho KS, Passarelli VC, Bellei N. Is Higher Viral Load in SARS-CoV-2 Associated with Death? Am J Trop Med Hyg 2020;103:2019–21. https://doi.org/10.4269/ajtmh.20-0954.
[157] Rueda-Garrido JC, Vicente-Herrero MT, Teresa M, Campo L, Reinoso-Barbero RE, Hoz GL. Return to work guidelines for the COVID-19 pandemic. Occupational Medicine 2020;70:300–5. https://doi.org/10.1093/occmed/kqaa099.
[158] Rao SN, Manissero D, Steele VR, Pareja J. A Systematic Review of the Clinical Utility of Cycle Threshold Values in the Context of COVID-19. Infect Dis Ther 2020;9:573–86. https://doi.org/10.1007/s40121-020-00324-3.
[159] Wang H, Zhang Y, Huang B, Deng W, Quan Y, Wang W. Development of an inactivated vaccine candidate, BBIBP-CorV, with potent protection against SARS-CoV-2 2020.
[160] Poon LLM, Leung CSW, Chan KH, Lee JHC, Yuen KY, Guan Y. Detection of human influenza a viruses by loop-mediated isothermal amplification. Journal of Clinical Microbiology 2005;43:427–30. https://doi.org/10.1128/JCM.43.1.427-430.2005.
[161] Brisco AA MJ & Morley. Quantification of RNA integrity and its use for measurement of transcript number. Nucleic Acids Research 2012;40:144. https://doi.org/10.1093/nar/gks588.
[162] Sanchez de Groot N, Armaos A, Graña-Montes R, Alriquet M, Calloni G, Vabulas RM, et al. RNA structure drives interaction with proteins. Nat Commun 2019;10:3246. https://doi.org/10.1038/s41467-019-10923-5.
[163] Jonsson O, Lundell A, Rosell J, You S, Ahlgren K, Swenson J. Comparison of Sucrose and Trehalose for Protein Stabilization Using Differential Scanning Calorimetry. J Phys Chem B 2024;128:4922–30. https://doi.org/10.1021/acs.jpcb.4c00022.
[164] Ahlgren K, Olsson C, Ermilova I, Swenson J. New insights into the protein stabilizing effects of trehalose by comparing with sucrose. Physical Chemistry Chemical Physics 2023;25:21215–26. https://doi.org/10.1039/D3CP02639F.
[165] Huelsmeyer M, Kuzman D, Bončina M, Martinez J, Steinbrugger C, Weusten J, et al. A universal tool for stability predictions of biotherapeutics, vaccines and in vitro

diagnostic products. Sci Rep 2023;13:10077. https://doi.org/10.1038/s41598-023-35870-6.
[166] Li M, Jia L, Xie Y, Ma W, Yan Z, Liu F, et al. Lyophilization process optimization and molecular dynamics simulation of mRNA-LNPs for SARS-CoV-2 vaccine. Npj Vaccines 2023;8:1–13. https://doi.org/10.1038/s41541-023-00732-9.
[167] Tyagi N. Live Biotherapeutics : importance of formulation and lyophilization parametersand an example of a clinical application. 2023. https://doi.org/10.54612/a.4g1r1pvjb4.
[168] Biopharma Industry Outlook: Key Trends Impacting the Industry | L.E.K. Consulting n.d. https://www.lek.com/zh-hant/insights/ei/looking-ahead-biopharma-key-trends-impacting-industry (accessed June 3, 2025).
[169] Cao Z, Zhang K, Yin D, Zhang Q, Yu Y, Wen J, et al. Clinical validation of visual LAMP and qLAMP assays for the rapid detection of Toxoplasma gondii. Frontiers in Cellular and Infection Microbiology 2022;12.
[170] Yu Y, Zhou JXY, Li B, Ji M, Wang Y, Carnaby E, et al. A quantitative RT-qLAMP for the detection of SARS-CoV-2 and human gene in clinical application. Microb Biotechnol 2022;15:2619–30. https://doi.org/10.1111/1751-7915.14112.
[171] Newman H, Hardie D. HIV-1 viral load testing in resource-limited settings: Challenges and solutions for specimen integrity. Rev Med Virol 2021;31:e2165. https://doi.org/10.1002/rmv.2165.
[172] Hansen S, Abd El Wahed A. Point-Of-Care or Point-Of-Need Diagnostic Tests: Time to Change Outbreak Investigation and Pathogen Detection. Trop Med Infect Dis 2020;5:151. https://doi.org/10.3390/tropicalmed5040151.
[173] Rossaki FM, Hurst JR, van Gemert F, Kirenga BJ, Williams S, Khoo EM, et al. Strategies for the prevention, diagnosis and treatment of COPD in low- and middle-income countries: the importance of primary care. Expert Review of Respiratory Medicine 2021;15:1563–77. https://doi.org/10.1080/17476348.2021.1985762.
[174] Moore C. Point-of-care tests for infection control: should rapid testing be in the laboratory or at the front line? J Hosp Infect 2013;85:1–7. https://doi.org/10.1016/j.jhin.2013.06.005.
[175] Blyth CC, Booy R, Dwyer DE. Point of care testing: diagnosis outside the virology laboratory. Methods Mol Biol 2011;665:415–33. https://doi.org/10.1007/978-1-60761-817-1_22.
[176] Adams ER, Schoone GJ, Ageed AF, Safi SE, Schallig HDFH. Development of a Reverse Transcriptase Loop-Mediated Isothermal Amplification (LAMP) Assay for the Sensitive Detection of Leishmania Parasites in Clinical Samples. The American Journal of Tropical Medicine and Hygiene 2010;82:591–6. https://doi.org/10.4269/ajtmh.2010.09-0369.
[177] Nikpey N. Nanomolecular Magnetic Probe for Colorimetric RT-LAMP of Viral RNA. Biointerface Res Appl Chem 2022;13:292. https://doi.org/10.33263/BRIAC133.292.
[178] Uribe-Alvarez C, Lam Q, Baldwin DA, Chernoff J. Low saliva pH can yield false positives results in simple RT-LAMP-based SARS-CoV-2 diagnostic tests. PLoS One 2021;16:e0250202. https://doi.org/10.1371/journal.pone.0250202.
[179] Vergara A, Boutal H, Ceccato A, López M, Cruells A, Bueno-Freire L, et al. Assessment of a Loop-Mediated Isothermal Amplification (LAMP) Assay for the Rapid Detection of Pathogenic Bacteria from Respiratory Samples in Patients with Hospital-Acquired Pneumonia. Microorganisms 2020;8:103. https://doi.org/10.3390/microorganisms8010103.

[180] Alian E, Semnani A, Firooz A, Shirani M. A Novel Sensitive Bulk Optode Based on 5-Br Salophen as an Ionophore for Determination of Zinc Ion in Real Samples. J Braz Chem Soc 2018;29:528–34. https://doi.org/10.21577/0103-5053.20170165.
[181] Wan YY, Chen QH, Yao JX. FAAS Determination of Zinc in Water Samples after Enrichment by Coprecipitation with Mn(II)-5-Br-PADAP. Advanced Materials Research 2014;997:745–8. https://doi.org/10.4028/www.scientific.net/AMR.997.745.
[182] Homsher R, Zak B. Spectrophotometric investigation of sensitive complexing agents for the determination of zinc in serum. Clin Chem 1985;31:1310–3.
[183] Makino T. A sensitive, direct colorimetric assay of serum copper using 5-Br-PSAA. Clin Chim Acta 1989;185:7–16. https://doi.org/10.1016/0009-8981(89)90125-3.
[184] Tanner NA, Evans TC. Loop-mediated isothermal amplification for detection of nucleic acids. Curr Protoc Mol Biol 2014;105:Unit 15.14. https://doi.org/10.1002/0471142727.mb1514s105.
[185] Yuen KKY, Jolliffe KA. Bis[zinc(II)dipicolylamino]-functionalised peptides as high affinity receptors for pyrophosphate ions in water. Chem Commun 2013;49:4824–6. https://doi.org/10.1039/C3CC40937F.
[186] Degobert G, Aydin D. Lyophilization of Nanocapsules: Instability Sources, Formulation and Process Parameters. Pharmaceutics 2021;13:1112. https://doi.org/10.3390/pharmaceutics13081112.
[187] I S, An R. A Review on Freeze-drying: A Stability Enhancement Technique. Research Journal of Pharmacy and Technology 2022;15:4841–6. https://doi.org/10.52711/0974-360X.2022.00813.
[188] Tuyen DT, Thang LV, Boukharev G. Effects of Freezing Treatments and Protective Agents on the Stability of Weissella cibaria TSL24.10 after Freeze-Drying. Moscow Univ BiolSci Bull 2022;77:272–8. https://doi.org/10.3103/S0096392522040150.
[189] Ward KR, Matejtschuk P. The Principles of Freeze-Drying and Application of Analytical Technologies. Methods Mol Biol 2021;2180:99–127. https://doi.org/10.1007/978-1-0716-0783-1_3.
[190] Nail SL, Jiang S, Chongprasert S, Knopp SA. Fundamentals of freeze-drying. Pharm Biotechnol 2002;14:281–360. https://doi.org/10.1007/978-1-4615-0549-5_6.
[191] Gatlin LA, Nail SL. Protein purification process engineering. Freeze drying: A practical overview. Bioprocess Technol 1994;18:317–67.
[192] Abdelwahed W, Degobert G, Fessi H. Investigation of nanocapsules stabilization by amorphous excipients during freeze-drying and storage. European Journal of Pharmaceutics and Biopharmaceutics 2006;63:87–94. https://doi.org/10.1016/j.ejpb.2006.01.015.
[193] Mehanna MM, Abla KK. Recent advances in freeze-drying: variables, cycle optimization, and innovative techniques. Pharmaceutical Development and Technology 2022;27:904–23. https://doi.org/10.1080/10837450.2022.2129385.
[194] Atanasov N, Trifonova E, Evstatieva Y, Nikolova D. Effect of two lyoprotectants on the survival rate and storage stability of freeze-dried probiotic lactic acid bacterial strains. JCTM 2023;58. https://doi.org/10.59957/jctm.v58i6.1.
[195] Laurent A, Scaletta C, Abdel-Sayed P, Raffoul W, Hirt-Burri N, Applegate LA. Industrial Biotechnology Conservation Processes: Similarities with Natural Long-Term Preservation of Biological Organisms. BioTech (Basel) 2023;12:15. https://doi.org/10.3390/biotech12010015.
[196] Liu Y, Zhang Z, Hu L. High efficient freeze-drying technology in food industry. Crit Rev Food Sci Nutr 2022;62:3370–88. https://doi.org/10.1080/10408398.2020.1865261.

[197] Assegehegn G, Brito-de la Fuente E, Franco JM, Gallegos C. Freeze-drying: A relevant unit operation in the manufacture of foods, nutritional products, and pharmaceuticals. Adv Food Nutr Res 2020;93:1–58. https://doi.org/10.1016/bs.afnr.2020.04.001.
[198] Ma Y, Wu X, Zhang Q, Giovanni V, Meng X. Key composition optimization of meat processed protein source by vacuum freeze-drying technology. Saudi J Biol Sci 2018;25:724–32. https://doi.org/10.1016/j.sjbs.2017.09.013.
[199] Yuan F, Li Y-M, Wang Z. Preserving extracellular vesicles for biomedical applications: consideration of storage stability before and after isolation. Drug Deliv 2021;28:1501–9. https://doi.org/10.1080/10717544.2021.1951896.
[200] Hozouri H, Norouzian D, Aboofazeli R. An Investigation into Improvement of Stability and Efficacy of Intravesical BCG Formulations Using Freeze-Drying Technique: Stability and efficacy of intravesical BCG formulations. Trends in Peptide and Protein Sciences 2020;5:1-9 (e7). https://doi.org/10.22037/tpps.v5i.33393.
[201] Singh S. Storage considerations as part of the formulation development program for biologics. American Pharmaceutical Review 2007;10:26–33.
[202] Zhang Y, Bi J, Huang J, Tang Y, Du S, Li P. Exosome: A Review of Its Classification, Isolation Techniques, Storage, Diagnostic and Targeted Therapy Applications. Int J Nanomedicine 2020;15:6917–34. https://doi.org/10.2147/IJN.S264498.
[203] Hansen LJJ, Daoussi R, Vervaet C, Remon J-P, De Beer TRM. Freeze-drying of live virus vaccines: A review. Vaccine 2015;33:5507–19. https://doi.org/10.1016/j.vaccine.2015.08.085.
[204] Drain PK, Hyle EP, Noubary F, Freedberg KA, Wilson D, Bishai WR, et al. Diagnostic point-of-care tests in resource-limited settings. Lancet Infect Dis 2014;14:239–49. https://doi.org/10.1016/S1473-3099(13)70250-0.
[205] Bissonnette L, Bergeron MG. Diagnosing infections—current and anticipated technologies for point-of-care diagnostics and home-based testing. Clinical Microbiology and Infection 2010;16:1044–53. https://doi.org/10.1111/j.1469-0691.2010.03282.x.
[206] Kumru OS, Joshi SB, Smith DE, Middaugh CR, Prusik T, Volkin DB. Vaccine instability in the cold chain: mechanisms, analysis and formulation strategies. Biologicals 2014;42:237–59. https://doi.org/10.1016/j.biologicals.2014.05.007.
[207] Preston KB, Randolph TW. Stability of lyophilized and spray dried vaccine formulations. Adv Drug Deliv Rev 2021;171:50–61. https://doi.org/10.1016/j.addr.2021.01.016.
[208] Juhl D, Mosel C, Nawroth F, Funke A-M, Dadgar SM, Hagenström H, et al. Detection of herpes simplex virus DNA in plasma of patients with primary but not with recurrent infection: implications for transfusion medicine? Transfus Med 2010;20:38–47. https://doi.org/10.1111/j.1365-3148.2009.00951.x.
[209] Young H, Ogilvie M. Herpes simplex virus (HSV-1; HSV-2) (Genital herpes). In: Young H, Ogilvie M, editors. Genitourinary Infections: November 1994, Dordrecht: Springer Netherlands; 1994, p. 184–238. https://doi.org/10.1007/978-94-017-5080-6_7.
[210] Zhu S, Viejo-Borbolla A. Pathogenesis and virulence of herpes simplex virus. Virulence 2021;12:2670–702. https://doi.org/10.1080/21505594.2021.1982373.
[211] Omarova S, Cannon A, Weiss W, Bruccoleri A, Puccio J. Genital Herpes Simplex Virus-An Updated Review. Adv Pediatr 2022;69:149–62. https://doi.org/10.1016/j.yapd.2022.03.010.
[212] Pinninti SG, Kimberlin DW. Neonatal herpes simplex virus infections. Semin Perinatol 2018;42:168–75. https://doi.org/10.1053/j.semperi.2018.02.004.

[213] Dichtl K, Osterman A, Forster J, Jakob L, Suerbaum S, Flaig MJ, et al. A retrospective evaluation of the Euroarray STI-11 multiplex system for the detection of eight STI causing agents. Sci Rep 2023;13:11382. https://doi.org/10.1038/s41598-023-38121-w.
[214] Williamson DA, Chen MY. Emerging and Reemerging Sexually Transmitted Infections. N Engl J Med 2020;382:2023–32. https://doi.org/10.1056/NEJMra1907194.
[215] Elden LJR van, Kraaij MGJ van, Nijhuis M, Hendriksen KAW, Dekker AW, Rozenberg-Arska M, et al. Polymerase Chain Reaction Is More Sensitive than Viral Culture and Antigen Testing for the Detection of Respiratory Viruses in Adults with Hematological Cancer and Pneumonia. Clinical Infectious Diseases 2002;34:177–83. https://doi.org/10.1086/338238.
[216] Koivikko T, Rodrigues PC, Vehviläinen M, Hyvönen P, Sundquist E, Arffman RK, et al. Detection of herpes simplex virus in oral tongue squamous cell carcinoma. Front Pharmacol 2023;14:1182152. https://doi.org/10.3389/fphar.2023.1182152.
[217] Tuddenham S, Hamill MM, Ghanem KG. Diagnosis and Treatment of Sexually Transmitted Infections: A Review. JAMA 2022;327:161–72. https://doi.org/10.1001/jama.2021.23487.
[218] Bradshaw MJ, Venkatesan A. Herpes Simplex Virus-1 Encephalitis in Adults: Pathophysiology, Diagnosis, and Management. Neurotherapeutics 2016;13:493–508. https://doi.org/10.1007/s13311-016-0433-7.
[219] Weber Z, Sutter D, Baltensperger A, Carr N. Economic Evaluation: Onsite HSV PCR Capabilities for Pediatric Care. Pediatr Qual Saf 2020;5:e266. https://doi.org/10.1097/pq9.0000000000000266.
[220] Scheithauer S, Manemann AK, Krüger S, Häusler M, Krüttgen A, Lemmen SW, et al. Impact of herpes simplex virus detection in respiratory specimens of patients with suspected viral pneumonia. Infection 2010;38:401–5. https://doi.org/10.1007/s15010-010-0036-x.
[221] Van TT, Mongkolrattanothai K, Arevalo M, Lustestica M, Dien Bard J. Impact of a Rapid Herpes Simplex Virus PCR Assay on Duration of Acyclovir Therapy. J Clin Microbiol 2017;55:1557–65. https://doi.org/10.1128/JCM.02559-16.
[222] Jamehdar SA, Aelami MH, Mehrabadi FY, Tabaei S, Hajghorbani ST, Malakuti P, et al. Molecular Epidemiology and Risk Factors of Herpes Simplex Virus Type 2 in Pregnant Women. Journal of Clinical and Nursing Research 2022;6:1–6. https://doi.org/10.26689/jcnr.v6i3.3576.
[223] Mirchandani D, Jawed R, Khawar N, Narula P, John M. Effectiveness of Early Antiviral Therapy in Disseminated Neonatal Herpes Simplex Virus 2 (HSV-2) with Fulminant Hepatic Failure. Am J Case Rep 2017;18:381–5. https://doi.org/10.12659/AJCR.902418.
[224] Ramgopal S, Wilson PM, Florin TA. Diagnosis and Management of Neonatal Herpes Simplex Infection in the Emergency Department. Pediatric Emergency Care 2020;36:196. https://doi.org/10.1097/PEC.0000000000002077.
[225] Samies NL, James SH. Prevention and treatment of neonatal herpes simplex virus infection. Antiviral Res 2020;176:104721. https://doi.org/10.1016/j.antiviral.2020.104721.
[226] De Rose DU, Bompard S, Maddaloni C, Bersani I, Martini L, Santisi A, et al. Neonatal herpes simplex virus infection: From the maternal infection to the child outcome. J Med Virol 2023;95:e29024. https://doi.org/10.1002/jmv.29024.
[227] Humisto A, Antikainen J, Holma T, Jarva H, Toivonen A, Loginov R, et al. Evaluation of the Novel CE-IVD-Marked Multiplex PCR QIAstat-Dx Meningitis/Encephalitis Panel. Microbiology Spectrum 2023;11:e05144-22. https://doi.org/10.1128/spectrum.05144-22.

[228] Kabani N, Kimberlin DW. Neonatal Herpes Simplex Virus Infection. NeoReviews 2018;19:e89–96. https://doi.org/10.1542/neo.19-2-e89.
[229] McIntosh K. The SARS coronavirus: rapid diagnostics in the limelight. Clin Chem 2003;49:845–6. https://doi.org/10.1373/49.6.845.
[230] The Story of Oxsed Limited. Oxford University Innovation n.d. https://innovation.ox.ac.uk/about/social-ventures/story-oxsed-limited/ (accessed October 16, 2024).
[231] Yu Y, Ahmadi, Yasaman. Development and clinical validation of extraction-free loop mediated Isothermal amplification assay for rapid detection and subtyping of herpes simplex virus 2024.
[232] Kessler HH, Mühlbauer G, Rinner B, Stelzl E, Berger A, Dörr HW, et al. Detection of herpes simplex virus DNA by real-time PCR. Journal of Clinical Microbiology 2000;38:2638–42. https://doi.org/10.1128/jcm.38.7.2638-2642.2000.
[233] Maret W. Inhibitory zinc sites in enzymes. Biometals 2013;26:197. https://doi.org/10.1007/s10534-013-9613-7.
[234] Perry DK, Smyth MJ, Stennicke HR, Salvesen GS, Duriez P, Poirier GG, et al. Zinc Is a Potent Inhibitor of the Apoptotic Protease, Caspase-3: A NOVEL TARGET FOR ZINC IN THE INHIBITION OF APOPTOSIS *. Journal of Biological Chemistry 1997;272:18530–3. https://doi.org/10.1074/jbc.272.30.18530.
[235] Takei F, Akiyama M, Nobusawa K, Sabani NB, Han H, Nakatani K, et al. PCR under Low Ionic Concentration Buffer Conditions. ChemistrySelect 2018;3:973–6. https://doi.org/10.1002/slct.201702542.
[236] Lee S, Kang H, Do Y, Lee G, Kim J, Han H. High-precision THz Dielectric Spectroscopy of Tris-HCl Buffer. Journal of the Optical Society of Korea 2016;20:431–4. https://doi.org/10.3807/JOSK.2016.20.3.431.
[237] Chashchina GV, Beniaminov AD, Kaluzhny DN. Stable G-Quadruplex Structures of Oncogene Promoters Induce Potassium-Dependent Stops of Thermostable DNA Polymerase. Biochemistry Moscow 2019;84:562–9. https://doi.org/10.1134/S0006297919050109.
[238] Leng X, Wang Y, Li R, Liu S, Yao J, Pei Q, et al. Circular exponential amplification of photoinduced electron transfer using hairpin probes, G-quadruplex DNAzyme and silver nanocluster-labeled DNA for ultrasensitive fluorometric determination of pathogenic bacteria. Microchim Acta 2018;185:168. https://doi.org/10.1007/s00604-018-2698-5.

END

Johnny Xiangyi Zhou

Linacre College

University of Oxford

2025